Schweizerische Eidgenossenschaft
Confédération suisse
Confederazione Svizzera
Confederaziun svizra

Department of the Environment,
Transport, Energy and Communication DETEC

Swiss Federal Office of Energy SFOE
Energy Research

Final report

Project VITES

Vacuum Insulated Thermal Energy Storage

Date: 6 November 2019

Place: Yverdon-les-Bains

Publisher:
Swiss Federal Office of Energy SFOE
Research Programme XY
CH-3003 Bern
www.bfe.admin.ch
energieforschung@bfe.admin.ch

Co-financed by:
HEIG-VD
Laboratoire d'énergétique solaire et de physique de bâtiment (LESBAT)
CH-1401 Yverdon-les-Bains
www.heig-vd.ch

Agent:
HEIG-VD
Laboratoire d'énergétique solaire et de physique de bâtiment (LESBAT)
Av. des Sports 20, CP 521
CH-1401 Yverdon-les-Bains
www.heig-vd.ch

TVP Solar SA
Place du Bourg-de-Four 36
CH-1204 Genève
www.tvpsolar.com

Author:

Sara Eicher, HEIG-VD	sara.eicher@heig-vd.ch
Martin Guillaume, HEIG-VD	martin.guillaume@heig-vd.ch
Xavier Jobard, HEIG-VD	xavier.jobard@heig-vd.ch
Jacques Bony, HEIG-VD	jacques.bony@heig-vd.ch
Stéphane Citherlet, HEIG-VD	stephane.citherlet@heig-vd.ch
Philippe Bonhôte, HEIG-VD	philippe.bonhote@heig-vd.ch
Vittorio Palmieri, TVP Solar	palmieri@tvpsolar.com
Francesco Di Giamberardino, TVP Solar	digiamberardino@tvpsolar.com

SFOE Head of domain: Stefan Oberholzer, stefan.oberholzer@bfe.admin.ch
SFOE programme manager: Stefan Oberholzer, stefan.oberholzer@bfe.admin.ch
SFOE contract number: SI/501690-01

SFOE Head of domain: Andreas Eckmanns, andreas.eckmanns@bfe.admin.ch
SFOE programme manager: Elimar Frank, elimar.frank@frank-energy.com
SFOE contract number: SI/501691-01

The author of this report bears the entire responsibility for the content and for the conclusions drawn therefrom.

Résumé

Aujourd'hui, le stockage de l'énergie thermique (TES de l'anglais thermal energy storage) joue un rôle important dans la transition vers des systèmes énergétiques durables à faibles émissions de carbone en permettant de répondre au décalage entre la demande et la disponibilité de l'énergie thermique provenant de sources d'énergie variables dans le temps. L'un des défis pour cette technologie réside dans la réduction des pertes de chaleur en augmentant la qualité de l'isolation. Les technologies actuelles pour le stockage d'eau chaude utilisent des matériaux d'isolation conventionnelles pour le bâtiment. Pour ces derniers, l'amélioration de la capacité d'isolation se limite à leurs conductivités relativement élevées et nécessite également une grande épaisseur. Une solution possible est d'utiliser le vide d'air en lieu et place à une isolation classique.

Ce projet vise à analyser la faisabilité technique et la viabilité économique d'une cuve de stockage thermique à double paroi et à haute performance, isolé sous vide, conçu pour minimiser les pertes de chaleur. Les applications de ce produit pourraient être des systèmes solaires thermiques intégrés dans des procédés de chauffage industriel pour des températures allant jusqu'à 180 °C, mais il peut également être utilisé pour des applications résidentielles à basse température (par ex. jusqu'à 70 °C) ainsi qu'en combinaison avec d'autres sources d'énergie. L'objectif final est d'offrir une alternative efficace, fiable et économique aux solutions de cuves isolées existantes pour le stockage de l'énergie thermique sous forme de chaleur sensible. Ce nouveau concept est ci-après dénommé VITES et la faisabilité déterminée pour les applications industrielles et résidentielles. Le concept VITES présente des caractéristiques spécifiques par rapport à d'autres approches d'isolation sous vide pour les TES :

- pas de matériau de remplissage dans l'espace sous vide entre la cuve intérieur et la cuve extérieur pour supprimer le transfert de chaleur par conduction
- revêtement de cuivre sur les parois de l'espace sous vide pour réduire l'échange de rayonnement infrarouge entre les parois
- un dispositif spécial pour maintenir le vide élevé dans l'espace entre la cuve intérieur et la cuve extérieur (moins de 0.001 mbar)
- entretoises et supports sur mesure pour réduire la conduction thermique entre l'intérieur et l'extérieur de la cuve

Afin de mener à bien cette étude, les activités suivantes ont été réalisées :

- recherche bibliographique sur l'état de l'art des systèmes TES, études et applications
- analyse structurelle du concept VITES
- analyse thermique du concept VITES
- l'analyse des performances thermiques pour les procédés de chauffage industriels et les applications résidentielles
- analyse économique et positionnement au sein du marché

La revue bibliographique indique qu'en dépit d'une importante activité de recherche visant à améliorer les pertes de chaleur des TES, le concept de l'isolation sous vide sans matériaux de remplissage n'a pas encore été entièrement étudié. Des conceptions appropriées de TES à double paroi isolées sous vide ont été étudiées. La conception de la cuve VITES a évolué en prenant en compte différentes considérations. Sur le plan externe, VITES ressemble aux cuves conventionnels existants sur le marché dans le but de minimiser les coûts d'investissement tout en présentant en interne un certain nombre de composants clés destinés à réduire les pertes de chaleur.

Ces travaux ont été suivis d'une analyse structurelle pour valider la conception proposée et assurer la conformité aux applications à haute température. La conception finale a ensuite fait l'objet d'une étude thermique afin d'évaluer l'impact des revêtements à faible émissivité sur les pertes radiatives dans l'espace sous vide. Une estimation des ponts thermiques de la tuyauterie, des raccords et des entretoises a également été effectuée. Une amélioration de la conception de ces composants a été effectuée permettant ainsi une réduction considérable des ponts thermiques. L'effet de l'humidité sur la capacité d'isolation des matériaux conventionnels a également été utilisé à des fins de comparaison. Pour maintenir et garantir le vide, une pompe getter, déjà brevetée et compacte a été choisie sur la base d'une technologie éprouvée.

Une évaluation du coût d'investissement du concept VITES a également été réalisée et des comparaisons ont été effectuées avec les TES commercialisés munis d'isolations conventionnelles. Cela a permis de positionner le concept VITES sur le marché actuel des TES en vue d'un déploiement futur. Un modèle numérique de la cuve a été développé et le comportement thermique a été étudié dans différentes conditions de fonctionnement. Une évaluation du coût d'investissement du concept VITES a également été réalisée et des comparaisons ont été effectuées avec les TES munis d'isolations conventionnelles disponibles sur le marché. Enfin, des aspects économiques sous la forme d'un calcul du temps de retour sur investissement ont présenté l'attrait par rapport aux solutions de stockage conventionnels disponibles sur le marché.

Dans l'ensemble, le concept VITES est clairement viable non seulement en termes de faisabilité technique, mais également en termes de viabilité économique. De cette étude, les paramètres techniques suivants peuvent être résumés :

- réservoir en AISI 304L
- pression de service maximale 16 bar
- température maximale de fonctionnement 180 °C
- capacité standard jusqu'à 10 m³.
- pour des capacités plus élevées, possibilité d'utiliser plusieurs cuves
- niveau d'isolation sous vide (inférieur à 0.001 mbar)
- pompe getter pour inspecter et maintenir le niveau de vide (garantie 20 ans)
- ponts thermiques inférieurs à 15% des pertes totales de la cuve (à 160°C)
- pertes de chaleur : 25 W/m² à 160 °C et 9 W/m² à 90 °C
- coût spécifique : 13500 à 5000 CHF/m³ pour 1 à 10 m³
- coût de la capacité de stockage : 130 à 47 CHF/kWh pour 1 à 10 m³

Summary

Today, thermal energy storages (TES) play an important role in the transition to low carbon, sustainable energy systems by coping with the mismatch between demand and availability of thermal energy from timely-based energy sources. One of the challenges for this technology lies in the reduction of the heat losses by increasing the quality of the insulation. The current technology state for hot water storages is conventional building insulation materials. For these latter, improving insulation ability is limited to their high conductivity properties and consequently, required large thickness. A possible solution is to use vacuum insulation.

This project aims to analyse the technical feasibility and the economic viability of a high performance, double-wall vacuum insulated thermal storage tank, designed to minimise heat losses. Applications for this product could be solar thermal systems integrated into industrial heating processes with temperatures up to 180 °C, but it can also be used for low temperature residential applications (e.g. up to 70°C) as well as in conjunction with other energy sources. The final objective is to provide an efficient, reliable and economic alternative to the existing insulated tank solutions for sensible thermal energy storage. This new concept is hereafter referred to as VITES and the feasibility determined for both industrial and residential applications. The VITES concept has some specific features when compared to other approaches of vacuum insulation for TES:

- no filling material in the evacuated gap between inner and outer tank to suppress conduction heat transfer
- copper coating on the walls of the evacuated gap to reduce longwave radiation exchange between the walls
- a special device to maintain the high vacuum in the gap (less than 0.001 mbar)
- customised spacers and supports to reduce thermal conduction between inner and outer tank

In order to carry out this study, the following activities were performed:

- literature review of the state of the art of TES systems and review of existing research on vacuum insulated tank technology and applications
- structural analysis of the designed VITES concept
- thermal analysis of the VITES concept
- thermal performance analysis for industrial heating processes and residential applications
- economic analysis and integrated market position

The literature review indicates that despite an important research activity to improve TES heat losses, the concept of no-filling evacuated annular gap investigated in this project has not yet been fully considered elsewhere. Suitable designs of double-wall vacuum insulated TES were then investigated, the final design evolved from a number of considerations. Externally, VITES resembles existing conventional insulated TES on the market in an attempt to minimise investment costs while internally it presents a number of key components designed to reduce heat losses.

This work was followed by a structural analysis to validate the proposed design and ensure conformity to high temperature applications. The final design was then thermally investigated to assess the impact of low emissivity coatings on the radiative heat transport in the evacuated gap. An estimation of the thermal bridges from piping connections, fittings and stability spacers was also conducted. The effect of moisture on the insulation ability of conventional materials was also used for comparison purposes. To maintain and inspect the vacuum, an existing, patented and compact getter pump was chosen based on well-proven technology.

All these studies have allowed positioning the VITES concept in the actual TES market for future deployment considerations. A numerical model of the tank was subsequently developed and the thermal behaviour investigated under different operating conditions. An evaluation of the investment cost of the VITES concept was also performed and comparisons were made with conventional insulated TES on the market. Finally, economic considerations in the form of a payback time calculation presented the investment attractiveness with respect to the common TES alternatives on the market.

Overall, the VITES concept is clearly viable not only in terms of technical feasibility but also in terms of economic practicality. From this study, the following technical parameters can be summarised:

- tank made of AISI 304L
- maximum operating pressure 16 bar
- maximum operating temperature 180 °C
- standard capacities up to 10 m^3
- for higher capacities possibility to use multiple tanks
- vacuum insulation level (less than 0.001 mbar)
- getter pump to inspect and maintain vacuum level (20 years warranty)
- thermal bridges less than 15% of the overall tank losses (at 160°C)
- heat losses: 25 W/m^2 at 160 °C and 9 W/m^2 at 90 °C
- specific cost: 13500 to 5000 CHF/m^3 for 1 to 10 m^3
- storage capacity cost: 130 to 47 CHF/kWh for 1 to 10 m^3

Table of Contents

List of abbreviations

AISI	American Iron and Steel Institute
ANF	Annuity factor
ATES	Aquifer thermal energy storage
BTES	Borehole thermal energy storage
DHW	Domestic hot water
ECES	Energy Conservation and Energy Storage
FEA	Finite Element Analysis
HX	Heat exchanger
HTF	Heat transfer fluid
LMTD	Logarithmic mean temperature difference
MFH	Multi-family house
PTES	Pit thermal energy storage
PUR-PIR	Polyurethane-polyisocyanurate
REC	Reference energy cost
SFOE	Swiss Federal Office of Energy
SH	Space heating
SHC	Solar Heating and Cooling
SHIP	Solar heating industrial process
TES	Thermal energy storage
UTES	Underground thermal energy storage
VIP	Vacuum insulation panels
VSI	Vacuum super insulation

1 Introduction

The Swiss Energy Strategy 2050 sets an approach to reach a sustainable energy supply in Switzerland by 2050. In addition to the phase-out of nuclear power, the strategic objectives include measures to increase the use of renewable energy and the energy efficiency of buildings, mobility, industry and appliances [1]. However, most renewable energy sources are intermittent in nature so that energy production is not in phase with energy demand. Energy storage has, therefore, become an important research topic and the development of efficient, inexpensive energy storage systems as important as the quest for new energy sources [2].

In Switzerland, more than 50% of the final energy consumption is used for space heating, domestic hot water production and industrial process heating [3, 4]. Moreover, the European average of process heat demand between 100 and 200°C [5] is reported to represent 21% for the industry sector. Corresponding statistics for Switzerland are not available but assuming that the energy demand profile for the Swiss industry is close to that of Germany and Austria, the Swiss value should be around 21%. In these applications, full use of renewable energy can only be achieved by providing adequate energy storage options. Therefore, thermal energy storage (TES) could play a major role in global energy efficiency improvement by increasing the share of renewable energy production and of waste heat recovery. In addition, the Federal Energy Research Masterplan [6] considers decentralised heat and cold storage as one of the research areas to be focused by 2020. Still, for a better market penetration, major challenges need to be overcome not only on the technical side (long-term capacity, longer lifetime, higher efficiency, improved safety) but also on the economic side with better payback periods.

Recent years have shown a number of different developments regarding cost-effective thermal insulation solutions for TES. Double-wall vacuum insulated systems for sensible heat storage, using low levels of vacuum and gap filling materials to increase thermal resistance, are one of them.

The goal of this project is to develop the concept of a high performance, double-wall hot water thermal storage tank with high vacuum and no filling material in the gap between the walls to decrease heat losses. Such a device must have an acceptable cost and should be of interest to solar thermal industrial and residential systems as well as to store thermal energy from any other energy source.

This research is in line with the Swiss Energy Strategy 2050 through:

- Valorisation of waste heat, solar heat and other renewable energies
- Improvement of the performance of sensible TES
- Improvement of energy efficiency in buildings and industrial processes
- Reduction of environmental impacts

Short initial participation to the Annex 30: Thermal Energy Storage for Cost-effective Energy Management and CO_2 Mitigation [7], have not only allowed to deepen the knowledge of this topic but also to evaluate current challenges in the development of TES, some of them addressed in this project.

Beginning 2017 a joint SHC Task 58/ECES Annex 33 entitled Material and Component Development for Thermal Energy Storage [8] was launched dealing with advanced materials for latent and chemical storage. Although the focus is on materials, the current project for which the development of a novel

TES concept is aimed, presents a good complement to the overall work developed in this joint task/annex.

2 Project aim

The aim of this project is to develop a high performance, double-wall vacuum insulated hot water thermal storage tank. In this concept, for which a high vacuum level (less than 0.001 mbar) is foreseen, losses by convection and conduction should tend towards zero. The main heat losses of the tank being limited to radiation and to the thermal bridges present in the wall of the tank and fittings. In addition, this new tank will have to be competitive from a financial point of view compared to standard insulated tanks on the market. To achieve this goal, several parameters will be investigated, in particular:

- the design and structural analysis of the VITES concept
- the optimisation between the level of vacuum achieved, the performance and cost
- the need to use reflective surfaces
- the need to minimise thermal bridges
- the cost and other economic aspects

Target applications for this device would be in the industrial sector, as temperature levels are normally higher than in building applications so that storing energy losses are equally larger. In addition, temperatures over 120 °C prevent the use of polyurethane foams (PUR-PIR), an insulating material commonly used on water storages. For these high temperatures, the available insulation options are limited to either low thermal performance, low cost inorganic fibrous materials (glass and rock wool), greatly vulnerable to moisture or high thermal performance, high cost superinsulator aerogels, greatly fragile and vulnerable to moisture [9]. The choice between these two insulation products bears a non-negligible impact on the final insulation costs of the storage system.

However, this project will also tackle the individual and collective housing market because the energy saving potential of this technology appears to be significant even at lower temperatures as the potential market is significantly larger. It has been estimated to about 1.4 million GWh/year, the potential savings from a wider use of hot and cold storage systems in the industrial and domestic sectors in Europe [10]. Within the Swiss context, the estimated value is about 4500 GWh/year in the building sector alone. The use of TES for industrial waste heat recovery is also of great importance with over 300 TWh/year of waste heat potential in the EU while for Switzerland, the estimated value is about 5.3 TWh/year [11, 12]. All these developments are in line with the strategy of meeting industry demands with the expertise of the industrial partner in this project (TVP Solar).

In terms of investment cost, the goal of this project is to design a storage device that does not exceed the maximum acceptable storage capacity cost (SCC_{acc}) as defined in the IEA SHC Task 42 / ECES Annex 29 [13], see Figure 1. Thus, based on the specifications provided for short-term TES investigated in the building sector [13], the cost of the TES should not exceed an average 336 CHF/kWh_{cap} (CHF per kWh of installed storage capacity). For the industry sector, acceptable average prices should be below 112 CHF/kWh_{cap} for a process that needs several cycles per year (e.g. 700 cycles/year). For further details, please refer to *cf.* 5.2.

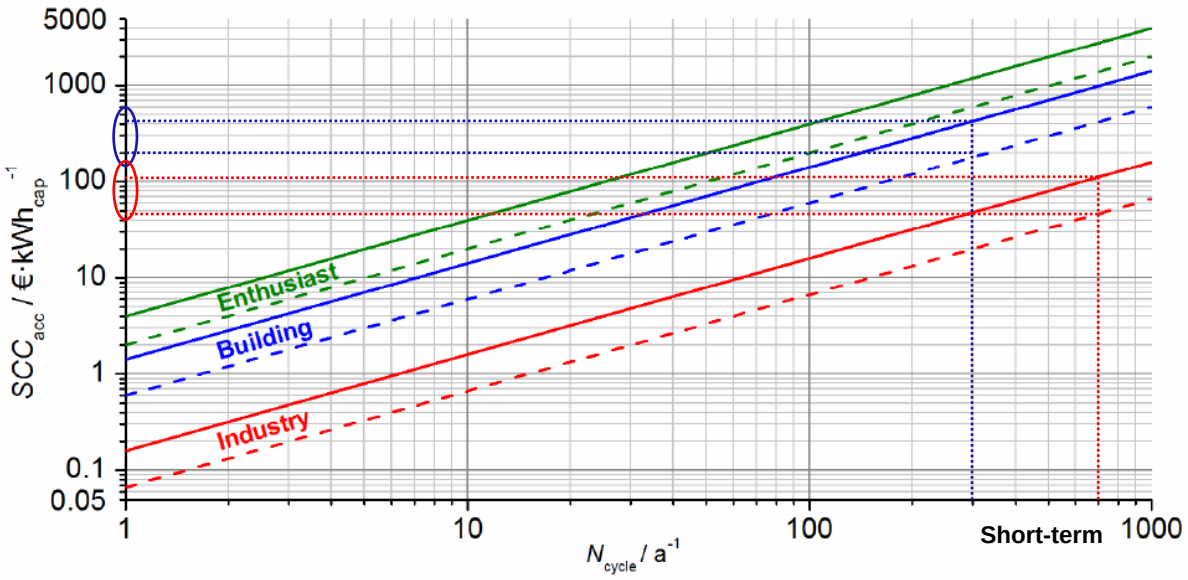

Figure 1 Maximum acceptable storage capacity costs SCC_{acc} for three user classes as a function of storage cycles per year Ncycle; enthusiast high/low case (green solid/dashed line), building high/low case (blue solid/dashed line), and industry high/low case (red solid/dashed line) [13].

To develop a sound vacuum insulated storage tank, this project leaned on the renowned and comprehensive experience of TVP Solar, experts on thermal vacuum power charged technology and industrial partner of this project.

2.1 Project steps

The project is divided into 3 work packages:

WP1: Concept development

WP2: System integration

WP3: Dissemination

In order to successfully develop the VITES storage device, the following objectives have been defined:

- literature review of existing concepts, products and research in the field of TES, particularly for hot water thermal storage
- structural analysis of the VITES tank to validate the proposed design, ensure conformity to the target applications and assess the impact of changing conditions
- thermal design analysis to assess the heat transmission process, estimate thermal bridges and the influence of several parameters on the overall thermal behaviour of the VITES tank
- numerical simulation of the annual performances of the VITES tank under different conditions and for different applications and assessment of potential gains
- cost estimation and economic considerations for market diffusion

3 Literature review

3.1 Thermal energy storage

Thermal energy storage is defined as the temporary storage of thermal energy at high or low temperature levels. These systems are required when the heat demand is not in phase with heat production. Of great importance in many engineering fields, they are particularly used in buildings for short-term storage of domestic hot water and for industrial processes. However, long-term storage is also possible but imply larger storage tanks to harvest large quantities of energy, such as waste heat from industrial processes, to use, for example, in large-scale central heating systems.

The technology offers, in this way, the possibility to offset the mismatch between demand and availability of thermal energy by collecting and storing energy for use at a later time. Primarily designed to store solar energy, these systems can also be employed to store any other timely-based energy source such as waste heat for which availability and utilisation periods differ.

The advantages of a well design TES system can be summarised as follows:

- improved energy efficiency
- increased reliability of the required supplied energy
- increase share of renewables
- reduced investment and maintenance costs

According to the storage mechanism, TES can be classified into:

- sensible heat storage: by heating or cooling a liquid or a solid storage medium
- latent heat storage: by the phase change of the storage medium (melts and solidification)
- thermochemical heat storage: by thermochemical reactions

Storage of heat has been traditionally in the form of sensible heat with water as the most common storage medium. Latent heat storage as become an important research topic in the last decade due to its operational advantages of smaller storage tanks and small temperature variations. Thermochemical heat storage, despite its potential to provide even higher storage capacities, is still in a development and demonstration phase. This review will concentrate on sensible heat storage for water heating applications.

A key aspect of TES systems is the insulation of the tank to reduce heat losses. The simplest and most cost-effective solution is insulation applied to the storage outside wall. In this case, conventional building insulation materials such as mineral wool, expanded polystyrene and polyurethane foam [14], dominate the market. Improving the current insulation ability of these materials is difficult because of their high thermal conductivities and corresponding large insulation thicknesses required to improve thermal resistance. Therefore, advanced insulation materials, the so-called superinsulators, have been developed and tested in real case studies, see for example [15,16].

Alternatively, insulation can be applied within the storage wall by creating an evacuated gap between two concentric vessels, the so-called vacuum super insulation (VSI). The open literature indicates an important research and development activity in Europe particularly for VSI filled with powders, a technology proven and widely used in cryogenic applications. The availability of some commercial products based on this technology is also reported in different case studies [9]. It seems that the no-

filling evacuated gap insulation concept for TES proposed in this project, has not been considered elsewhere.

3.2 Sensible heat storage technologies

The most common material used in sensible heat storage is water as it has a high specific heat capacity and is cheap in comparison to any other storage medium. Applications types vary widely across buildings, industrial processes and district heating. At low temperature, water is one of the best storage medium and the most widely used for solar water heating applications. Due to the boiling point constraint of water, high temperature applications require increasing the system pressure [17].

Research have shown that water tank storage is a cost-effective option but with room for improvement in terms of internal stratification temperatures and thermal insulation [18]. For this latter, research is now focus on vacuum insulation solutions with much lower effective thermal conductivities and, in some cases, with no moisture deterioration, as is the case in the most common insulation materials [19]. In Switzerland, small water storage tanks with capacities up to several m^3 used as short-term storage in the domestic and industry sectors represent the majority.

As for large-scale applications, underground storage of sensible heat is normally used and is well suited for seasonal storage, i.e. using summer season stored heat in the heating season. In Switzerland, very large tanks (up to thousands m^3) are not common and are out of the scope of this study.

According to a recent review [20], TES systems based on sensible heat storage have storage efficiencies between 50 to 90% depending on the storage medium and insulation technology. In general, sensible heat storages are simpler in design and relatively inexpensive when compared to latent or thermochemical storages but are bigger in size. The proposed VITES solution provides an interesting alternative to the common employed insulation solutions by avoiding moisture effects in addition to reducing heat losses without increasing the tank size due to improved insulation properties of vacuum. For this latter, the reason is that the no-filling evacuated gap solution is able to further supress the solid conduction occurring in the gap due to the absence of filling material.

3.3 Vacuum insulated materials

Superinsulating materials have been used in the past to insulate passive houses. [21] reported a building related application with the integration of vacuum insulation into different building elements. The market is now offering two types of solutions: vacuum insulated panels (VIP) and silica aerogels. VIP consists of an open, highly porous evacuated core, wrapped in a sealed envelope. Silica aerogels is a highly transparent, highly porous, exceptionally lightweight composite material. Vacuum insulation panels and aerogel based products have 6 to 10 times lower thermal conductivity [22] and, consequently, lower insulation thickness when compared to traditional insulating materials. They offer a suitable option for insulating TES.

The characterisation of the effective thermal conductivity of the most widely proposed nanostructured insulants, such as expanded perlites and fumed silica, under different operating conditions lead to a number of publications [16, 19, 23, 24]. Results demonstrate that superinsulating materials are best for TES with certain dimensions being less effective and not economical for large TES. The study [16] demonstrated that the use of evacuated powders with expanded perlite is an appropriate and economic method for high temperature (up to 300 °C) since effective thermal conductivities remain low.

In practice, VIP and aerogels are fragile in handling, vulnerable to moisture and quite expensive when compared to traditional insulation materials. On the other hand, there are concerns regarding gas leakages into the evacuated powder containing space that could negatively affect the insulation

performance of this type of VSI. The potential robustness of the proposed VITES concept lies in the excellent proven characteristics of the getter pump chosen to inspect and maintain the vacuum in the gap.

3.4 Vacuum insulated TES: research and market

The potential of vacuum insulation materials for different hot water storage sizes and operating temperatures has also been addressed in the open literature.

The use of concrete cylindrical long-term hot water thermal storage of 100 m^3 with vacuum insulated panels (fumed silica) in a seasonal TES system design to reach 90% reduction in emissions and 80% in storage losses [15] was experimentally tested. The measured thermal resistance was about 30% of the original theoretical estimation. The observed discrepancy was attributed to thermal bridges and defects in the thermal insulation, clearly demonstrating the fragility of these panels. Results also indicate that improvements are necessary in the sizing and mounting design of these type of panels. The additional cost for the vacuum insulation tank was estimated to be about 25 000 EUR.

Another storage concept was developed and tested for hot water applications [22]. The 15.5 m^3 evacuated double vessel filled with perlite and containing water at 86 °C presented an overall cooling rate of 0.23 K/day including thermal bridges. This development led to a commercialised German product capable to ensure long-term operation without considerable heat losses [25]. Manufacturing of the tank is indicated to be a major issue because it requires precise welding and leaks inspection. The evacuation process also takes long. The price for 10 to 15 m^3 vacuum storages is indicated to range from EUR 20 000 to 25 000. From 35 m^3 onwards, the price of a vacuum TES and a conventional tank are reported to be the same.

The work carried out in [26] in a kind of thermos flask storage with a vacuum level of 1 mbar showed that a low-cost production is possible if the evacuated gap is filled with silica materials. A lab version of the thermos flask was built to assess the technical properties and validate the preliminary theoretical studies. Deviations from measurements suggested the need for further research on filling materials.

Within the framework of a research project financed by SFOE (COLAS) [27], the LESBAT had the opportunity to measure the performance of two TES tanks in an industrial application for bitumen storage. It was observed that the 40 years old thermal insulation in place was no longer effective, which lead the industrial partner to replace them. Despite this measure, one of the new TES tanks presented heat losses up to 10 times higher than the expected theoretical value for this type and thickness of insulation. In some cases, heat losses could represent 15 to 40% of energy consumption like in the COLAS project [28]. The reason for this problem was the permeability of mineral wool to air and the effect of moisture on the air conductivity. In [29], measurements have confirmed the sensitivity of mineral wools to condensation of water vapour in the material. For long-term exposure to humidity, conductivity values were significantly affected and the insulating ability reduced. This case highlights the importance of using insulation that is not affected by moisture or aging, such as in a vacuum TES.

In Switzerland, efforts are currently being made to develop high temperature TES relevant to industrial applications such as the case of VITES. A comprehensive analysis of the potential of integration of vacuum insulated TES in Swiss industries found that 70% could profit from this technology [30]. For retrofitting purposes, it is not possible to replace existing TES insulation with evacuated annular gap technologies.

Research is also focusing on low temperature seasonal TES for building applications: space heating, domestic hot water and industrial processes [31]. Seasonal storage is a fundamental domain of action to meet the Energy Strategy 2050 objectives.

Overall, research on TES vacuum insulation concepts is well underway with a few reported real experiments of TES using VIP or VSI. The proposed VITES attempts to overcome some of the limitations encountered in those cases, by avoiding moisture effects and ensuring the tightness of the system while limiting the investment cost.

3.5 Market today and future developments in Switzerland

In the residential sector, small hot water tanks (up to several m³) for short-term use are well established. About 90% of the buildings have a central heating system. Less than 5% are connected to district heating (DH). The industry sector also employs a number of these small hot water tanks for different heating processes. Research is expected to continue on efficiency improvement of hot water storages by pursuing the development and characterisation of superinsulation technologies for domestic and industrial applications. Medium size hot water storages (up to hundreds m³) are found in small DH systems serving small communities. No information was found for uses in the industry sector.

Large hot water systems (up to thousands m³) are not common in Switzerland but recent developments in the DH sector have shown the potential uptake of this technology. Switzerland has not a long tradition in using DH but the need to accelerate measures to achieve the energy strategy goals set in 2017 seems to push developments quite quickly. According to [32] district heat sales have been rising in Switzerland and this tendency is expected to last. Of particular interest, two district heating developments with large hot water storages have been identified in the country. In Basel, a 100 MWh heat storage unit consisting of nine insulated steel tanks with a total volume of 1260 m³ containing pressurised hot water tank is under construction, see Figure 2 [33].

Figure 2 Storage facility for Dolderweg district heating in Basel [33]

Built to cover short-term consumption peaks of households and industry, it will replace the energy currently produced by gas-firing heating plants. The aim is to provide better production-to-consumption flexibility while enabling the use of local resources such as wood and waste products. The reported investment cost is approximately 50 000 CHF/MWh.

Another example is the 50 m high, 28 000 m³ insulated hot water tank, see Figure 3, that supplies the Schwyz region enough to guarantee security of supply during two consecutive cold winter days when fully charged [34]. Investment costs are reported to be about 7700 CHF/MWh.

Figure 3 The Schwyz large hot water storage [34]

Another interesting system is the 2500 m³ underground reservoir in the administration building of the Swiss Federal Office of Statistics in Neuchâtel that is used for seasonal storage [35]. These large hot water storage developments are believed to set the pace for future TES systems in Switzerland.

Other technologies, such as underground TES technologies: aquifer (ATES) and pit (PTES) have seen no significant uptake. Only borehole (BTES) is undergoing considerable development.

ATES uses natural underground water-bearing permeable layers as storage medium. In the 80', the first European ATES was development in Neuchâtel, followed by other ATES developments in Lausanne but by lack of funding these slowly disappeared from the Swiss panorama. Recently, two ATES pilot projects have been identified, pushed forward by the new energy strategy objectives [36]. In Geneva, the potential for the development of a high temperature ATES connected to a waste-to-energy plant is under assessment. In Bern, the feasibility of storing waste heat from a nearby power generation site is also investigated.

PTES are based on shallow pits dug in the ground, lined and filled with gravel or water for heat storage but none have been identified in the country.

Regarding BTES, vertical heat exchangers are installed underground to transfer heat to and from the ground. Some hundred or so, low-temperature systems in combination with heat pumps, are currently operated in Switzerland for applications such as residential, DH and office buildings, please refer to [36, 37] for a few examples. Additional information on underground TES can be found in [10].

The current and future use of hot water storages in Switzerland seems to indicate the pertinence of the proposed concept and of this type of research within the national context.

3.6 Costs of sensible hot water TES

Costs for sensible hot water TES are highly sensitive to the insulation solution applied as well as to the storage volume, which in turn relates to the application. Some studies reported on TES costs based on European prices and including installation and operation costs, see for example [10, 38, 39]. However, the wide disparity of reported costs, reminds the difficulty and uncertainty linked to cost estimation of TES. Others studies presented updated cost values, representative of international markets, for thermal insulation materials for TES systems [9].

In an attempt to provide a cost estimation method to evaluate TES systems, Task42/Annex29 developed a simple tool based on two approaches [13]. The top-down approach seeks to estimate the maximum acceptable storage cost (SCC_{acc}) based on current energy costs (REC) and the annuity factor (ANF). This latter is a function of the interest rate (i) assigned to the capital and of the expected payback time (n):

$$SCC_{acc} = \frac{REC.N_{cycle}}{ANF} \quad \text{with} \quad ANF = \frac{(i+1)^n . i}{(i+1)^n - 1}$$

where,

Ncycle is the annual number of cycles

The bottom-up approach focus on the cost of existing storages on the market. The realised storage capacity cost (SCCreal) is the investment cost (INC) divided by the energy storage capacity (SC):

$$SCC_{real} = \frac{INC}{SC}$$

Figure 4 presents the results for the top-down approach. It is clear that SCC_{acc} depends on the application sector (e.g. domestic or building) because of the differences on the base assumptions specific to each application. The largest influence on SCC_{acc} is the number of storage cycles. Typically, for industry, a process requiring a low number of storage cycles could differ by a factor of 1000 in costs when compared with a process with a high number of storage cycles.

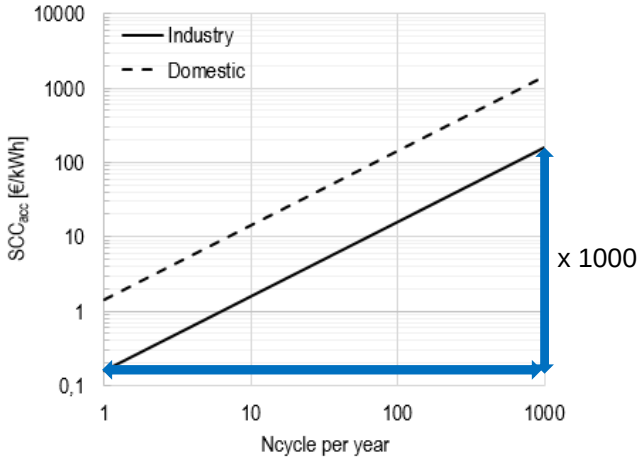

Figure 4 Maximum acceptable storage costs (SCC_{acc}) as a function of storage cycles per year for two applications [13]

For the bottom-up approach, cost data on existing TES systems is necessary. For water storages, the main investment cost is that of the material, manufacturing and insulation of the tank. Material relates to the costs of different components such as end caps, cylinder and fittings. Manufacturing includes costs of welding, labour and pressure control (if pressurised tank). Insulation costs includes insulation material and labour. This kind of data can be gathered from various sources such as product lists from internet sites, requested catalogues and directly quotes from manufacturers and suppliers.

3.7 Overview considerations

Overall, the literature review shows that the vacuum insulation concept investigated here has not been fully addressed elsewhere nor have the VSI cases reported dealt with high temperature applications. From the current state-of-the-art for TES insulation, it can be seen that VITES could provide an efficient, reliable and economic alternative to common insulation options besides presenting some other advantages with respect to other vacuum insulation solutions. A summary of the VITES features and a comparison to real case studies of vacuum insulation TES from the literature is presented in Table 1.

Table 1: Characteristics of the VITES concept and comparison to vacuum insulation solutions from the literature

Sensible hot water vacuum insulated TES Comparison of available vacuum concepts (real case studies)									
	Insulation technology	**Insulation mechanisms**			**Range of temperature applications °C**	**Storage volume m³**	**Vacuum level mbar**	**Overcost CHF**	**Major issues**
		conduction	***convection***	***radiation***					
Sengenthal TES [15]	VIP	reduced	suppressed	reduced	up to 90	n/a	n/a	25000 (100 m³)	Mounting process and material fragility
ZAE Bayern commercialised TES [22]	VSI filled with powders	reduced	suppressed	reduced	up to 95	5-50	0.05	10000 (10 m³)	Manufacturing process : welding and leaks inspection
VITES	VSI without filling powders	suppressed	suppressed	reduced	up to 180	1-10	0.001	8500* (10 m³)	n/a

* value derived from *cf.* 5.1

The main advantages of VITES are:

- the wide range of temperature applications (up to 180 °C)
- the vacuum reliability through a robust getter pump
- the reduced heat losses due to conduction heat transfer suppression in the evacuated gap and radiation reduction due to low emissivity coatings on the evacuated gap walls
- the no-filling material that translates into lower technology costs
- the intrinsic moisture protection
- the less space requirements: smaller tank dimensions for the same water volume (compared to typical insulated hot water storages)

The disadvantages are:

- Not suitable for TES renovation, like all others VSI concepts

4 VITES design conception

The VITES concept is a vacuum insulated hot water heat storage that can be charged with solar energy or any other renewable energy and even waste heat. Its functional principle is to store heat in the form of temperature-layered hot water over long periods.

By definition, vacuum (space devoid of matter) is often considered to be the best known insulator. In fact, the lack of matter greatly minimises heat losses by conduction and convention and only radiation prevails. In the VITES concept, the vacuum insulation is obtained in the gap between the two concentric metal cylinders that form the tank. The VITES target design specifications are presented in Table 2.

Table 2: Target design specifications of the VITES concept

Purpose	Heat storage for industrial applications
Tank volume	Up to 10 m^3 (reference 1 m^3)
Storage medium	Water
Storage medium temperature	Up to 180 °C (reference 160 °C)
Storage medium pressure	Up to 16 bar
Tank material	AISI 304L or 316L
Insulated material	Vacuum
Vacuum level	Less than 0.001 mbar
IR surface coating material of outer wall of inner tank	copper
Design cost from Task 42/Annex29 (please refer to Figure 1)	Up to 112 CHF/kWh (industrial sector) Up to 340 CHF/kWh (residential sector)

4.1 Structural analysis

Because of the design operating pressures: up to 16 bar inside the tank, less than 0.001 mbar in the double-wall gap and atmospheric pressure at the outside, the structural assessment of the proposed design was performed. The geometry and the structural analysis of the VITES concept is presented here.

VITES consists of two concentric stainless steel cylindrical tanks with end caps. The inner tank contains pressurised hot water. The outer tank must withstand the vacuum between the two cylindrical shells to isolate the inner tank and minimise the heat exchange between the water and the outside ambient conditions.

For the structural analysis, the following characteristics are considered:

- Tank capacity : 1 m^3
- Lateral spacers between the two cylindrical shells
- Four pipes for water circulation
- Minimised thermal bridges
- Attachment points on the top of the tank
- Minimised gap between the two cylindrical shells

There are two major categories leading to the failure of a mechanical component: material failure and structural instability, often called buckling. While material failures are related to the mechanical strength of the material, the load at which buckling occurs depends on the stiffness of the component and is independent of material strength. To predict the mechanical failure of the VITES concept, a Finite Element Analysis (FEA) was performed with ANSYS [40]. It aimed to ensure adequate strength for the design loadings (resistance and deformation analysis) and the buckling safety (stability analysis). Design loadings comprise the pressure loads: internal (16 bar) and external (1 bar) and mechanical loads present on the tank due to the weight of the structure and of the inner fluid.

The final design of the VITES tank evolved from three base design models. The aim was to arrive at an external configuration close to that of typical glass wool insulated tanks on the market and used by the industrial partner for high temperature solar fields, in an attempt to minimise additional costs due to the

new vacuum insulation concept. The final design has therefore optimised characteristics that bear an impact on the size, weight, heat losses and ultimately cost of the tank while preserving the strength and stability for safe operation. Modifications from the initial design were performed mainly in the supporting feet, thicknesses of the concentric tanks, end caps shape and lateral and bottom supports design, see Figure 5.

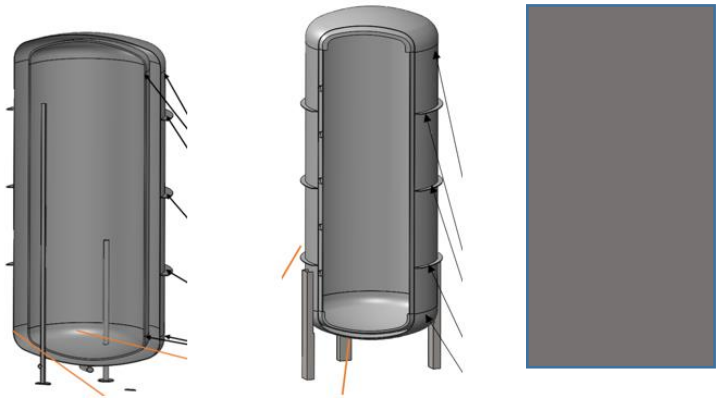

Figure 5 The three design prototypes considered for the VITES tank (design 3 TVP confidential)

The main geometrical dimensions of designs 1 to 3 are provided in Table 3.

Table 3 Main geometrical dimensions of designs 1 to 3 for 1 m³

	AISI 316L		
	Design 1	**Design 2**	**Design 3**
Length	2127		2668
Outer tank external diameter, mm	1000		880
Inner tank external diameter, mm	800		800
Inner tank thickness, mm: cylindrical body	8	5	6
Inner tank thickness, mm: end caps		12	
Outer tank thickness, mm: cylindrical body and end caps	3		
Number of reinforcement C rings	3		
Number of supporting feet	4		

4.1.1 Material properties and allowable stresses

In the preliminary study discussions, AISI 316L was initially considered in designs 1 to 3. However, in an attempt to limit costs and in accordance with our industrial partner, it was decided to employ AISI 304L in the final design, a material equally used in vacuum applications but considerably cheaper than AISI 316L. The material proposed for the VITES concept is therefore AISI 304L stainless steel. This iron-chromium-nickel bearing austenitic stainless steel is commonly used for vacuum applications as it shows enhanced corrosion resistance and ductability [41]. The mechanical properties of this stainless steel are given in Table 4 [42].

Table 4 Material properties used for the VITES concept at 160 °C [42]

Material	AISI 304L
Young's modulus	200 GPa
Poisson's ratio	0.3
Density	8000 kg/m^3
Yield strength	185 MPa
Ultimate tensile strength	398 MPa

4.1.2 Design 1

Figure 6 shows the design of prototype 1.

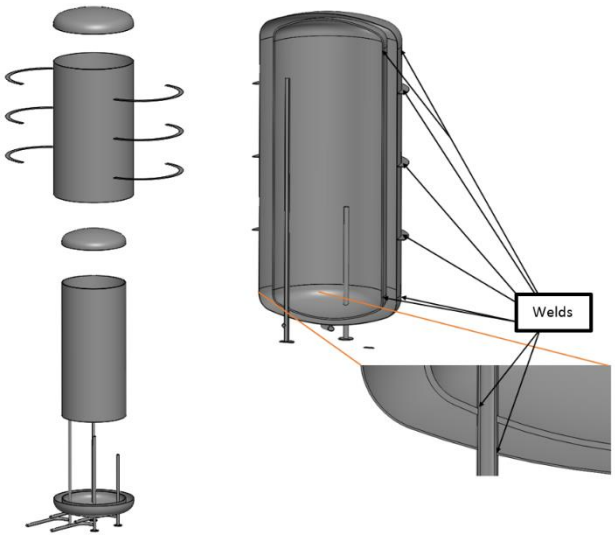

Figure 6 Overview of design 1

In here, a preliminary simple design was developed from the core requirements stated in Table 2. In this way, C shape rings were considered to reinforce the outer tank in order to resist buckling caused by the vacuum between the two tanks. The inner tank is positioned and supported by four inlet/outlet pipes welded to the elliptic bottom end, that serve equally as feet to the tank. The idea was to verify the possibility for multifunction components, such as the use of inlet/outlet pipes as outer tank support and to position and provide mechanical stability to the inner tank. However, the FEA results (see 11.1) have shown an important plastic deformation at the pipes welding and on the bottom end cap of the inner tank that lead to the development of design 2.

4.1.3 Design 2

Figure 7 shows the design of prototype 2.

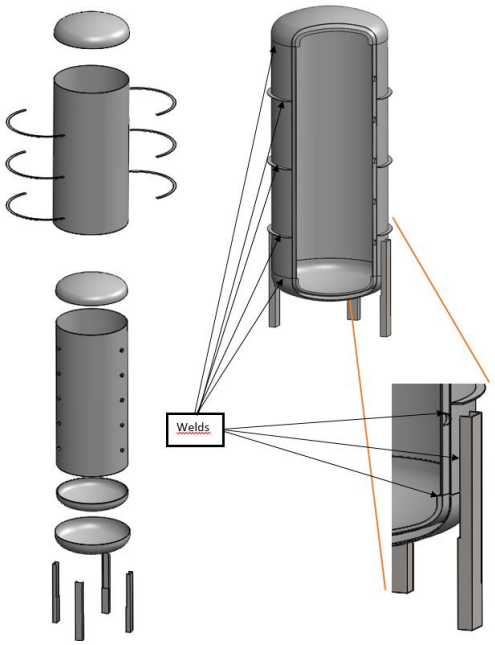

Figure 7 Overview of design 2

To improve the lack of mechanical resistance detected in some parts of design 1, a new design was developed. Here, no inlet/outlets were considered in the FEA analysis as these components do not interfere directly with the new structure behaviour. The outer tank remains reinforced with C shape rings to resist buckling caused by the vacuum between the two tanks. The inner tank is now supported by 15 ring spacers welded at the inner side of the outer tank and the outer side of inner tank but not on the elliptic end caps. The spacer material, a choice between borosilicate glass and stainless steel, is defined from the FEA study. The supporting feet are welded at the outer side of the outer tank cylindrical body for assembly simplicity. The different thicknesses of the cylinder and end caps of the inner tank meant to minimise constraints in the curved part, particularly of the bottom end cap.

The FEA results (see 11.1) have shown that design 2 is structurally adapted to the operation core requirements. However, the tank design was incomplete, missing important details such as a drainage pipe at the bottom, a top pipe connection for venting purposes as well as the inlet/outlets at different heights. In addition, the industrial partner also suggested a few more changes to improve the structure mechanical strength that lead to design 3.

4.1.4 Design 3

Figure 8 shows the design of prototype 3.

Figure 8 Overview of design 3 (TVP Solar confidential)

As mentioned before, a third design was further considered in order to account for additional components and increase the mechanical strength while minimising thermal bridges:

- to improve strength of inner tank, the elliptical caps were replaced with hemispherical ones. These latter are the ideal shape for an end cap (pressure in the vessel equally divided across the surface of the end cap) and are commonly used in high pressure applications where material savings are important (overall thinner thicknesses);
- replacement of lateral ring spacers by flat springs spacers to minimise heat transfer;
- added bottom support flat springs to provide mechanical stability of the inner tank;
- integration of inlet/outlet pipes of different heights for stratification that were not included in design 2;
- added top spiral pipe connection for non-condensable venting allowing to absorb the thermal expansion of the inner tank while minimising heat transfer;
- added drainage pipe at the bottom;
- integration of straight thin wall pipe jackets to inlet/outlet pipes for reduced heat transfer

The resultant structure is now higher than the previous designs due to the hemispherical end caps and heavier, despite thinner thicknesses, due to the additional components that were missing in design 2.

4.1.5 Finite element analysis (FEA) results

The main results of the structural analysis are provided in

Table 5. See section 11, for detailed results on this study.

Table 5 Comparison of the structural analysis results for designs 1 to 3 (AISI 316L)

	Design 1	Design 2	Design 3
Mass, kg	655	462	545
Global stress of inner tank, MPa (limit value 172 MPa)	189	96	98
[1]**Membrane stress of inner tank, MPa** (limit value 258 MPa)	120	84	103
Buckling (load multiplication)	6.2	9.6	4.3

The first FEA results show that due to the different cylinder and end cap thicknesses, design 2 is more efficient in handling stresses than design 1, as indicated by the lower global and membrane constraints. It can also be seen that design 2 presents a reduced overall mass when compared to design 1, most probably due to the missing inlet/outlet pipes. Other results from the FEA study revealed that the use of stainless steel ring spacers in design 2 is recommended because of its mechanical resistance, see section 11.1 for details. The use of borosilicate glass for the ring spacers, a commonly used material for this type of application, was excluded because the stress will exceed its mechanical resistance, making it yield.

The modifications introduced in design 3, aimed to complete the missing elements while keeping the strength and stability of the structure together with reduced thermal bridges. With a weight higher than in design 2 but significantly lower than in design 1, design 3 presents constraints sufficiently lower than the limit values, still placing it as a mechanically strength structure. A buckling analysis was also performed to check the stability (collapsing of the VITES tank) of the prototype designs for the two critical loads: external pressure and combined weight of the structure and of the inner fluid. Design 3 presents a buckling load 4.3 times higher than the nominal load, meaning that the critical pressure is 4.3 times the atmospheric pressure. According to [43], and for this type of application, a buckling load factor over 3 is recommended to ensure safety against buckling. Therefore, under these conditions no risk of buckling is foreseen. Given the results, design 3 was chosen as the most structurally suitable for the design applications.

During the study, it was necessary to adapt design 3 to resemble, from the external point of view, typical mineral wool insulated tanks on the market. The reason was to be able to properly compared performance and cost of the VITES concept against commercialised TES. At this point, the material was changed to AISI 304L to minimise costs. The revised design 3 has the same internal volume, but the overall dimensions are modified to be one-to-one comparable to the commercialised glass wool insulated tank used by our industrial partner for high temperature solar fields and manufactured inside their ovens, see Figure 9 . The result is a shorter (semi-elliptic end caps) and heavier (thicker thicknesses) tank than in design 3.

[1] Stress along the thickness of the shell

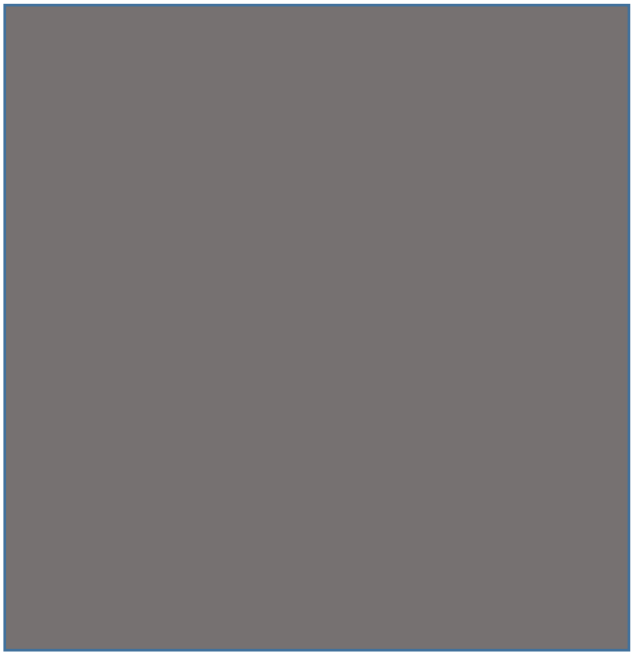

Figure 9 Overview of revised design 3 (TVP Solar confidential)

The main geometrical dimensions of the revised design 3 are provided in Table 6.

Table 6 Main geometrical dimensions of the revised design 3

Length, mm	2097 mm
Outer shell external diameter, mm	974 mm
Inner shell external diameter, mm	884 mm
Inner shell thickness: cylindrical body and elliptic caps	8 mm
Outer shell thickness: cylindrical body and elliptic caps	3 mm
Number of reinforcement C rings	3
Number of supporting feet	4

The structural analysis of the revised design 3 is presented in Table 7 .

Table 7 Structural analysis results for revised design 3 (AISI 304L)

	Revised design 3
Mass, kg	570
Global stress of inner tank, MPa (limit value 114 MPa)	106
[1]Membrane stress of inner tank, MPa (limit value 185 MPa)	117
Buckling (load multiplication)	5.9

The results show that the revised version of design 3 remains structurally suitable and the design safe for the required applications with maximum stresses lower than the limit values and buckling load over 3. Given this results, the revised version corresponds to the final VITES design and will be used for the remaining part of the study.

Please refer to Appendix 1 and 2 for further details of the FEA results.

4.2 Thermal analysis of the VITES tank

To assess the heat transmission process, estimate thermal bridges and the influence of several parameters on the overall thermal behaviour of the VITES tank, a thermal analysis was performed.

4.2.1 Radiation heat transfer – Emissivity impact of gap walls

As previously mentioned, vacuum insulation reduces dramatically the heat transfer by conduction and convention with no effect on the radiation transfer that becomes the dominate heat exchange mode, which depends on the emissivity of the walls and their temperatures. In order to anticipate the performance simulations, a thermal loss calculation for the radiation component was undertaken to evaluate the effect of emissivity coatings, applied to the walls of the annular gap, on the heat losses of the VITES design.

For this calculation, the VITES tank is assumed to be a closed cylinder with flat ends instead of elliptic end caps. Wall emissivity for the two concentric tanks was assumed to be 0.03 over the temperature range of 200 to 600 K [44], a value easily achieved with a copper based coating on the evacuated side surfaces of the gap between the cylinders, to reduce the net radiation transfer.

Thus, two calculations are performed: one for the cylindrical body of the tank and the other for the upper and lower flat ends of the tank. The theoretical heat losses of the VITES tank can be calculated as the net radiation exchange between the two flat plates added to that between the two concentric cylinders as given by [44]:

For flat plates:

$$q_p = \frac{A_p \sigma (T_1^4 - T_2^4)}{\frac{1}{\varepsilon_1} + \frac{1}{\varepsilon_2} - 1}$$

For concentric cylinders:

$$q_c = \frac{A_1 \sigma (T_1^4 - T_2^4)}{\frac{1}{\varepsilon_1} + \frac{1 - \varepsilon_2}{\varepsilon_2}\left(\frac{r_1}{r_2}\right)}$$

with :

q : specific heat transfer [W/m²]

A_p : flat plate area (top and bottom) – mean value between diameter of inner and outer tank [m²]

A_1: inner cylinder surface area [m²]

σ : Stefan-Boltzmann constant 5,67.10^{-8} [W/m²/K⁴]

ε_1, ε_2 : Emissivity of surface 1 (inner tank) and 2 (outer tank) [-]

T_1, T_2 : surface temperature 1 (inner tank) and 2 (outer tank) [K]

The radiation heat losses for the vacuum insulation was compared to the case where the VITES tank is insulated with 100 mm mineral wool material. Two cases were considered: one where the mineral wool was affected by vapour in the form of humid air with a thermal conductivity (*k*) of 0.06 W/m K [29] and a second dry mineral wool case with a thermal conductivity of 0.04 W/mK. The convection heat losses were estimated for a natural convection heat transfer coefficient of 10 W/m²K. Ambient temperature was taken at 20 °C. The results are illustrated in Figure 10.

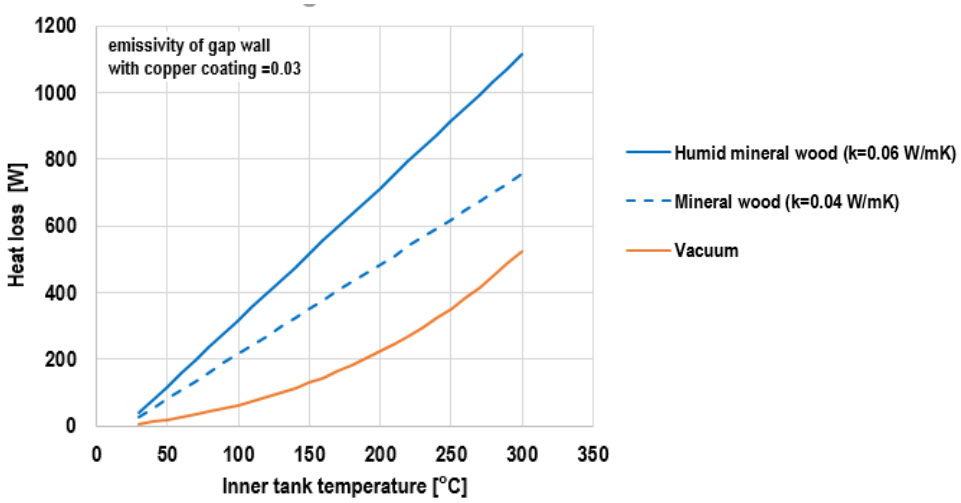

Figure 10 Comparison of the heat loss rate between the VITES concept and an equivalent typical mineral wool insulated storage tank

As expected, the higher the temperature difference between the inner tank and the ambient conditions, the higher the heat loss to the outside. Vacuum insulation is seen to be more effective in preventing heat losses over the entire range of temperatures that are of interest to this study (up to 180 °C) but also beyond when compared to both mineral wool insulation cases. In comparison to dry mineral wool insulation, heat loss reductions of about 70 to 50 % are predicted using vacuum insulation in the range of 100 to 200 °C, respectively. The heat loss reduction decreases with the increasing temperature of the inner tank. Usual insulation materials such as mineral wool can be affected by moisture that heavily deteriorates their insulation properties due to an increase in the thermal conductivity. For the reference operating temperature of 160 °C, heat loss is estimated to be nearly four times lower when using vacuum insulation with a low emissivity coating when compared to conventional humid mineral wool insulation. This result demonstrates that a low emissivity coating in the evacuated gap offers a tremendous advantage in the development of vacuum insulated TES. Heat loss results are displayed in Table 8 for the operating temperature of 160 °C.

Table 8 Heat loss results for conventional insulation and VITES technology at 160 °C

Conventional insulation			
	humid	conv.	
Conductivity (**mineral wool**)	0.06	0.04	W/m/K
Convection heat transfer coeff.	10	10	W/m²/K
Insulation thickness	0.1	0.1	m
Heat losses	**95**	**64**	**W/m²**

VITES		
Wall emissivity (copper coating)	0.03	-
Convection heat transfer coeff.	not taken into acc.	
Vacuum thickness	0.037	m
Heat losses	**25**	**W/m²**

The use of more advanced coatings such as silver coatings were not considered because of their high cost.

4.2.2 Thermal bridges – Supports and connections heat loss results

In the VITES prototype, spacers are used to maintain the space and properly position the two cylindrical concentric tanks. Spacers are available in a variety of shapes and materials to meet the particular needs of different applications. For this case, the choice of a proper spacer was defined by performing a conduction heat loss calculation in order to evaluate thermal bridges and minimise their impact. In the preliminary designs, ring spacers made either of borosilicate or stainless steel were investigated. Borosilicate with their low thermal expansion and high surface strength was found not resistant enough

as stainless steel, *cf.* 4.1.5. Losses from ring spacers were found to amount to nearly 7.5 W which led to a revised version of the spacers design since thermal bridging would, in this case, represent nearly 20% of the total losses at 160 °C.

In the revised design 3, flat spring stainless steel shape spacers and bottom supports were considered to reduce heat losses, see Table 9. Losses through the water connections, including a top spiral gas purge port and a bottom drain port, were also calculated to evaluate the impact of thermal bridging and provide solutions to minimise it. In this feasibility study, connections and water pipes diameters are not final. The final dimensions will be considered and optimised in a follow-up project.

According to Figure 10, the overall radiation heat loss of the VITES concept with applied copper coating, at the reference operating temperature of 160 °C is about 145 W, for an ambient temperature of 20 °C. The theoretical conduction heat losses from spacers, supports and water connections were calculated from the conduction rate equation [44]:

$$q_x = -k\mathrm{A}\frac{\Delta \mathrm{T}}{\mathrm{L}}$$

with :

q_x : heat transfer rate [W]

k : thermal conductivity [W/m K]

A : cross-sectional area [m²]

ΔT: temperature difference [K]

L: element length [m]

Table 9 presents the results of the conduction heat losses in the spacers, supports and water connections under these conditions.

Table 9 Conduction heat losses from spacers, supports and water connections of the revised design 3

	Piping		Drain and purge spiral pipes		Spacers	Bottom supports
	Material					
	Stainless steel	Water	Stainless steel	Water	Stainless steel	Stainless steel
Conductivity, W/m K	15	0.688	15.000	0.688	15	15
Length, m	0.390	0.390	1.900	1.900	0.175	0.257
External diameter, m	0.060	0.053	0.017	0.014	0.003	0.010
Internal diameter, m	0.053	0.000	0.014	0.000	0.005	0.015
Conduction surface area , m²	0.001	0.002	0.000	0.000	0.000015	0.000150
Coefficient, W/K	0.025	0.004	0.001	0.000	0.001	0.009
Conduction heat transfer, W	3.498	0.545	0.096	0.008	0.181	1.227
Number of elements	4	4	2	2	6	3
Total conduction heat transfer, W	**13.99**	**2.18**	**0.19**	**0.02**	**1.08**	**3.68**

The addition of the different conduction heat losses amounts to about 21 W, representing less than 15% of the overall losses of the tank at 160°C. Given the results, the proposed spacers, supports and water connections are considered suitable for the remaining part of the study.

4.3 Final design considerations

In this study, the use of an external heat exchanger for the VITES concept was chosen for simplicity reasons. Four inlets/outlets at different heights are considered but no further investigations are made at this stage regarding the final positions.

Mandatory for any vacuum device, an exhaust baking process is performed to reduce, among others, water vapour outgassing. Ovens exist for this process but in this study and for economic reasons, tanks are limited to a maximum volume of 10 m^3. The outgassing of baked systems is dominated by H_2 diffusing out of the metallic walls of the tank. To reduce this outgassing, a getter pump, an alloy gas sorber able to store hydrogen, will be used. This proven technology has been used for more than 10 years in the MT-Power from TVP Solar, a high-vacuum flat solar collector [45]. The reactive alloy powder is compressed into pills and assembled together to form the getter that will be placed on the outer tank to be activated by induction. For the VITES vacuum gap surface area, about 20 pills are estimated to be necessary. After activation, the getter sorbs gases without requiring power and when the surface capacity is reached, the getter must be reactivated. Vacuum level is guaranteed 20 years even with partial regeneration.

5 VITES cost estimation

The uptake of any new technology requires, in addition to reliability assurance, cost-effective evidence over the common alternatives on market. In this way, a cost estimation of the VITES tank was performed and the result compared with the cost of a conventional storage with 100 mm mineral wool insulation, illustrated in Figure 11 without insulation. The investment cost of the storage is determined based on catalogue prices and quotes. Economic evaluation of the VITES tank was performed using the methodology developed within the framework of Task42/Annex29 [13].

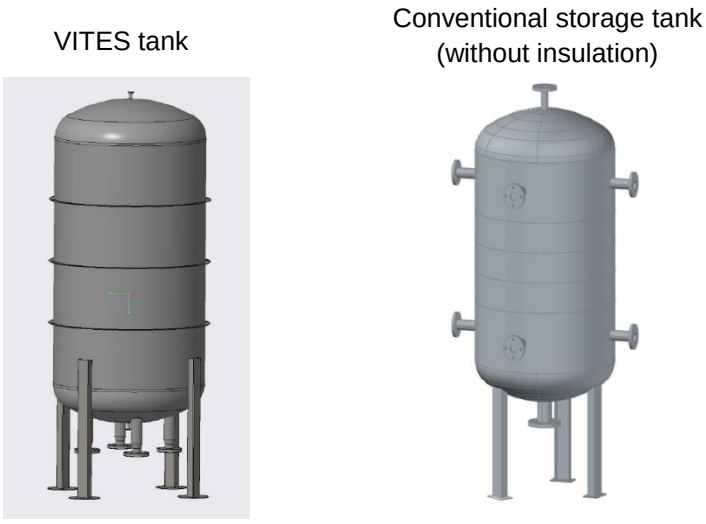

Figure 11 Simplified representation of 1 m^3 VITES and a one-to-one comparable conventional tank (without insulation)

5.1 Investment cost evaluation

In this method, the total investment cost is the sum of all costs to produce the storage unit and is expressed as the combination of components, manufacturing and insulation costs. Component costs

relate to the costs associated with different tank parts such as end caps, cylinder and fittings and were obtained from catalogue prices and quotes. Manufacturing costs, including welding and labour together with pressure control costs in case of pressurised tanks, were also obtained from quotes. Finally, insulation costs are those associated with the chosen insulation solution (traditional or vacuum). Two type of applications were considered: industrial high temperature processes and residential low temperature usage.

For industrial processes requiring water above 120°C, the storage is usually in the form of a pressurised stainless steel tank with either internal or external heat exchangers. For residential applications for which water is required below 100°C, tanks are either made of enamelled steel or stainless steel with one or two internal spiral heat exchangers. In this study, both conventional and VITES tank are made from stainless steel 304L with external heat exchangers. For the industrial application, both tanks are pressurised at 16 bars. For the residential application, stainless steel tanks are pressurised at 6 bars.

As previously mentioned, prices of components, insulation, manufacturing and pressure control were gathered from a mix of sources including product prices from internet sites, literature values, private communications with welding institutes and local quotes. Only investment cost (excluding the transport cost) are considered and the values in CHF are taken for a reference size of 1 m³. For comparison purposes, the specific cost is related to the water storage volume. It is important to note that the VITES inner tank is taken to be the same as the tank of the conventional insulated option. Only the insulation solution makes up for the cost difference. The 1 m³ conventional storage cost estimated using this methodology was validated with a quote.

A scale-up exercise was also carry out for volumes up to 10 m³, the maximum size for which VITES is designed. Here the scale-up method was to keep the same end caps and hold constant the tank diameter while adding constant height cylindrical parts to reach the required maximum volume. Therefore, the additional cost for the inner tank takes into account the cylindrical parts to be added as well as the additional welding to be done and the higher pressure control in terms of labour. The insulation cost, mineral wool for the conventional case and double wall with vacuum for the VITES case, also considers the enlargement of the tank.

Figure 12 shows the cost breakdown for both VITES and conventional insulated tank for the high temperature industrial application.

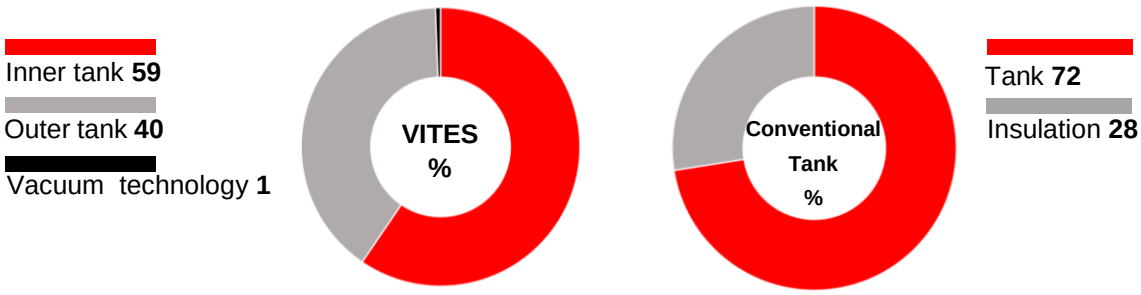

Figure 12 Cost breakdown of VITES and conventional insulated tank for the high temperature industrial application

The major fraction of investment costs associated with the investigated tanks relate to the water storage container (red colour label). The vacuum technology (oven and getter), often considered expensive, accounts for less than 1% of the overall VITES investment cost.

For residential applications, the non-pressurised VITES tank presents a cost breakdown equally distributed between the inner and outer tank with the vacuum technology remaining negligible.

For both applications, Figure 13 indicates that total costs are slightly higher for the VITES tank.

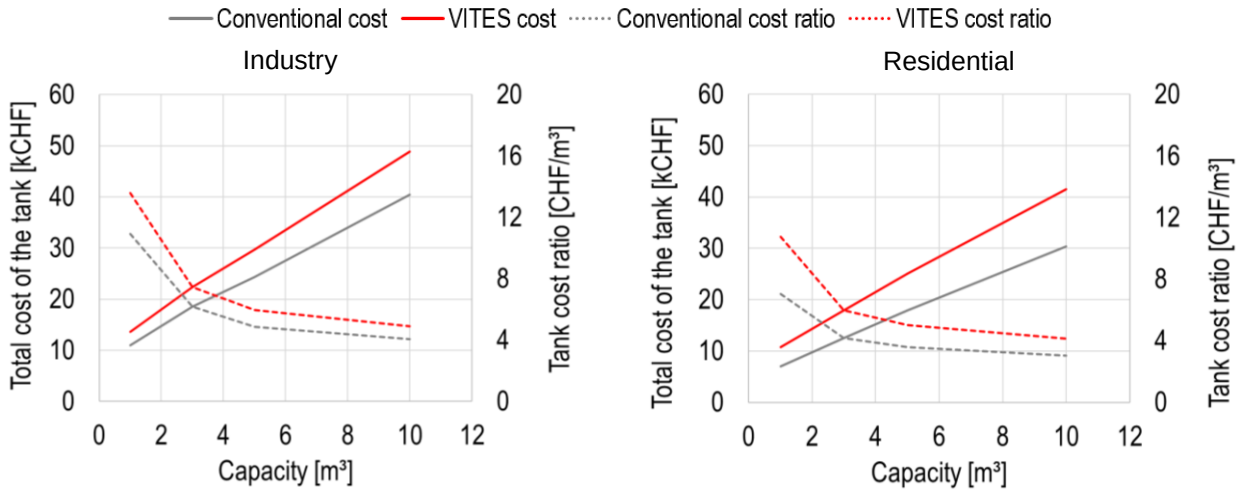

Figure 13 Cost comparison between VITES and conventional insulated tank for industrial and residential applications

For example, the insulated 100 mm mineral wool stainless steel tank for a nominal operating pressure of 16 bar costs about 11000 CHF whereas the VITES tank sums up to 13500 CHF. A cost difference of only 2500 CHF. In both applications, the over cost still places VITES has an interesting cost-effective technology with the additional advantage that VITES is moisture protected and has lower heat losses.

For the scale-up cases, VITES average specific costs for industry applications were found to range from 13500 CHF/m³ to 5000 CHF/m³ for volumes ranging from 1 to 10 m³ in comparison with 11000 and 4000 CHF/m³ for a conventional insulated tank.

Lower costs were obtained for multi-family houses, with VITES values ranging from 11000 CHF/m³ to 4000 CHF/m³ for volumes from 1 to 10 m³ in comparison with 7000 and 3000 CHF/m³ for a conventional insulated tank. It is clear the advantages of scale as specific costs progressively reduce as the size of the store increases.

5.2 Economic evaluation according to Task42/Annex29 methodology

The economic assessment of the VITES technology was also performed using Task 42/Annex 29 methodology [13]. As previously referred, *cf.* 3.6, these costs can be easily computed from the interest rate (*i*) assigned to the capital cost, the expected payback time (*n*), the reference energy cost (REC) and the annual number of storage cycles. However, these parameters differ from one application to another.

According to [13], interest rates over 10% and short payback times of less than 5 years are usual in the industry sector. In contrast, moderate interest rates of 5% and longer payback times of 15-20 are more common in residential applications. Theoretical limits for SCC_{acc} are also defined by considering a high and a low case corresponding to a max. REC with a min. ANF and min. REC with a max. ANF, respectively. The annuity factor, ANF, is a function of *i* and *n* and represents the annual payment for the storage investment, see [13] for further details. For industry, ANF ranges from 0.25 to 0.30 while for the

building sector these are within 0.07 and 0.10. As a reminder, the realised storage capacity cost (SCCreal) is the investment cost, as calculated in section 5.1, divided by the energy storage capacity.

Figure 14 shows the results for industry applications. Four storage capacities for the VITES tank containing pressurised water temperature at 180 °C with a return flow at 90 °C were analysed. Swiss industries gas prices are taken between 0.05 – 0.1 CHF/kWh.

For short-term storage with several hundred storage cycles, VITES seems quite attractive with specific costs ranging from 130 to 47 CHF/kWh (black full lines) for 1 to 10 m³, respectively. Compared to an existing 1 m³ industrial short-term storage with conventional insulation (dotted blue line) with an SCC_{real} of 107 CHF/kWh [46], it can be seen that VITES is totally within the range of acceptable storage cost.

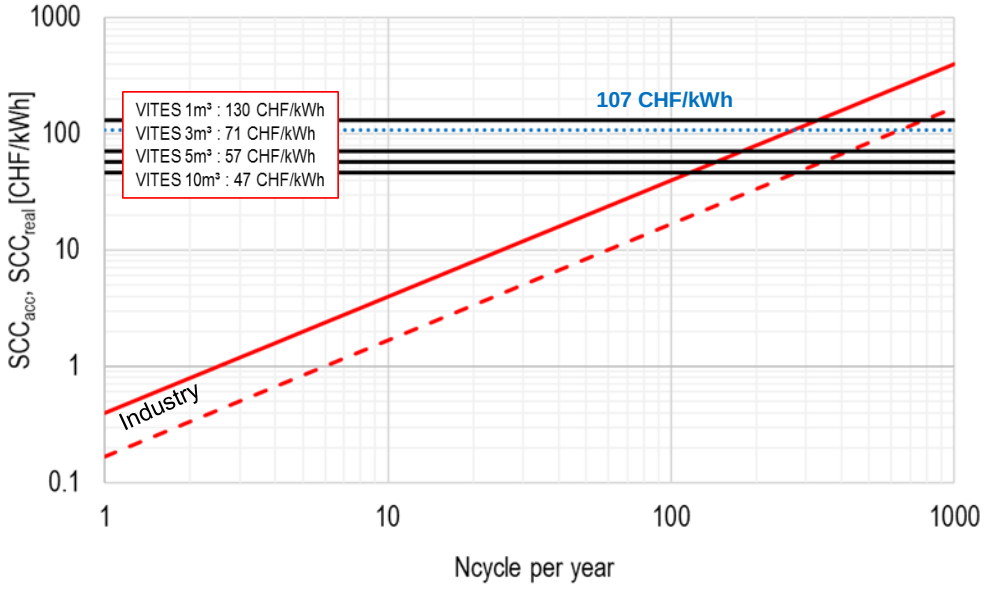

Figure 14 SCC_{real} for the VITES storage (solid black lines) and SCC_{real} for an equivalent conventional insulated storage (dotted blue line) for industrial applications (i=10%; n=5 years, REC_{gas}=0.05-0.1 CHF/kWh). Solid and dashed red lines are the SCC_{acc} theoretical limits for industry

For short-term, residential applications, SCC_{acc} between 40 and 103 CHF/kWh render the VITES storage economically competitive in comparison to a conventional insulated storage tank for which values between 70 and 170 CHF/kWh were found, see Figure 15. Here, energy costs for residential conventional insulated storages were calculated based on Swiss catalogue prices for PUR insulated stainless steel tanks with capacities ranging from 0.5 m³ and 2 m³ [47, 48, 49 and 50]. REC is taken from Swiss residential gas prices [51]. Energy cost are highest for residential consumers because the individual consumer use less energy in comparison to an industrial consumer.

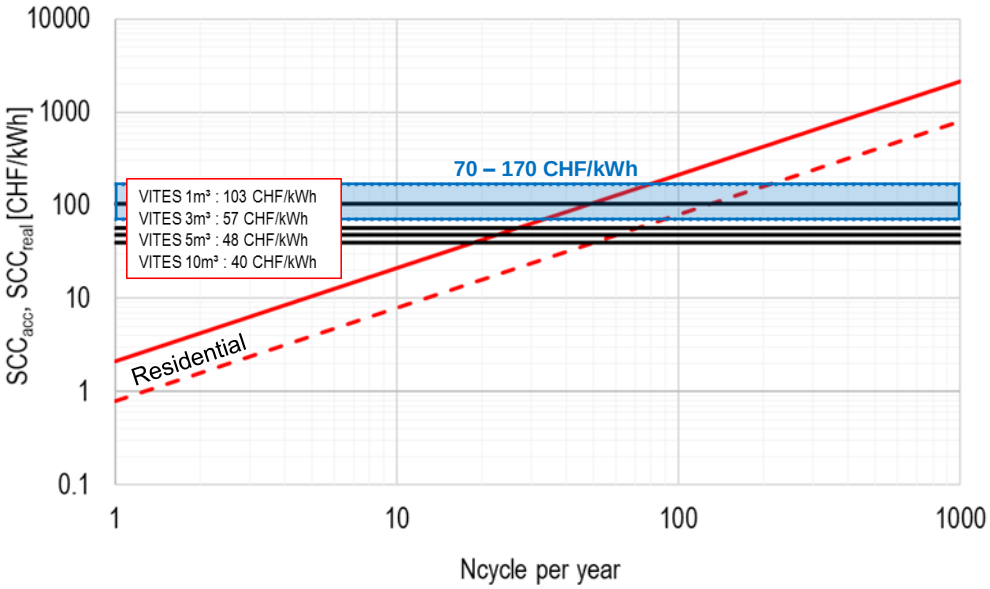

Figure 15 SCC_{acc} for the VITES storage (solid black lines) and SCC_{real} for conventional insulated storages (blue rectangle) for residential applications (i=5%; n=15 years, $REC_{residential}$=0.08-0.15 CHF/kWh). Solid and dashed red lines are the SCC_{acc} theoretical limits for residential sector

5.3 VITES market integrated position

Figure 16 illustrates the potential integrated position of the VITES technology within the current TES market.

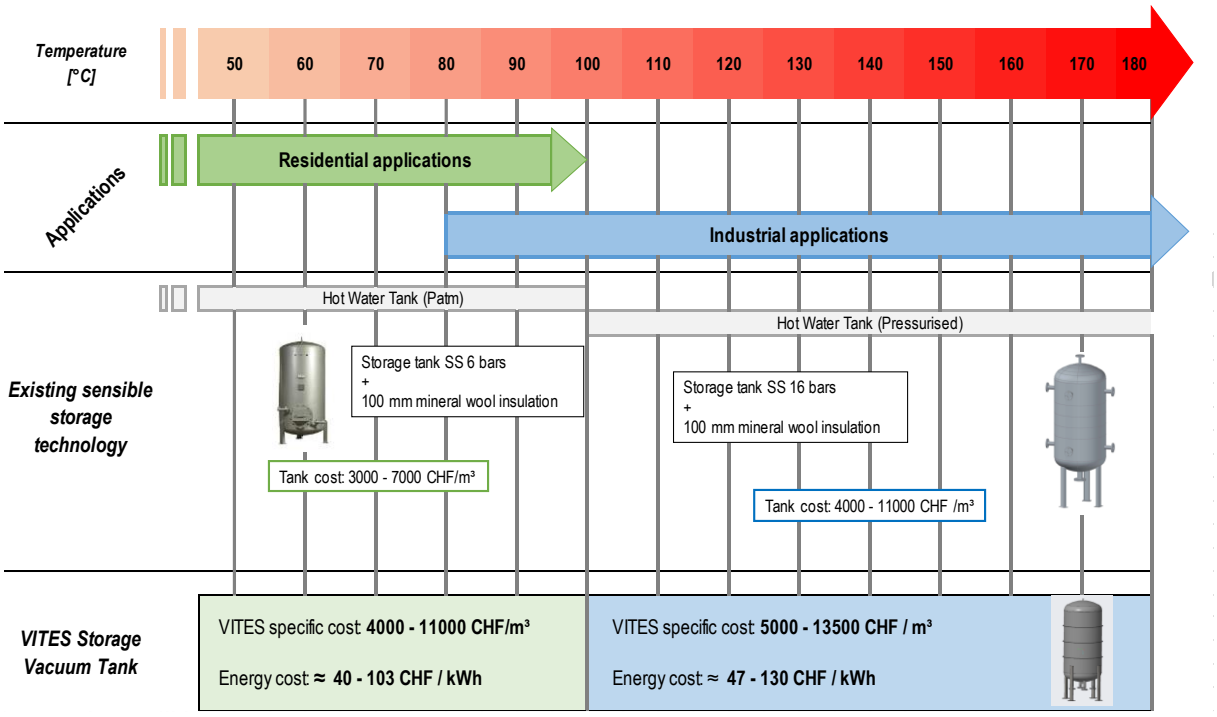

Figure 16 Integrated position of the VITES technology in the current TES market

The cost estimation results have shown the potential for VITES to be integrated in a variety of applications, from residential hot water production to high-temperature industrial processes. Despite a slightly higher cost, VITES storages are shown to be economically competitive or within reach for both industry and residential applications with the additional advantages of moisture protection and reduced heat losses.

6 Simulation analysis

The simulation investigates the VITES tank charged with solar energy for an industrial application and provides comparisons with conventional insulated tanks. The main elements of the simulated system are, therefore, solar thermals collectors, the tanks (VITES and conventional insulated) and the heating loads. The final objective of the simulation is to provide the potential gains of the VITES concept under different operating conditions for the investigated case study. Since the main application envisaged for the VITES tank is in the industrial sector, it was decided to focus on this case and simplify the calculation of the required energy gains in the residential sector, see section 7.2.

6.1 Simulation environment

The reference conditions and the simulation environment for the annual simulations of the VITES tank for an industrial application under the Swiss climate are described here. A first numerical modelling of the VITES and conventional insulated tanks is developed followed by the annual simulations of the overall system under different conditions for different solar thermal system sizes. The simulations were carried out in TRNSYS 17 [52] with standard components or with validated, well-known third-party models. The reference weather conditions are taken from the Meteonorm package provided with TRNSYS for the city of Bern-Liebenfeld.

6.1.1 VITES and conventional insulated TES numerical model

Both VITES and conventional insulated tanks were modelled with the standard TRNSYS type 60. This type models a stratified tank with a certain numbers of nodes here set arbitrary to 50. The thermal losses are calculated for each node *i* according to equation:

$$q_{loss,i} = (U_{loss} + \Delta U_i)\, A_{s,i}\, (T_{env} - T_i)$$

ΔU_i accounts for the insulation disparity along the tank and is neglected in this study. $A_{s,i}$ is the storage surface area for node *i*. The heat loss coefficient, $U_{loss,}$ is a parameter and cannot be changed so it remains constant for the whole simulation. This means that U_{loss} cannot be expressed as a function of a variable temperature and needs therefore, to be linearised at a fixed temperature. The linearisation method such as described in [44] is not applicable for high temperature. To estimate the thermal losses of the VITES tank at temperature higher than 100°C, the ambient temperature T_{env} is modified with the introduction of an offset parameter τ_{offset} which is added to the actual ambient temperature T_{amb} where the storage is installed. The following equations described this model:

$$Q_{loss,i} = U_{loss}\, A_{s,i}\, (T_{env} - T_i)$$

with

$$U_{loss} = 4\sigma\, T_m^4 \left(\frac{1}{1/\varepsilon_1 + 1/\varepsilon_2}\right)$$
$$T_{env} = T_{amb} + \tau_{offset}$$

For the considered application, storage temperatures between 100°C and 180°C are foreseen, it was then chosen to calculate U_{loss} from a mean temperature T_m of 140°C and the specified emissivity of the considered coating (ε_1, ε_2) . τ_{offset} is identified by minimising the relative error between the linearised model and theoretical radiative losses given in section 4.2.1.

Figure 17 shows nonlinear theoretical heat losses compared to the linear relation presented above and the error in temperature range of 100 °C to 180 °C. It is seen that the error is smaller than ±5% and therefore acceptable for numerical estimation of the thermal losses of the VITES concept.

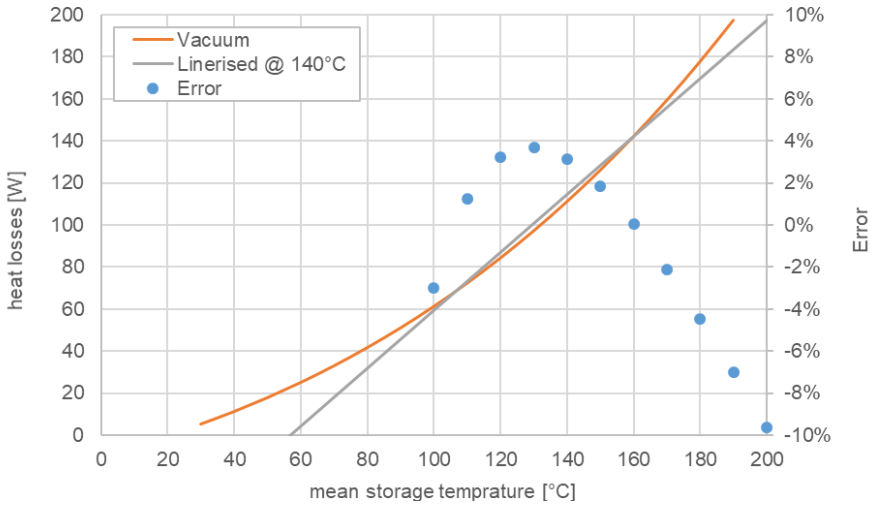

Figure 17 Comparison of the detail radiative losses calculation with the linearised model at 140°C

The tank upscaling method induces a change in the overall heat loss coefficient U_{loss} for conventional insulated tanks. For the latter, a change of 6% was calculated, whereas the difference for the VITES tank was smaller than 1%. Therefore, in order to carry out investigations on the different solar plant sizes, a regression model was developed based on a simplified calculation of U_{loss} for four different tank volumes and for the two quality of insulations considered here. Table 10 and Figure 18 present the calculation for the well-insulated tank.

Table 10 Geometric characteristic of the conventional tank and the calculation of the overall heat loss coefficient for the well-insulation tank

Tank volume	litres	1000	3000	5000	10000
Equivalent tank height (interior)	m	1.63	4.89	8.15	16.29
Inner diameter	m	0.884	0.884	0.884	0.884
Cylinder area	m²	4.525	13.575	22.624	45.249
Bottom and top areas	m²	0.614	0.614	0.614	0.614
Cylinder linear heat loss coef.	W/m K	1.189	1.189	1.189	1.189
Bottom and top heat loss coef.	W/m² K	0.385	0.385	0.385	0.385
Thermal losses calculation					
Cylinder thermal losses	W	271	814	1356	2713
Bottom and top thermal losses	W	99.4	99.4	99.4	99.4
Total heat losses	W	371	913	1456	2812
Inner surface specific heat losses	W/m²	64.4	61.7	61.0	60.5
Overall heat loss coefficient	W/m² K	0.460	0.441	0.436	0.432

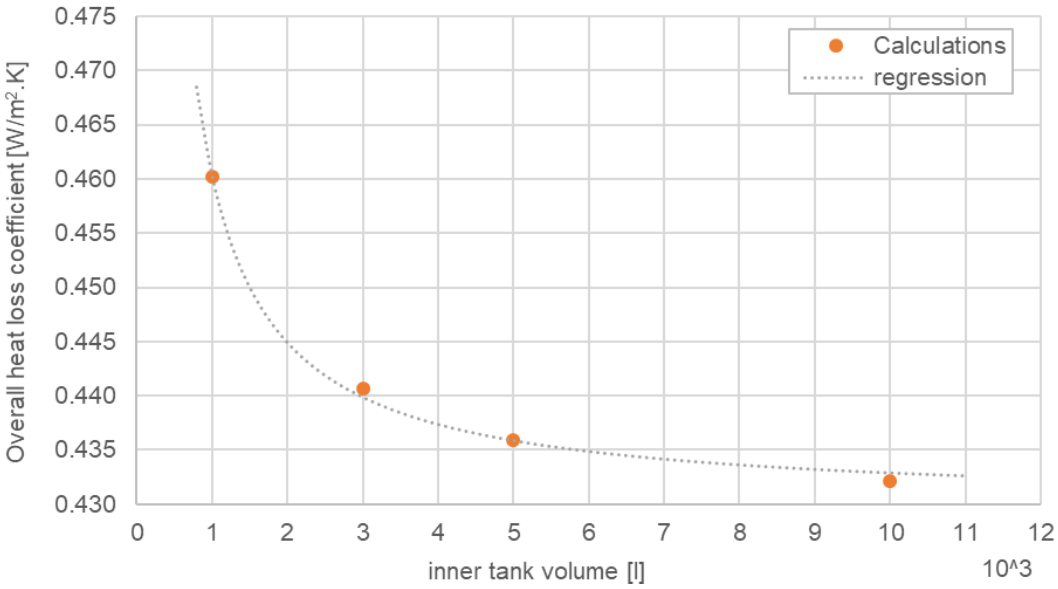

Figure 18 Evolution of the overall heat loss coefficient of the conventional insulated tank in function of the tank size

U_{loss} is related to the tank volume V by an inverse exponential function of the form :

$$U_{loss} = a\, e^{b/V}$$

The coefficient a and b where identified with a python script for the two conventional insulations (k is the conductivity value), see Table 11.

Table 11 Summary of the tank parameters for the regression of the overall heat loss coefficient

	a [W/(m².K)]	b [l⁻¹]	SSE[2] [W/(m².K)]
Well-insulated tank (*k*=0.04 W/m K)	4.299e^{-1}	6.879e^{-2}	8.3e^{-6}
Low-insulated tank (*k*=0.06 W/m K)	6.338e^{-1}	6.822e^{-2}	9.3e^{-6}

6.1.2 Solar Collectors

The solar collectors are modelled with the TRNSYS third party model Type 832 [52]. Compared to a standard collector model, this type is discretised in the flow direction and reproduces very well the transient behaviour of the collector at start-up. The chosen collector is the MT-Power v4, currently commercialised by [45], see characteristics in Table 12.

Table 12 Parameters of the MT-Power v4 solar collector according to the Solar Keymark Certificate 011-7S1890F

Collector: TVP Solar – MT Power v4			
Zero-order efficiency	η_0	0.737	[-]
First-order heat loss coefficient	c_1	0.504	[W/(m²K)]
Second-order heat loss coefficient	c_2	0.006	[W/(m²K²)]
Incidence angle modifier of diffuse radiation	K_d	0.957	[-]

6.2 Description of the case study

To evaluate and compare the performances of the VITES tank in industrial applications, a case study was defined from literature data. Figure 19 show a simplified hydraulic scheme of the chosen process and the integration of a solar thermal system. The integration of the solar heat is implemented at the process level with a preheating strategy. This means that the heat exchanger (HX) is placed before the conventional one, this latter will deliver the rest of heat needed for the process. The solar system is set to work between 128°C and 180°C with storage temperatures between 100°C and 180°C.

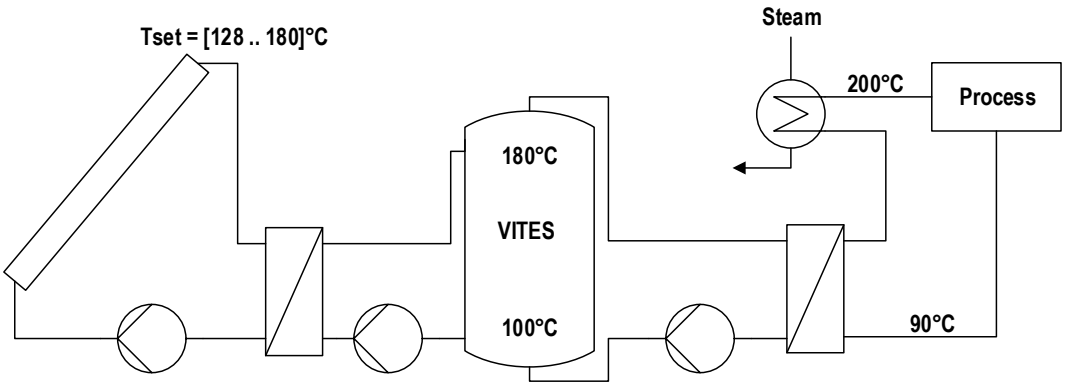

Figure 19 Simplified hydraulic scheme of the solar thermal system and integration into the industrial process

[2] sum squared error

The investigation is focused on the TES with the simulation of three different type of tanks:

1. The VITES concept as presented before in section 4.
2. A well-insulated tank with 10 cm of mineral wool with a conductivity of 0.04 W/m K
3. A low-insulation tank with 10 cm of humid mineral wool with a conductivity of 0.06 W/m K

In order to analyse the performances of the storage and investigate up-scaling capabilities, four different solar system sizes are investigated for the same process and for a constant TES capacity to solar collector area ratio of 50 litre/m^2. This means that for the given process, four different solar fractions are obtained.

6.2.1 Process and Load Profile

The process considered is a spray dryer in the food and beverage industry using humid air as the HTF, with a required temperature of 200 °C. The HTF leaves the spray drier at 100 °C and is then regenerated with fresh air at 25 °C reducing the temperature further to 90 °C corresponding to a HTF recirculation factor of 87%. The process was designed according to the tank volumes investigated in the project. This resulted in a daily energy consumption of 159 kWh and a nominal heat flow rate of 10 kW. Table 13 gives a summary of the process characteristics.

Table 13 Characteristics of the spray drying industrial process

High temperature process			
Industry		Food & Beverage	
Process		Spray dryer	
Profile type		Constant	
Heat transfer fluid (HTF)		air	
Daily consumption	E_p	159	kWh
HTF thermal capacity	Cp_p	1017	J/kg K
HTF density	ρ_p	0.83	kg/m^3
Inlet process temperature	$T_{p,e}$	200	°C
Return process temperature	$T_{p,s}$	90	°C
HTF mass flow rate	$\dot{m}_p$	320	Kg/h
Process nominal heat flow rate	P_p	10.0	kW

The process is modelled with an hourly load file where the required flow rate and temperature are defined. The process runs 24 hours per day and 7 days a week with the profile given in Figure 20. The process schedule was adapted to stress the solar thermal system with short pauses (1h) during the day, specifically between 12:00 and 13:00 where high solar production is expected. The process HX heat transfer coefficient is set to 3000 W/K for every case and corresponds to a LMTD of 3 K.

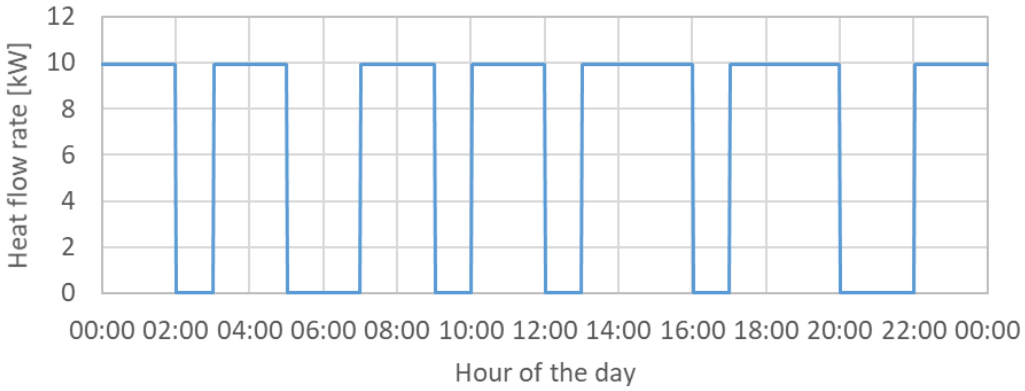

Figure 20 Daily hourly profile of the spray drying industrial process

6.2.2 Solar field and TES sizing

Given a maximum temperature of 180 °C for the solar heat provided to the process and a return flow at 100°C, the maximum heat flow covered by the solar field falls roughly under 80% taking into account the HX pinch of 5 K. From the mean absorber temperature of 145 °C, the specific peak power of the TVP solar collector is 379 W/m² for an ambient temperature of 30 °C. In order to cover 80%, e.g. 8 kW of the process heat flow rate, the area of the solar field is estimated to be around 20 m² for an irradiance of 700 W/m². The collector loop design conditions are presented in Table 14 .

Table 14 Design conditions of the solar field

Collector loop		
Design Irradiance on collector	700	W/m²
Mean absorber temperature	145.00	°C
Fluid temperature difference	80.00	°C
Heat capacity of the heat transfer fluid	2.319	kJ/(kg.K)
Density of heat transfer fluid	784.6	kg/m³
Specific heat rate @ Tamb = 30 °C	379	W/m²
Collector efficiency for Tamb = 30 °C	0.541	-
Aperture area	20	m²
Specific flow rate	7	kg/(h.m²)

For every case, the hot water tank is sized with a constant specific volume of 50 litre/m². To investigate other solar fractions, the storage and solar field is enlarged to the investigated storage volumes of 1, 3, 5 and 10 m³. For each solar field, the overall heat transfer coefficient of the HX is calculated according to the following equation [53]:

$$UA_{HX,c} = (88.561 * A_c + 328.19)$$

Table 15 summarises the parameters for the four solar field sizes investigated during the simulation work. The information on the peak power is given for an irradiance of 700 W/m² on the collector plane and for a temperature difference of 115 °C ($T_{collectors}$ = 145 °C, T_{amb} = 30 °C). The mean summer daily

solar production is an estimated value taken from May to August to evaluate the size of the field compared to the daily consumption of the process (149 kWh). This shows that for tank sizes of 5 and 10 m³, the system is oversized and the production of an average summer day is superior to the daily needs of the process.

Table 15 Summary of the characteristics of the sizing of the solar field as a function of the tank size

Storage volume	**m³**	**1**	**3**	**5**	**10**
Solar field	**m²**	20	60	100	200
Peak power @ (700 W/m²; 115 °C)	**kW**	7.6	22.7	37.9	75.7
Mean summer daily production	**kWh**	44	133	221	442
$UA_{HX,c}$	**W/K**	2099	5642	9184	18040

6.2.3 Control strategy

The solar field is controlled with an ON/OFF controller and a variable flow controller in the collector and secondary loop. The ON/OFF controller switch the pumps on both sides of the solar HX, while a PID controller sets the flow in the collector loop according to a temperature set point placed at the collector array output. The mass flow of the secondary loop is then set according to the ratio of the HTF thermal capacities.

The ON/OFF threshold of the controller is set according to the temperature set point of the collector output and a dead band of 7 K. Figure 21 gives an example of the function of the ON/OFF controller for a collector set point of 130 °C. Since the set point takes into account a relatively large pinch for the HX, the cut-off threshold is set to 5 K under the set point and the switch-on to 2 K over it.

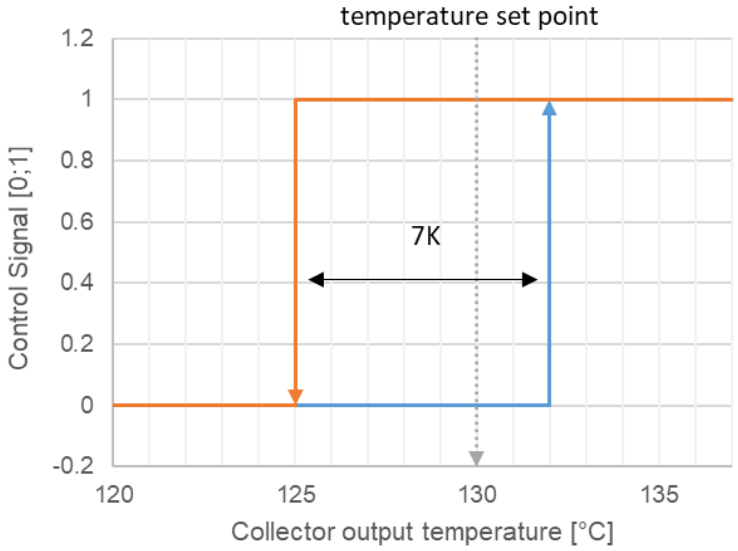

Figure 21 Example of the function of the ON/OFF controller for the solar pump

In order to maximise the solar production, the collector output temperature set point is variable according to the tank temperature placed at a relative height of 0.82. The function is given in Figure 22, the upper

bound is the maximum temperature given by the collectors' manufacturer and the lower bound corresponds to the temperature set for the discharge of the tank, 120 °C, plus 8 K to account for the pinch of the HX.

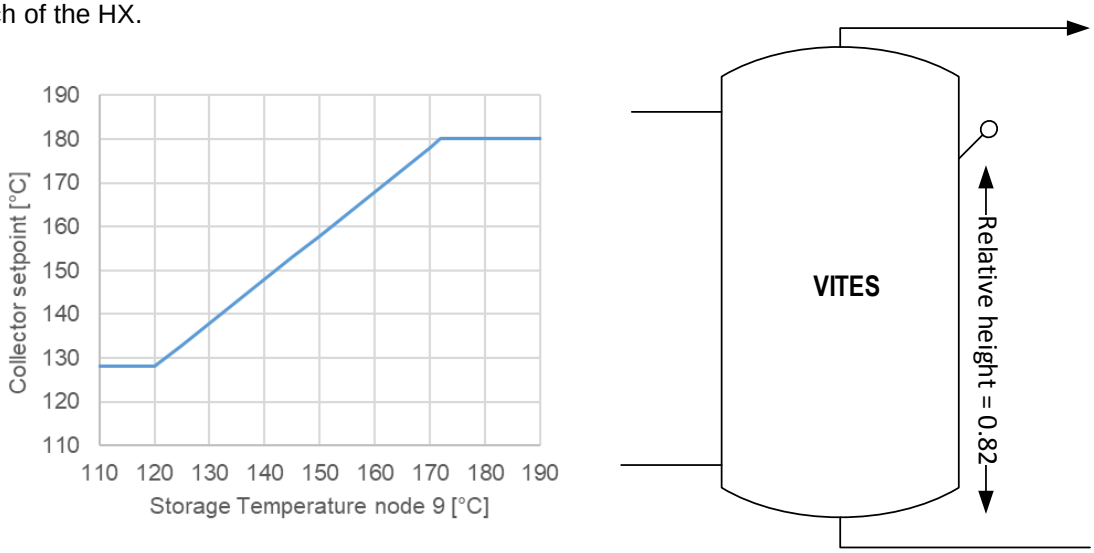

Figure 22 Output collector set point as a function of the storage temperature

The discharge of the tank is controlled with the same temperature sensor, the switch-on and cut-off thresholds are set to 120 °C and 100 °C, respectively.

6.3 Simulation results

Simulations were run according to the parameters defined above in 6.1. The results were processed with a python script to obtain yearly and monthly energy values. Moreover, two indicators are used to analyse the results, the solar fraction f_{sol} and the TES efficiency η_{TES}, given in the following equations:

$$f_{sol} = \frac{Q_{sol}}{Q_{sol} + Q_{stm}}$$

$$\eta_{TES} = \frac{Q_{TES,out} + \Delta Q_{int}}{Q_{TES,i}}$$

The solar fraction is the ratio of the solar field energy yield Q_{sol} over the sum of solar yield and the steam consumption Q_{stm}. As for the TES efficiency, it is the ratio of the total energy discharged from the TES $Q_{TES,out}$ corrected by the internal energy change between the start and end of the simulation ΔQ_{int} over the total energy supplied to the tank $Q_{TES,in}$.

Figure 23 presents on the left the solar fraction and on the right the TES efficiency as a function of the tank volume and for three tank insulation solutions: VITES, conventional low-insulated tank (k=0.06 W/m K) and conventional well-insulated tank (k=0.04 W/m K). It can be seen that VITES presents high TES efficiency with values as high as 0.9 while the conventional insulated tanks have efficiency below 0.74.

Thanks to the improved insulation capacity of the VITES tank, the energy savings lead to higher solar fractions, meaning that the avoided losses are used to supply the process with solar thermal energy. As expected, the efficiency of the storage decreases when the system size is increased. However, this

decrease is less pronounced in the case of the VITES tank meaning that high solar fractions can be reached without increasing significantly the heat losses of the system.

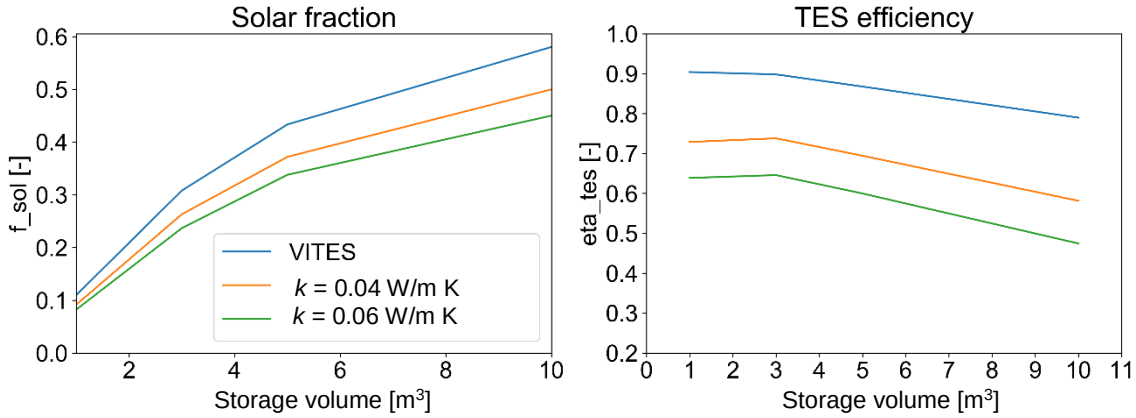

Figure 23 Solar fraction (left) and TES efficiency (right) as a function of the volume of the tank and for the three tank insulation solutions: VITES, conventional low-insulated tank (*k*=0.06 W/m K) and conventional well-insulated tank (*k*=0.04 W/m K)

Figure 24 shows that the monthly mean storage temperature according to each system size for the VITES tank on the left and the low-insulated conventional tank on the right. For the 1 m³ tank the monthly mean temperature is low, around 100°C, which is the cut-off threshold for the tank discharge. This indicates that most of the solar heat is consumed directly and that very little is stored from one day to another.

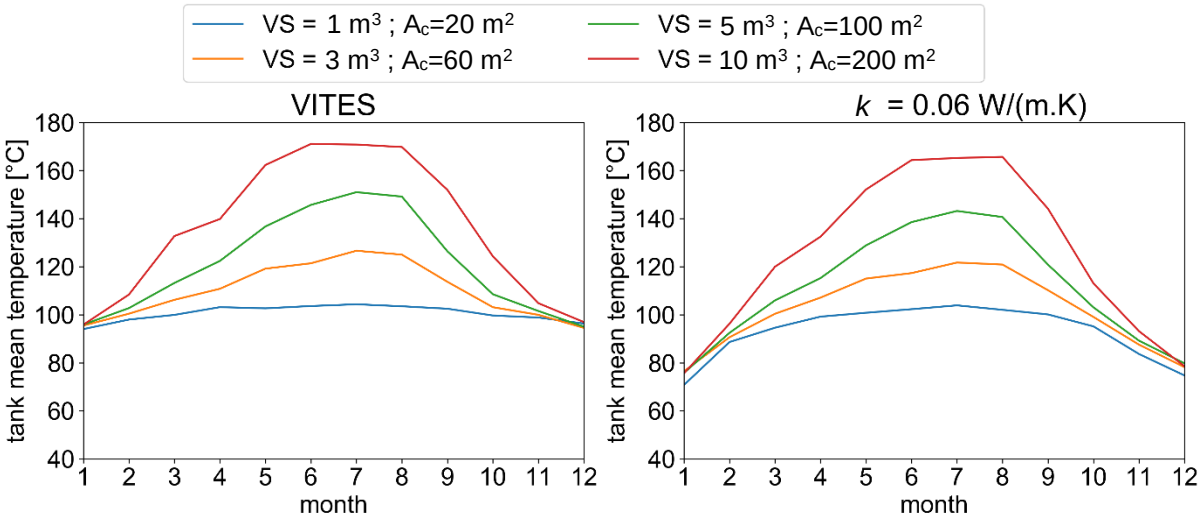

Figure 24 Monthly mean storage temperature according to each system size for the VITES tank (left) and for the low-insulated conventional tank (right)

For systems with higher solar fractions (larger solar fields and storage capacities), the VITES tank reaches higher temperatures with the largest difference occurring in the winter period as it can be seen in Figure 25 for a storage size of 3 m³. VS stands for storage volume and A_c for collector field surface area.

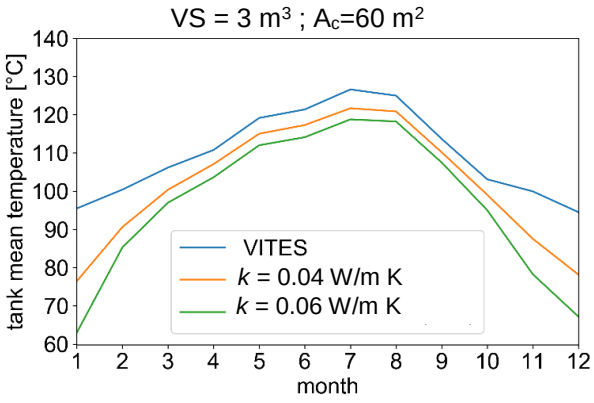

Figure 25 Monthly mean storage temperature for a TES capacity of 3 m^3 and for the three tank insulation solutions: VITES, conventional low-insulated tank (k=0.06 W/m K) and conventional well-insulated tank (k=0.04 W/m K)

Figure 26 presents the evolution of the heat losses of the three considered tank insulation solutions as a function of the storage volume. As expected, the VITES tank shows the lowest losses. When compared with the conventional insulated tanks, the heat losses are reduced by 65 to 75% according to the conventional insulation level, high and low, respectively.

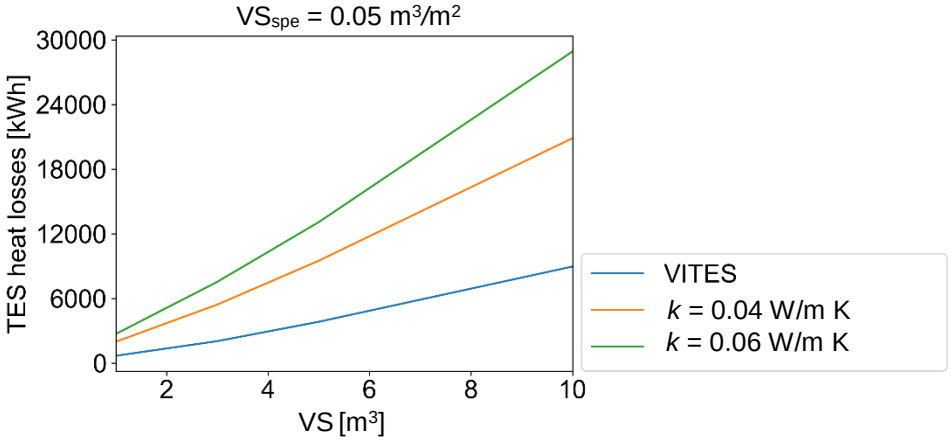

Figure 26 Evolution of the yearly heat losses of the three considered tanks

In conclusion, the VITES tank performs better than the conventional insulated tanks considered in this study. The improved insulation ability substantially reduces the losses, which translates into higher TES efficiencies and solar fractions. As the consumption is constant on a daily basis, the stored solar energy is directly discharged, thus the storage period is relatively short but it allows a high number of cycles. If the process is scheduled over half a day and mismatch from the solar resource, the VITES concept will perform even better than for the case study presented here. This could open the way to new applications for solar thermal systems and therefore the increase in the share of renewable energy use.

7 Economic considerations

The economic feasibility of the VITES concept was evaluated by comparing the payback period of the VITES technology against that of a conventional mineral wool insulated tank. For market deployment, it is essential to rank the VITES concept to determine its investment attractiveness with respect to the common TES alternatives on the market.

The payback period is a common investment evaluation and a quick ranking measure to gauge the cost-effectiveness of competing technologies. It calculates the length of time required to recover the initial or additional investment through savings generated by the investment. For TES, it provides the level of profitability of a TES technology in relation to time. The shorter the payback period, the better.

The payback period is calculated by dividing the additional investment (over cost) of VITES by the cost of the annual energy savings computed from the simulations. The energy savings are specific to the application and depend on the energy demand (amount and profile).

7.1 Economic viability for industrial applications

To assess the economic viability of the VITES tank, simulation results from section 6 as well as the cost of the VITES tank for industrial applications, estimated in 5.1, was used. The payback period calculation was performed comparing the VITES tank to a conventional storage tank with the same size and using mineral wool as insulation material. The influence of humidity in the insulation of the conventional tank was also taken into account.

7.1.1 Summary of the industrial process simulation results

As a reminder, the integration scenario is the preheating of a spray drying process with a solar thermal system, with a typical storage capacity ratio of 1 m³ for 20 m² of solar collectors, see Figure 19 . In this case, TES is useful to buffer the solar heat when the process is in stand-by.

Table 16 summarises the simulation results for the expected annual energy savings for the VITES storage for the four volume capacities investigated in this study.

Table 16 Expected annual energy savings for VITES as a function of the storage capacity

	Storage capacity (m³)	**1**	**3**	**5**	**10**
Annual energy saving (kWh)	VITES vs. humid mineral wool insulated tank	1593	4135	5541	7557
	VITES vs. mineral wool insulated tank	1048	2611	3567	4668

As expected, results show that larger energy savings are expected in cases where the insulating ability of the mineral wool is reduced due to moisture.

7.1.2 Swiss reference energy cost

Computing the resulting saving costs from the annual energy savings, requires knowledge of the actual costs of energy from the Swiss industrial market. These values besides varying with location are also expected to change over time. To evaluate the impact of the evolution of the Swiss industrial REC, three

different scenarios are considered based on average Swiss industrial gas prices and takes into account the efficiency of the gas-to heat supply loop. The first scenario corresponds to the Swiss actual average REC (0.07 CHF/kWh). The second scenario (0.1 CHF/kWh) corresponds to an upper limit of the actual Swiss REC and the third one (0.13 CHF/kWh) accounts for an enthusiast scenario where fossil energy becomes expensive.

The corresponding VITES annual cost savings for the three REC scenarios are presented in Table 17 when compared with a low-insulated (humid mineral wool) insulated tank.

Table 17 Dependence of the annual cost savings on the REC scenarios (VITES vs. low-insulated tank)

	Storage capacity (m³)	**1**	**3**	**5**	**10**
Annual cost saving (CHF)	Actual average Swiss REC (0.07 CHF/kWh)	112	289	388	529
	Upper limit of actual Swiss REC (0.1 CHF/kWh)	159	413	554	756
	Enthusiast scenario for Swiss REC (0.13 CHF/kWh)	207	538	720	982

7.1.3 VITES over cost estimation

The estimated VITES over cost in comparison to a conventional insulated storage was calculated in 5.1 using the investment cost evaluation method.

Table 18 presents a summary of the over cost obtained for the four volume capacities investigated in this study.

Table 18 Over cost estimation from the investment cost evaluation method (cf. 5.1)

Storage capacity (m³)	**1**	**3**	**5**	**10**
VITES investment cost (CHF) (*cf.* 5.1)	**13576**	**22314**	**29744**	**48850**
VITES estimated over cost (CHF)	2643	3748	5395	8412

7.1.4 Economic analysis for industrial applications

As previously mentioned, the payback period is calculated by dividing the VITES over cost by the annual cost savings. To illustrate the case, Figure 27 presents a comparison between VITES and a low-insulated (humid mineral wool) tank based on the actual average REC scenario. Solid lines indicate the over cost of VITES for different storage capacities while dotted lines the cumulative cost savings.

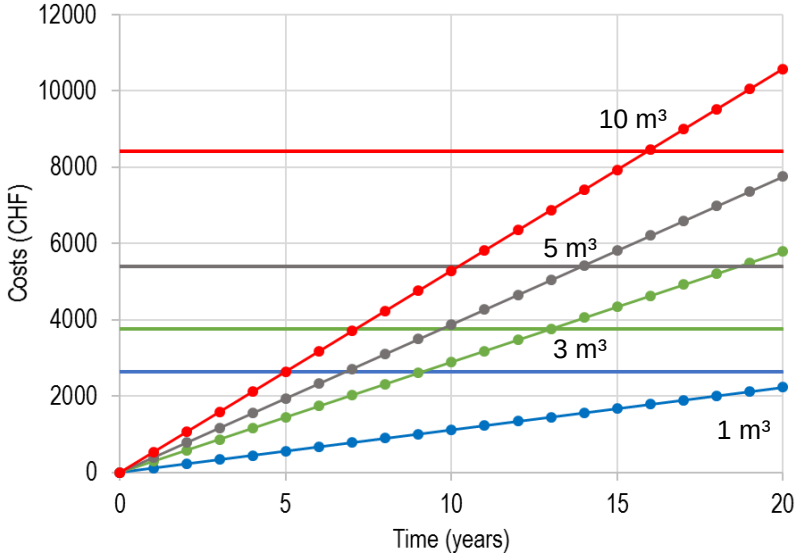

Figure 27 Payback time as a function of the storage capacity and based on the actual average REC (VITES vs. low-insulated tank) Solid lines indicate over cost and dotted lines cumulative cost savings

Results show clearly the dependence of the payback period with the storage capacity. For example, for a 10 m³ the estimated payback time is nearly 16 years while a 1 m³ results in over 20 years.

The variation of the payback time with storage capacity also suggests an optimum storage capacity for the investigated industrial process where the payback period is minimum, see Figure 28. Solid lines correspond to humid mineral wool and dashed lines to normal dry mineral wool insulation. Coloured lines account for the three Swiss REC scenarios: blue for actual average REC, grey for the upper limit REC and red for enthusiast scenario (*cf.* 7.1.2).

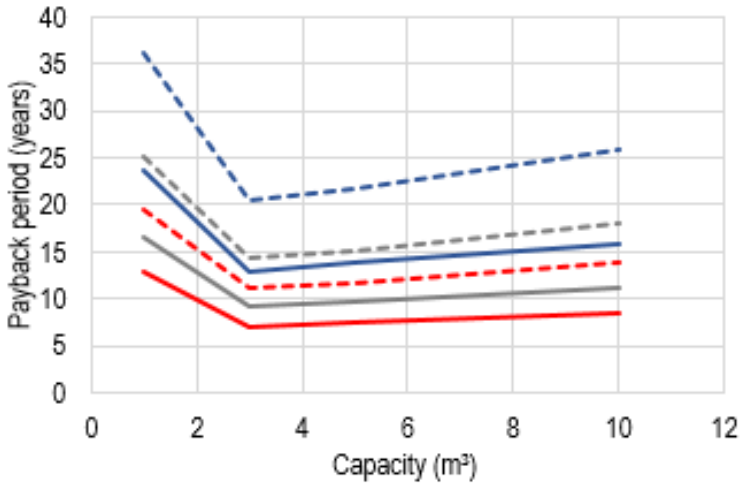

Figure 28 Economic optimum of the payback period for the investigated industrial process comparing VITES with conventional insulation (solid lines: humid insulation and dashed lines: dry insulation) for three Swiss REC scenarios; actual average REC (blue solid/dashed line), upper limit REC (grey solid/dashed line) and enthusiast scenario (red solid/dashed line)

The variation is U-shaped, the payback period declines with capacity up to 3 m³ (minimum) after which rises less steeply. The economies of scale seem to be more effective up to 3 m³, capacity beyond which the payback time starts to increase. This suggests that a capacity between 3 to 5 m³ is the adequate storage dimensioning for the specific industrial process investigated. Here, the payback period is relatively long (13 years) when considering low-insulated tank in the actual REC scenario. The use of conventional tanks with low insulating materials, shifts the curves downwards because the resulting energy savings are also more significant. It is clear that the closer the energy savings are from the over cost, the more interesting the technology investment becomes.

Overall, in this case, the investment is not interesting as the payback period is not below 5 years, value commonly found in the industry sector. In general, the higher the REC, the lower the payback time for a given storage capacity. Apart changes in the REC, other ways to obtain short payback periods are to reduce the over cost or benefit from financial incentives to promote high efficiency TES.

7.2 Economic viability for residential applications

The payback period for residential MFH for DHW applications was computed in a similar way. However, as previously mentioned, the energy savings values were obtained in a simplified manner from the annual DHW load and assuming average efficiencies of 80% and 90% for the conventional and the VITES tanks, respectively. The reference residential case is a two storey MFH with three flats per storey. The overall effective heating floor area of the building is 920 m². The annual DHW load of 20.8 kWh/m² was taken from SIA 380/2016. The resulting energy savings amount to 2658 kWh.

For this application, the over cost estimated in section 5.1 for 1 m³ stainless steel tank pressurised at 6 bar is about 3700 CHF. The payback period is presented in Table 19 for three residential REC scenarios in a similar approach to the one used for industry. Swiss residential gas prices are taken from [51].

Table 19 Payback period of the VITES tank for MFH DHW applications

Energy cost (residential)	Payback period
0,08 CHF/kWh	17 years
0,10 CHF/kWh	13 years
0,15 CHF/kWh	9 years

The payback period is seen to be within the range of acceptable residential values, usually between 15 to 20 years. For this type of application, the investment is considered good as the recovered investment cost is less than 20 years for all REC scenarios.

8 Key findings

The main findings of this project are presented here:

Literature review

- ✓ large number of studies related to TES developments are available in the open literature, in particular research on insulation solutions
- ✓ No study fully addressed the vacuum insulation concept investigated in this project

Concept design (structural and thermal analysis)

- ✓ final external design close to that of typical mineral wool insulated TES on the market to minimise the eventual additional costs of a new insulation concept
- ✓ final design structurally suitable for high temperature applications (up to 180 °C)
- ✓ 50 to 70% radiation loss reduction for low emissivity coatings applied to the walls of the evacuated gap when compared to conventional well and low insulated (moisture affected) TES, respectively
- ✓ customised design of key components: flat spring spacers and supports to minimise thermal bridges (less than 15% of total losses at 160 °C)

Cost estimation

- ✓ costs higher (19%) for the VITES tank in comparison with existing conventional insulated TES on the market
- ✓ advantages of scale identified as specific costs progressively reduce as the size of the store increases
- ✓ storage capacity costs within the range of acceptable SCC for both industry and residential applications (according to Task42/Annex29)

Simulation results for a specific industrial application

- ✓ VITES has higher efficiency than conventional insulated tanks, up to 0.9 compared to 0.74 at yearly storage temperature of 110 °C
- ✓ the solar fraction can be increased by 20%
- ✓ the solar heat supply for VITES in Winter and interseason (from October to March) can be increased by up to 70%

Economic considerations

- ✓ for the investigated industrial application, the investment is currently not interesting with payback values well over the acceptable 5 years

- ✓ for residential applications, the investment is considered good with payback periods in line with acceptable values from Task42/Annex 29 (15 to 20 years)

9 Conclusions

The technical feasibility and the economic viability of a high performance, vacuum insulated sensible thermal energy storage tank was investigated for uses in the industrial and residential sectors.

The literature review indicates that despite a considerable amount of research activities related to reducing TES heat losses, no concept has so far fully investigated the feasibility of using a vacuum annular gap without filling materials as insulating TES concept.

From the structural point of view, VITES was developed to ensure adequate strength for the design loadings (resistance and deformation analysis) and the buckling safety (stability analysis) while minimising heat losses. Design loadings comprise the pressure loads: internal (16 bar) and external (1 bar) and mechanical loads present on the tank due to the weight of the structure and of the inner fluid. Through careful design, the preliminary problematic plastic deformation found at the bottom end cap and at the pipes welding was eliminated. The tank design evolved then, progressively, to externally resemble conventional storage tanks on the market, for adequate comparisons and costs reduction purposes. From this study, the selected design was found to be structurally suitable and the design safe for the required high temperature applications with all tank stresses and stability factors found to remain within the limits.

To improve the insulating capability of the concept beyond the integrated vacuum technology, the use of reflective, low emissivity, coatings on the inner wall of the evacuated gap, was found to improve substantially the radiation losses. For the nominal operating temperature of 160 °C, thermal losses reductions from 40% to 75% were predicted in comparison with conventional well-insulated and low-insulated (humid affected) storage tanks, respectively. Thermal bridges due to piping, fittings and spacers, initially accounted for nearly 20% of the losses at 160 °C, were reduced through a customised redesign of spacers and supports to reach less than 15%.

Scalability of the investigated VITES concept was also investigated. Size and cost of current baking ovens for vacuum processes were found to set the maximum storage capacity for VITES to 10 m^3. To maintain and inspect the high vacuum level (<0.001 mbar) over the entire lifetime of the tank, a patented and compact getter-pump is used. This proven technology has been used for more than 10 years in a high-vacuum flat solar collector on the market.

In terms of investment cost, the major fraction is associated to the materials and manufacturing of the inner and outer tank. The vacuum technology, often considered expensive, accounts for less than 1% of the overall VITES investment cost. In both investigated applications, the slightly higher cost of VITES still places it as an interesting cost-effective technology with the additional advantage that VITES is moisture protected and has lower heat losses. In addition, the advantages of scale were clearly shown with specific costs progressively reduced as the size of the store increased.

The economic assessment of the VITES technology according to the Task 42/Annex 29 methodology provided additional economic arguments where the investment cost was found not to exceed the application related, maximum acceptable storage capacity cost. Overall cost estimation results have shown the potential for VITES to be integrated in a variety of applications, from residential hot water production to high-temperature industrial processes.

Simulations indicate that for the specific industrial application, the VITES tank performs better than the conventional insulated tanks considered in the study. The improved insulation ability substantially reduces the losses, which translates into higher TES efficiencies and solar fractions.

The economic viability of VITES evaluated through the payback period, revealed that for industry applications, the investment is currently not interesting with values well over 5 years but is still within reach. As for residential applications, the estimated values are quite interesting, all under the usual 20 years.

Overall, this study clearly indicates the viability of the VITES concept not only in terms of technical feasibility but also in terms of economic practicality. The key advantages of VITES are:

- the wider range of applications (up to 180 °C);
- the vacuum reliability through the use of a robust getter pump, a proven technology in high temperature commercialised solar collectors;
- the intrinsic moisture protection capability;
- the reduced heat losses through suppression of conduction and convention heat transfer and reduced radiation due to low emissivity coatings in the evacuated gap;
- the estimated cost that makes it quite competitive in comparison to conventional insulation TES and to other vacuum insulation solutions

The research should therefore pursuit to validate the performed technical and economic analysis. Potential reductions of the radiative component as well of the thermal bridges should be further investigate based on experimental results. The final characteristics of the inlet/outlet system should also be defined and the stratification process studied for a better characterisation of the VITES tank.

10 References

[1] Energy Strategy 2050 once the new energy act is in force, OFEN document (2018)

[2] Energy for the future. Highlights from three years of research at the Swiss Competence Centers for Energy Research (SCCERs). Topic report (2017)

[3] Statistique globale suisse de l'énergie, OFEN (2017)

[4] Analyse des schweizerischen Energieverbrauchs 2000-2018 nach Verwendungszwecken, OFEN (2019)

[5] Heat and cooling demand and market perspective, Pardo, N., Vatopoulos, K., Krook-Riekkola, A., Moya, J.A. and Perez, A., Publications Office of the European Union (2012)

[6] Federal Energy Research Masterplan for the period from 2017 to 2020, CORE (2015)

[7] ECES Annex 30: Thermal Energy Storage for Cost-effective Energy Management and CO2 Mitigation. www.eces-a30.org

[8] Task 58/ECES Annex 33: Material and Component Development for Thermal Energy Storage. www.task58.iea-shc.org

[9] A review and evaluation of thermal insulation materials and methods for thermal energy storage systems, Villasmil, W., Fischer, L.J. and Worlitschek, J., Renew. Sustain. Energy Rev. 103 (2019)

[10] The energy technology systems analysis programmes (ETSAP): Technology Brief E17, IRENA (2013)

[11] Industrial waste heat: Estimation of the technically available resource in the EU per industrial sector, temperature level and country, Papapetrou, M., Kosmadakis, G., Cipollina, A., La Commare, U. and Micale, G., Applied Thermal Engineering, 138, pp:207-216 (2018).

[12] Potential for adsorption technology and possible applications, Padey, P., Pahud, D. and Duret, A., THRIVE SP4 report (2015)

[13] IEA SHC Task 42 / ECES Annex 29 - A simple tool for the economic evaluation of thermal energy storages, Rathgeber, C., Hiebler, S., Lävemann, E., Dolado, P., Lazaro, A., Gasia, J., de Gracia, A., Miró, L., Cabeza, L.F., König-Haagen, A., Brüggemann, D., Campos-Celador, A., Franquet, E., Fumey, B., Dannemand, M., Badenhop, T., Diriken, J., Nielsen, J.E. and Hauer, A., Energy Procedia 91 (2016)

[14] Traditional, state-of-the-art and future thermal building insulation materials and solutions – properties, requirements and possibilities, Jell, B.P., Energy and Buildings 43 (2011)

[15] Vacuum insulated thermals storage in Sengenthal, Fuchs, B., Hofbeck, K. and Faulstich, M., 5th Int. renewable Energy Storage, Berlin (2010)

[16] Heat transport in evacuated perlite powders for super-insulated long-term storages up to 300 °C, Beikircher, T. and Demharter, M., Journal of Heat Transfer 135 (2013)

[17] A review of thermal energy storage technologies and control approaches for solar cooling, Pintaldi, S., Perfumo, C., Sethuvenkatraman, S., White, S. and Rosengarten, S., Renew. Sustain. Energy Rev. 41 (2015)

[18] Energy conservation through energy storage (ECES) programme. IEA Brochure (2016)

[19] Thermal conductivity of vacuum insulation materials for thermal energy stores in solar thermals systems, Lang, S., Gerschitzka, M., Bauer, D. and Drück, H., Energy Procedia 91 (2016)

[20] A comprehensive review of thermal energy storage, Sarbu, I. and Sebarchievici, C., Sustainability 10 (2018)

[21] Vacuum insulation panels – exciting thermal properties and most challenging applications, Fricke, J., Schwab, H., Heinemann, U., Int. J. Thermophysics 27 (2006)

[22] On vacuum insulated thermal storage, Fuchs, B., Hofbeck, K. and Faulstich, M., Energy Procedia 30 (2012)

[23] Vacuum super insulated heat storage up to 400 °C, Beikircher, T., Reuss, M. and Streit, G., Conference paper (2015)

[24] Thermal energy storage with super insulating materials: a parametrical analysis, Fantucci, S., Lorenzati, A., Kazas, G., Levchenko, D. and Serale, G., Energie Procedia 78 (2015)

[25] Vacuum-buffer storage, HummelsbergerStahl-und Metallbau, www.vacuum-storage.com (last accessed July 2019)

[26] ThermosTank Grundlegende Untersuchungen zur Entwicklung eines marktfähigen Wasserwärmespeichers mit Vakuumisolation – Thermoskannenspeicher, Gunczy, S., Enzinger, P., Felberbauer, K-P., Halb, F., Pucker, J., Stiglbrunner, R., Altenburger, F., Fink, C., Hausner, R. and Pink, W., Blue Globe Report, Smart Energies (2012)

[27] Projet Colas : Campagne de mesures : Installation solaire thermique à haute température de Colas Suisse, Bunea, M., Duret, A, Péclat, L, Bornet, P., Maranza, M., Wendling, J.-B and Pauletta, S., OFEN Annual report (2014)

[28] Projet Colas : Campagne de mesures : Installation solaire thermique à haute température de Colas Suisse, Bunea, M., Hildbrand, C., Duret, and Citherlet, S., OFEN Annual report (2016)

[29] The impact of moisture on the thermal conductivity value of stone wool based insulating materials, Chadiarakou, S., Papadopoulos, A.M., Karamanos, A. and Aravantinos, D., 2nd PALENC Conf. and 28th AIVC Conf. Build. Low Ener. Cooling and Adv. Vent. Tech. in the 21st century (2007).

[30] Anwendungen und potenziale von vakuum spalt isolation, Tischhauser, H. and Staufert, G., (2013)

[31] Thermal Energy Storage, Swiss Competence Center for Energy Research, www.sccer-hae.ch (last accessed July 2019)

[32] Euroheat&Power, https://www.euroheat.org/knowledge-hub/district-energy-switzerland, (last accessed July 2019)

[33] IWB, https://www.iwb.ch/Ueber-uns/Projekte/Waermespeicher-Dolder.html (last accessed July 2019)

[34] Agro Energie Schwyz, https://agroenergie-schwyz.ch/energiezentrum/waermespeicher/ (last accessed July 2019)

[35] BFS, https://www.stat20ne.bfs.admin.ch/fr/durabilite.html (last accessed July 2019)

[36] HeatStore project, https://www.heatstore.eu/index.html (last accessed July 2019)

[37] ETH Zurich, https://ethz.ch/en/news-and-events/eth-news/news/2017/01/geothermal-storage-for-our-cities.html (last accessed July 2019)

[38] Department for Business, Energy & Industrial Strategy. Evidence Gathering: Thermal Energy Storage (TES) Technologies. London; 2016.

[39] CETIAT, http://www.recuperation-chaleur.fr (last accessed July 2019)

[40] ANSYS software, www.ansys.com

[41] Materials for high vacuum technology: an overview, Sgobba, S., CERN document (2006)

[42] ASM Material Data Sheet

[43] Tuyauteries. Résistance des éléments – 1 partie, Pitrou, B., BM6720 (2001)

[44] Introduction to Heat Transfer, Incropera, F. and DeWitt, D., Wiley (1985)

[45] TVP Solar, https://www.tvpsolar.com (last accessed July 2019)

[46] TVP Solar, private communication, April 2019.

[47] CTA, https://www.cta.ch/file/file/de/Waerme/liste-de-prix_FR.pdf, p. 89-90

[48] DOMOTEC, https://domotec.ch/wp-content/uploads/2019/05/1.1.2-pl-allgemein-2019-FRA.pdf, pp 1-22

[49] VIESSMANN, https://www.viessmann.ch/content/dam/vi-brands/CH/Preisliste_listedeprix/FR/2018/Vitotec/Register_10_Preisliste%20Schweiz%2008-2018%20CH-FR.pdf/_jcr_content/renditions/original./Register_10_Preisliste%20Schweiz%2008-2018%20CH-FR.pdf, p. 10.6-2 and 10.6-14

[50] ELCO, http://elcoshop.ch/catalog/data/b1600/b160021/pdf/catalog.pdf, p. 9.30 and 9.33

[51] Bundesamt für Energie BFE, Ex-Post-Analyse des Energieverbrauchs der schweizerischen Haushalte 2000 bis 2017 nach Bestimmungsfaktoren und Verwendungszwecken

[52] Klein, S. A. et al. (2017) 'TRNSYS 17: A Transient System Simulation Program'. Madison, USA: Solar Energy Laboratory, University of Wisconsin. Available at: http://sel.me.wisc.edu/trnsys

[53] Heimrath, R. and Haller, M., The Reference Heating System, The Template Solar System of Task 32 - Report A2 of Subtask A, IEA SHC Task 32, in IEA SHC - Task 32 - Advanced storage concepts for solar and low energy buildings (2007)

11 Appendix

11.1 Appendix 1: FEA structural analysis report of designs 1 and 2

HAUTE ÉCOLE D'INGÉNIERIE ET DE GESTION DU CANTON DE VAUD
www.heig-vd.ch

Project :	VITES			Version: V2
Subject :	Structural analysis			
From :	COMATEC	To :	TVP Solar	Date :
Author(s) :	Philippe Bonhôte			

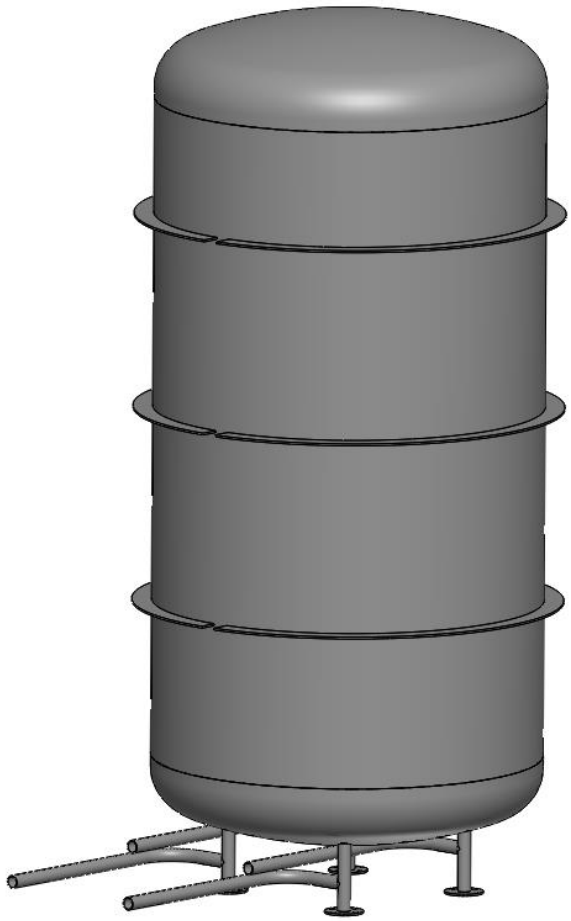

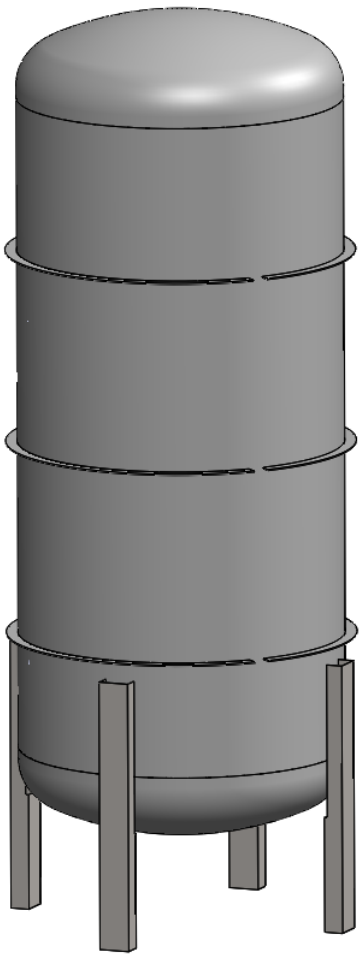

Table of contents

Introduction

This report present the geometry and the structural analysis of a tank under vacuum. This tank is made of two tanks, an inner one to contain water and an outer one. The outer tank must allow a vacuum between the two shells to isolate the inner tank and minimize the heat exchange between the water and the exterior.
The characteristics of the tank are:

- Capacity : 1000 [l]
- Minimize the heat exchange
- Four pipes for water circulation
- Attachment points on the top of the tank
- Minimize the gap between the two shells

Analytical calculation: formulas
The complete calculation is available in the Excel file “Dimensionnement.xlsx”.
The following equations are valid for thin wall tubes. The criteria for thin wall are:

$$\frac{a}{R_m} \leq 0.1 \qquad or \qquad \frac{D_a}{D_i} \leq 1.2$$

Thickness of the wall	a	[mm]
Medium raduis	R_m	[mm]
Outer diameter	D_a	[mm]
Inner diameter	D_i	[mm]

Table 20 : calculation parameters (thin wall)

The minimal wall thickness is determined separately for the cylinder part and the curved bottoms. The following equations are from Decker Maschinenelemente [1].
These values will be use for the 3D model and will be check with the simulation.
The minimal thickness for the wall of the cylinder parts of the two tank is determined with:

$$s_{min} = \frac{D_a \cdot p_i}{2 \cdot \frac{K}{S} \cdot v + p_i} + c$$

For the curved bottoms, the minimal thickness is:

$$s_{min} = \frac{D_a \cdot p_i \cdot \beta}{4 \cdot \frac{K}{S} \cdot v + p_i} + c$$

[2] Any corrosion allowance, which leads to the standard formula commonly used for thin tubes “ c”

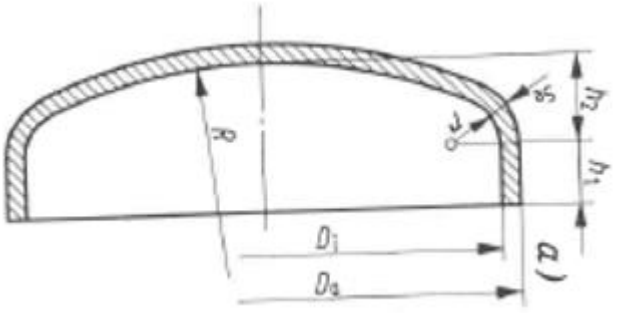

$$r = 0{,}1\,D_a, \quad h_1 \geqq 3{,}5s, \quad h_2 = 0{,}1935\,D_a - 0{,}455\,s_e, \quad \frac{s_e - c}{D_a} = 0{,}001 \ldots 0{,}1$$

Figure 29 : geometry of the curved bottom

The parameters of the previous equations are the followings:

Outer diameter	D_a	[mm]
Characteristic of material resistance	K	[MPa]
Security factor	S	[-]
Welding factor	v	[-]
Over thickness	c	[mm]
Inner pressure	p_i	[bar]
Coefficient	β	[-]

Table 21 : Calculation parameters (minimal thickness, Decker Maschinenelemente)

The outer tank must also resist linear buckling. To check the buckling resistance, the critic pressure is determined with the material and geometry parameters. This pressure has to be higher than the working pressure for the tank to resist buckling.
The determination of the critic pressure comes from “Techniques de l’ingénieur : tuyauteries. Résistance des éléments” [3].

.

$$p_{cr} = \frac{2.42 \cdot E}{(1-\mu^2)^{0.75}} \cdot \frac{\left({}^{a}/_{D_e}\right)^{2.5}}{\left({}^{L}/_{D_e}\right) - 0.45 \cdot \left({}^{a}/_{D_e}\right)^{0.5}} \geq x \cdot p_{atm}$$

-Security factor x=3
-Steel μ=0.3

Wall thickness	a	[mm]

Young's modulus	E	[GPa]
Poisson's ratio	μ	[-]
Outer diameter	D_e	[mm]
Distance between reinforcement	L	[mm]
Security factor	x	[-]
Atmospheric pressure	p_{atm}	[bar]
Critic pressure	p_{cr}	[bar]

Table 22 : calculation parameters (critic pressure)

The last verification point is the resistance of the feet (compression and buckling):

$$\sigma_{feet} = \frac{m_{tot} \cdot g}{n \cdot S_{feet}}$$

$$F_k = \frac{\pi^2 \cdot E \cdot I_y}{l_k^2}$$

Constraint in one foot	$\boldsymbol{\sigma_{feet}}$	[MPa]
Total mass (water and tank)	m_{tot}	[kg]
Quantity of feet	n	[-]
Area of one foot	S_{feet}	$[mm^2]$
Young's modulus	E	[GPa]
Second moment of area	I_y	$[mm^4]$
Buckling length	l_k	[mm]
Maximum length of one foot	l	[mm]
Equivalent of Buckling length	$l_k = 2 \cdot l$	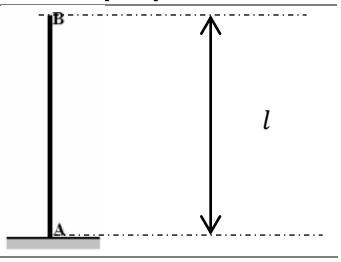

$l_k = l$	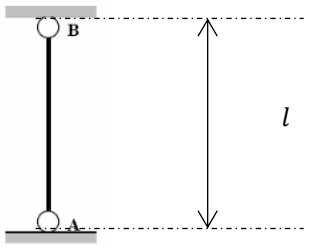
$l_k = 0.7 \cdot l$	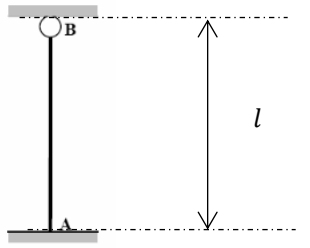
$l_k = 0.5 \cdot l$	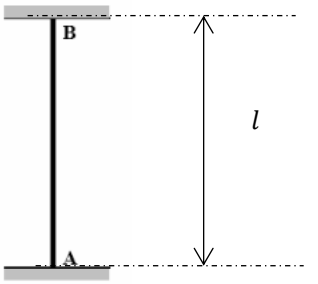

Table 23 : calculation parameters (compression and buckling)

Simulation: CODAP criteria **[4]**

The simulation will be perform on Ansys. The output will be constraint to check the resistance, the deformation and the multiplication factor for the buckling. The different criteria used for the interpretation are visible in Table 24.

The CODAP criteria are used to verify constraint given by the simulation. There are two different type of constraint:

- Primary constraint : constraint that participate at the mechanical equilibrium (forces)
- Secondary constraint : constraint generated by the necessary compatibility of the common deformation of different parts

These two type of constraint can be general or local. General constraint are located on zones that are relatively straight with no sudden geometric variation and local constraint are the one near these variations. The bellowing table shows the criteria for local and general constraint.

$\boldsymbol{R_{p\ 1.0}}$ plastic stretching to 1.0%, $\boldsymbol{R_m}$: tensile strength

Type of constraint depending meshing	Linearized constraint	Solid mesh
	Membrane constraint	Shell mesh
Nominal constraint for calculation		$f = min\left\{\left(\frac{R_{p\ 1.0}}{1.2}\right); \left(\frac{R_m}{3}\right)\right\}$

		Table in ASMEB31.3-1[5]
Equivalent stress (Tresca)		$\sigma_{eq} = max\{\lvert\sigma_1 - \sigma_2\rvert, \lvert\sigma_2 - \sigma_3\rvert, \lvert\sigma_3 - \sigma_1\rvert\} = 2 \cdot \tau_{max}$
Type of constraint	Primary general constraint (membrane)	$(\sigma_{eq})_{Pm} \leq 1.1 \cdot f$
	Primary local constraint (membrane)	$(\sigma_{eq})_{Pl} > 1.1 \cdot f$
Primary constraint	Primary general constraint (membrane)	$(\sigma_{eq})_{Pm} \leq f$
	Primary local constraint (membrane)	$(\sigma_{eq})_{Pl} \leq 1.5 \cdot f$
	Primary global constraint (membrane and bending)	$(\sigma_{eq})_{P} \leq 1.5 \cdot f$
Local constraint	Local zone without form discontinuity	$l_1 \leq \sqrt{R \cdot e}$
	Local zone around a form discontinuity	$l_1 \leq \frac{\sqrt{R_1 \cdot e_1} + \sqrt{R_2 \cdot e_2}}{2}$
	Minimal distance between two local zone	$l_2 \leq 2.5 \cdot \sqrt{R \cdot e}$

Table 24 :CODAP

Prototype one

Overview

This view shows the construction of the tank. The outer tank is reinforced with C parts to resist buckling because of the vacuum between the two tanks. The positioning of the inner tank is made with the four tubes (outer diameter 33.4 [mm], inner diameter 25.4 [mm]) that are welded in the two curved bottoms.

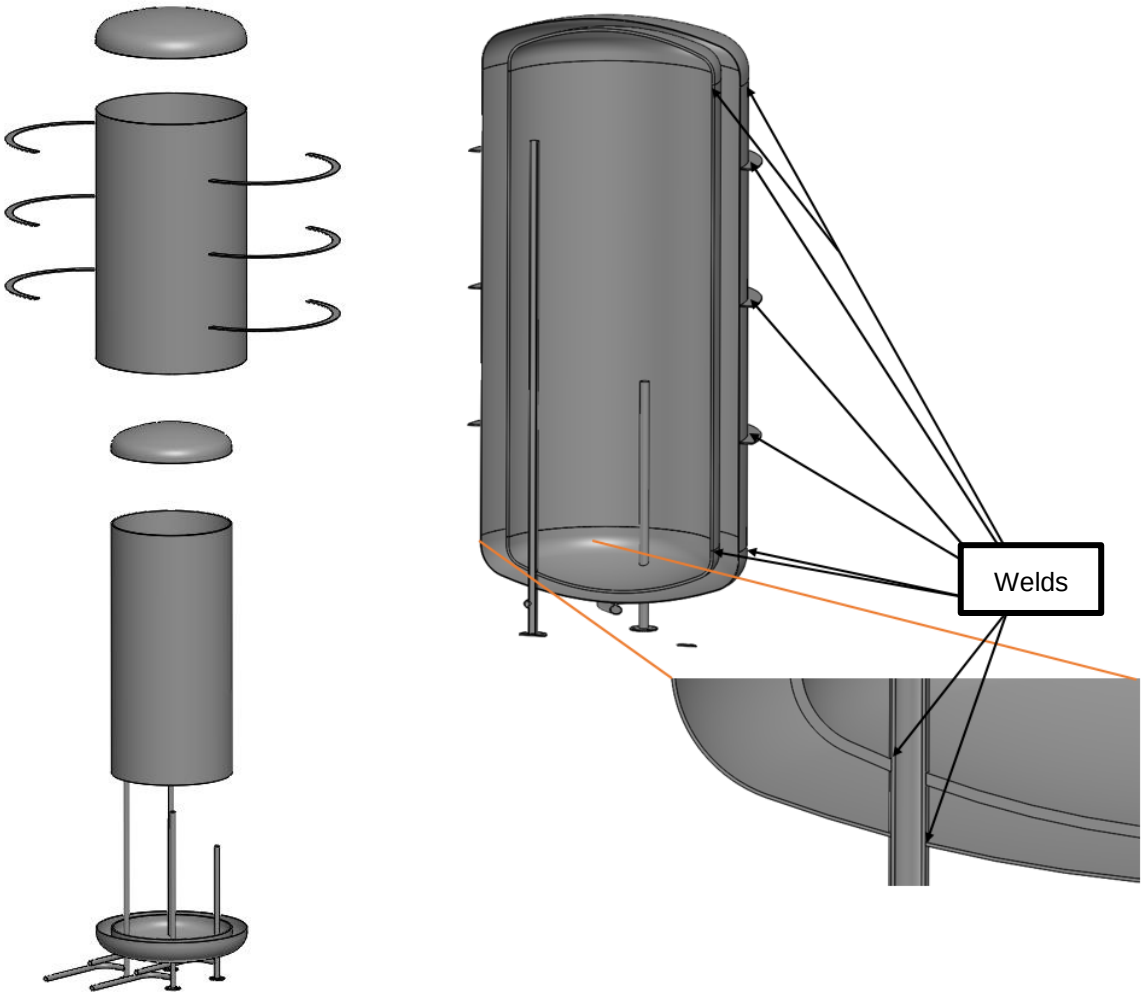

Figure 30 : overview of the tank

A

Inner tank

Outer diameter	D_a	800	[mm]
Characteristic of material resistance	K	200	[MPa]
Security factor	S	2	[-]
Welding factor	v	0.8	[-]
Over thickness	c	1.5	[mm]
Inner pressure	p_i	1.6	[MPa]
Minimal thickness	s_{min}	***9.3***	***[mm]***

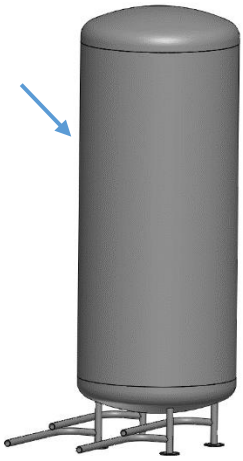

Table 25: inner tank, cylindrical part

Outer diameter	D_a	800	[mm]
Characteristic of material resistance	K	200	[MPa]
Security factor	S	2	[-]
Welding factor	v	0.8	[-]
Over thickness	c	1.6	[mm]
Inner pressure	p_i	1.6	[MPa]
Coefficient	β	4.6	[-]
Minimal thickness	s_{min}	***19.9***	***[mm]***

Table 26 : inner tank, curved bottom

The thickness of the two parts will be adapt depending the results of the simulation. The curved bottom and the cylinder part will have different thickness giving the big difference between the two analytical values.

Caractéristique matériau		
Type	316L	1.4404
Rp 0.2	220	[MPa]
Rp 1.0		[MPa]
Re		[MPa]
Rm	520	[MPa]

Technical Pocket Guide (Schaffler)

Outer tank

Outer diameter	D_a	1000	[mm]
Characteristic of material resistance	K	200	[MPa]
Security factor	S	2	[-]
Welding factor	v	0.8	[-]
Over thickness	c	1.4	[mm]
Outer pressure	p_e	0.1	[MPa]
Minimal thickness	s_{min}	***2.0***	***[mm]***

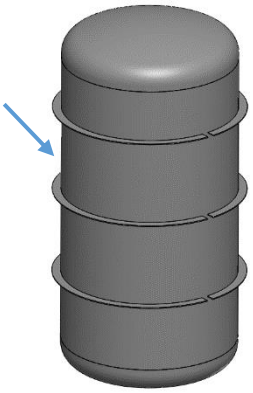

Table 27 : outer tank, cylindrical part

Outer diameter	D_a	1000	[mm]
Characteristic of material resistance	K	200	[MPa]
Security factor	S	2	[-]
Welding factor	v	1	[-]
Over thickness	c	1.4	[mm]
Outer pressure	p_e	0.1	[MPa]
Coefficient	β	4.6	[-]
Minimal thickness	s_{min}	***2.5***	***[mm]***

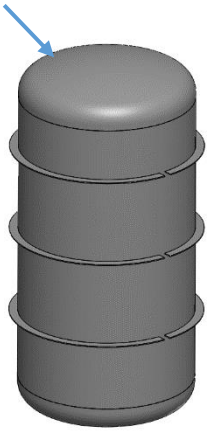

Table 28 : outer tank, curved botom

Outer diameter	D_a	1000	[mm]
Wall thickness	a	3	[mm]
Young's modulus	E	210	[GPa]
Poisson's ratio	v	0.3	[-]
Distance between reinforcement	L	500	[mm]
Critical pressure (with reinforcement)	p_{cr}	***5.66***	***[bar]***

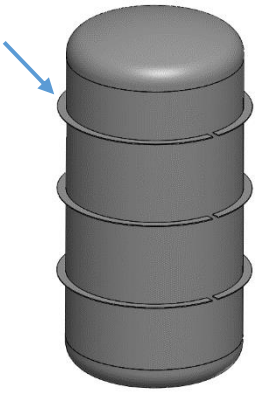

Table 29 : critical pressure (buckling)

For the outer tank, the thickness for the cylinder part and the curved bottom is nearly the same, so a common thickness will be use in the simulation.
The solution with three reinforcement is acceptable because the critical pressure is 5.6 times higher than the atmospheric pressure, pressure that is the same anywhere on earth.
Feet

Tubes			
Outer diameter	R_e	16.7	[mm]
Inner diameter	R_i	12.7	[mm]
Area	S_{feet}	369.5	[mm^2]
Second moment of area	I_y	40656.3	[mm^4]
Quantity of feet	n	4	[-]
Material			
Young's Modulus	E	210	[GPa]
Poisson's ratio	v	0.3	[-]
Load			
Tank mass	m_{res}	664	[kg]
Water mass	m_{eau}	1000	[kg]
Overall weight	F_g	16323.8	[N]
Compression			
Compression constraint	**σ_{feet}**	**11.05**	**[MPa]**
Yield strength	F_e	207	[MPa]
Buckling			
Maximal length	l	170	[mm]
Buckling length (case l_k = 0.7 l)	l_k	119	[mm]
Maximal load before buckling	F_k	5866	[N]
Load per foot	**$F_{g,1}$**	**4081**	**[N]**

Table 30 : feet calculation (compression and buckling)

With four feet, the compression constraint is much lower than the yield strength. The maximal buckling load is 5866 [N], which is 30% higher than the actual load. In conclusion, the use of the water tubes as feet is possible.

Simulation

Geometry and loads

Mesh	Inner pressure	Outer pressure
Shell, quadrilateral	$p_i = 16\ [bar]$	$p_e = 1\ [bar]$
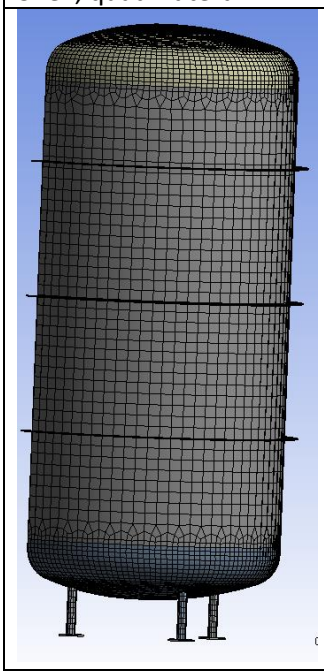	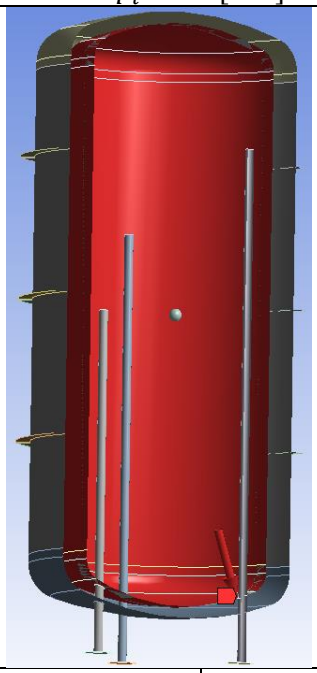	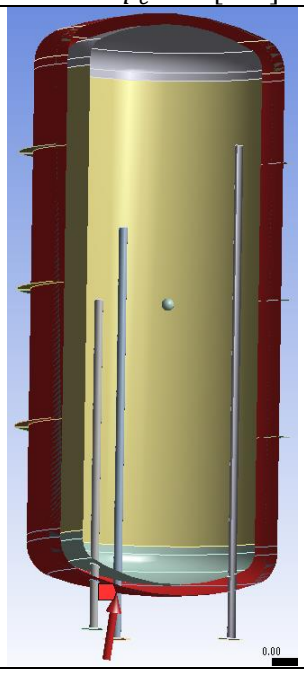
Water		**Gravity**
$m = 1000\ [kg]$		$g = 9.81\ \left[{}^{m}/_{s^2}\right]$
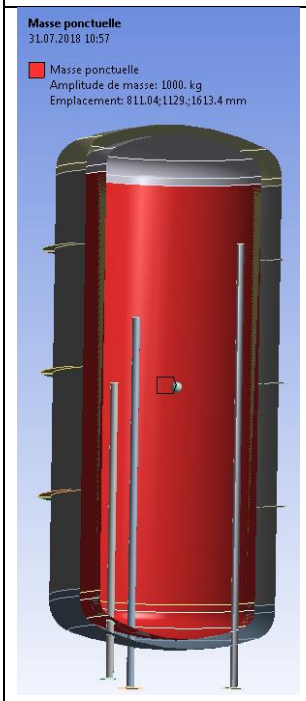		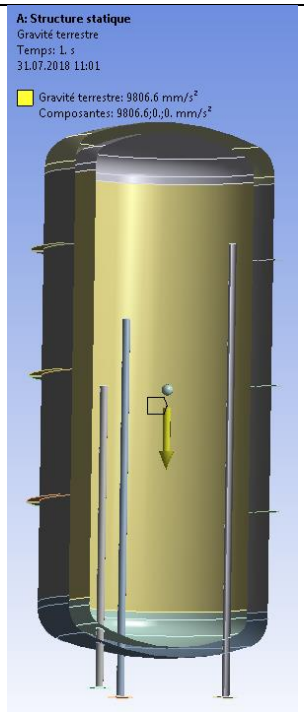

Table 31 : loads, prototype 1

Thickness	
Inner tank, cylindrical part	8 [mm]
Inner tank, top	8 [mm]
Inner tank, bottom	8 [mm]
Outer tank, cylindrical part	3 [mm]
Outer tank, top	3 [mm]
Outer tank, bottom	3 [mm]
C's reinforcements	3 [mm]
Overall mass	
655 [kg]	

Table 32 : geometry, prototype 1

Shear constraint

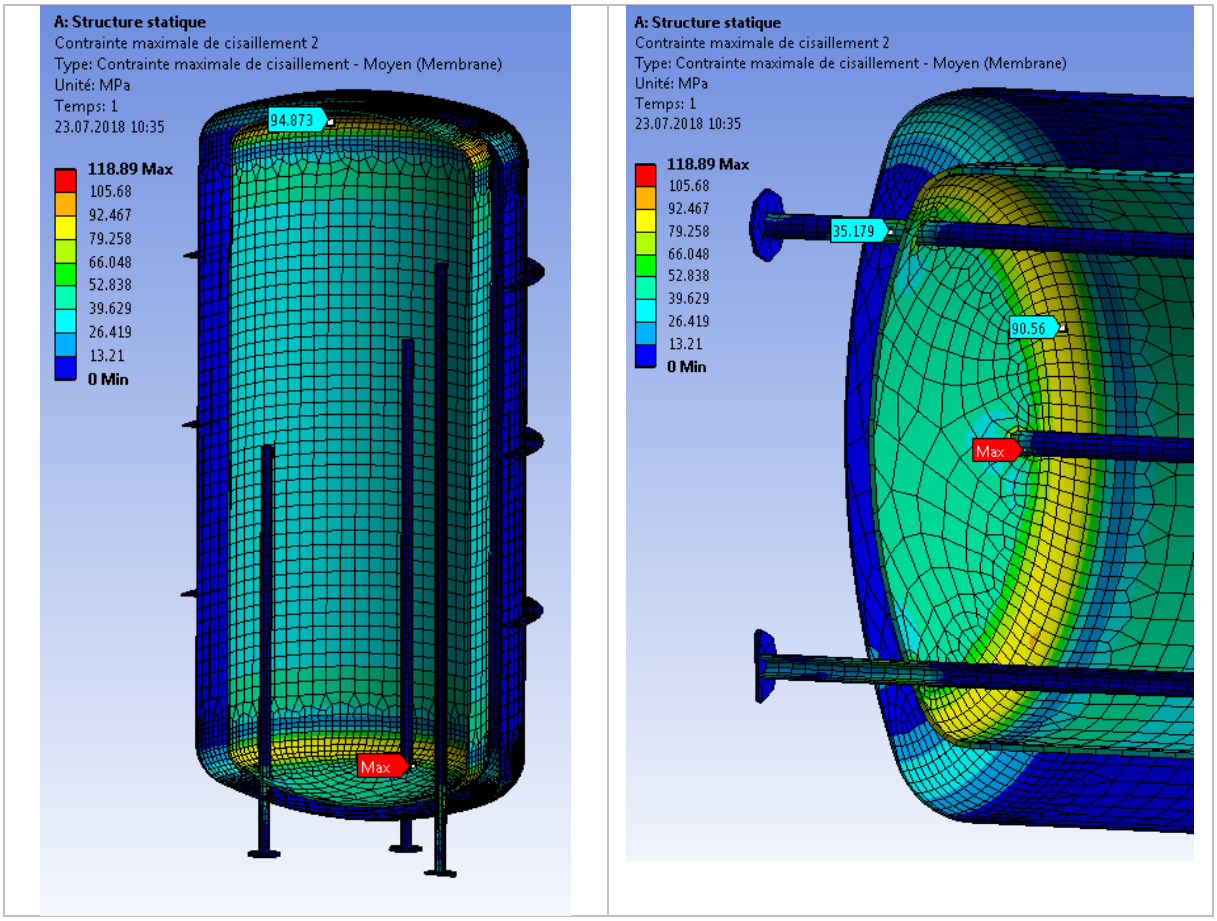

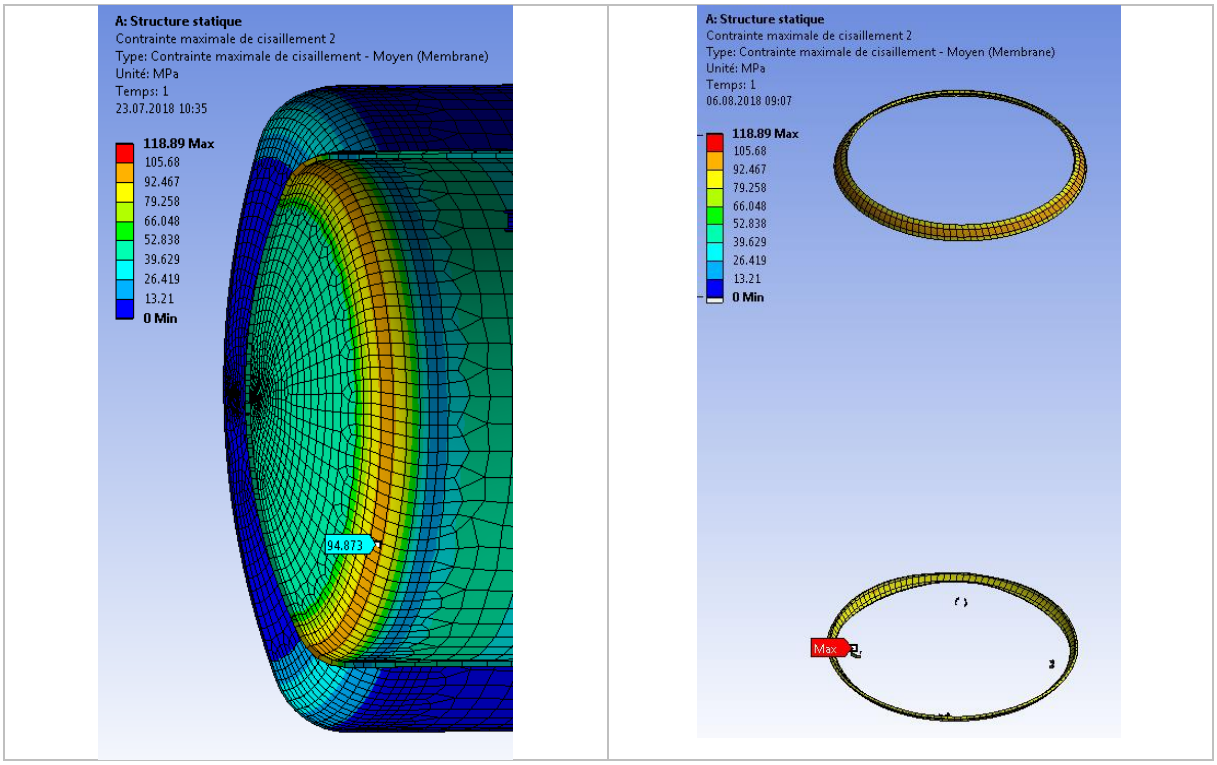

Table 33 : membrane constraint, prototype 1

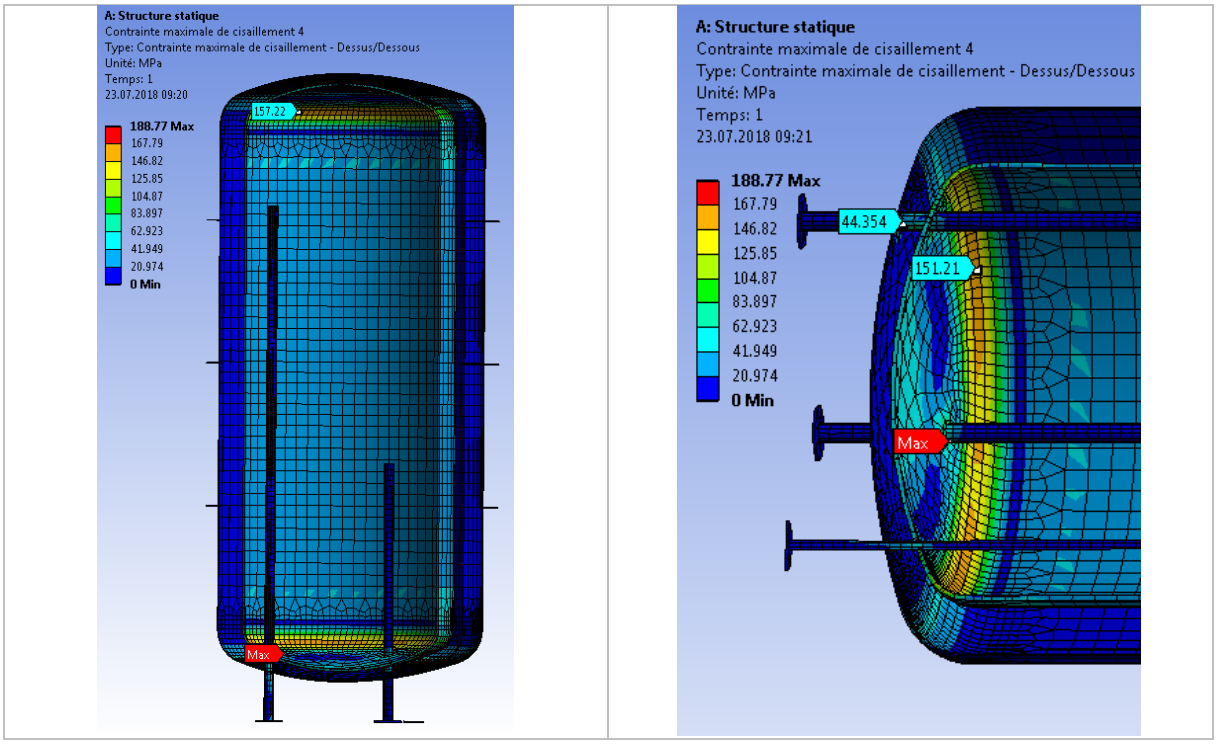

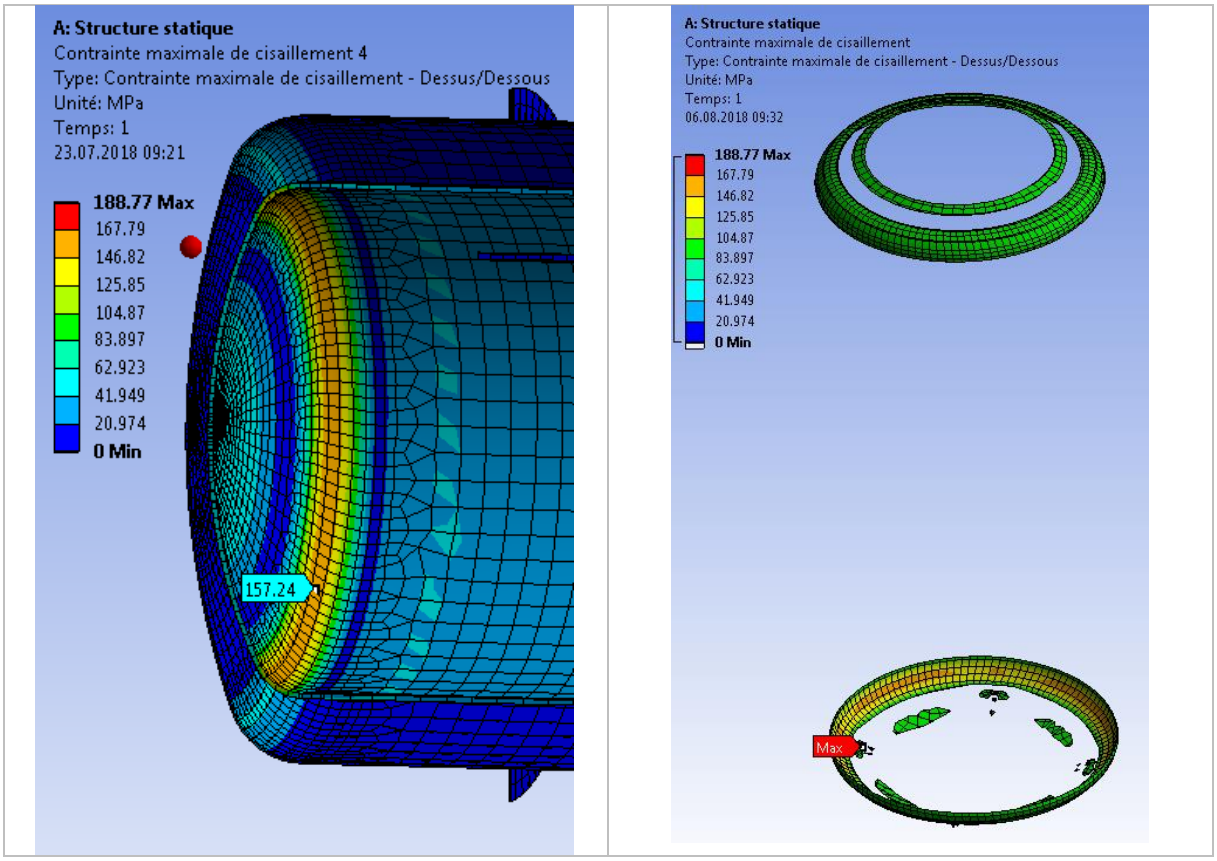

Table 34 : global constraint, prototype 1

Membrane			
Primary general constrain		$f = 172.4\ [MPa]$	$\sigma_{eq} = 2 \cdot \tau_{max} = 2 \cdot 94.873 = 189.746\ [MPa]$
Primary local constrain		$1.5 \cdot f = 258.6\ [MPa]$	$\sigma_{eq} = 2 \cdot \tau_{max} = 2 \cdot 118.89 = 237.78 [MPa]$
		Theoretical	Effective
Local zone	Inner tank	$l_1 \leq \sqrt{R \cdot e} = 54.8\ [mm]$	$l_1 \cong 50\ [mm]$
	Outer tank	$l_2 \leq \sqrt{R \cdot e} = 80\ [mm]$	-
Global			
Primary global constraint		$1.5 \cdot f = 258.6\ [MPa]$	$\sigma_{eq} = 2 \cdot \tau_{max} = 2 \cdot 188.77 = 377.54\ [MPa]$
		Theoretical	Effective
Local zone	Inner tank	$l_1 \leq \sqrt{R \cdot e} = 54.8\ [mm]$	$l_1 \cong 60\ [mm]$
	Outer tank	$l_2 \leq \sqrt{R \cdot e} = 80\ [mm]$	-

Table 35 : constraints results, prototype 1

Constraints of the major parts is lower than the nominal constraint for calculation. The critical parts are the curved bottom, which constraints are superior to the nominal constraint for calculation. The maximal solicitation is in the welds of the feet.
The local zone (see definition in Table 33) are visible on the last picture of the previous table. The length of these zones is nearly equal to the theoretical length (around 50 [mm] VS 55 [mm]) and the constraints is too high.

Buckling

Mode 1 Load multiplicator : 6.13	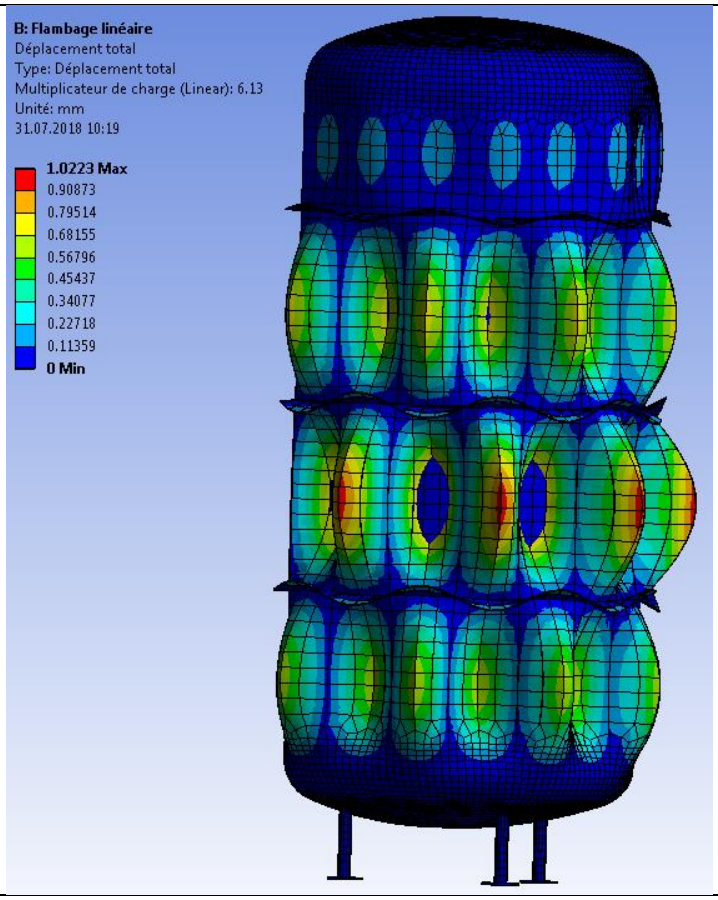

Table 36 : buckling, prototype 1

The minimal buckling load is 6.13 times higher than the nominal load. There is no risk of buckling of the structure with the actual load parameters.
Displacement

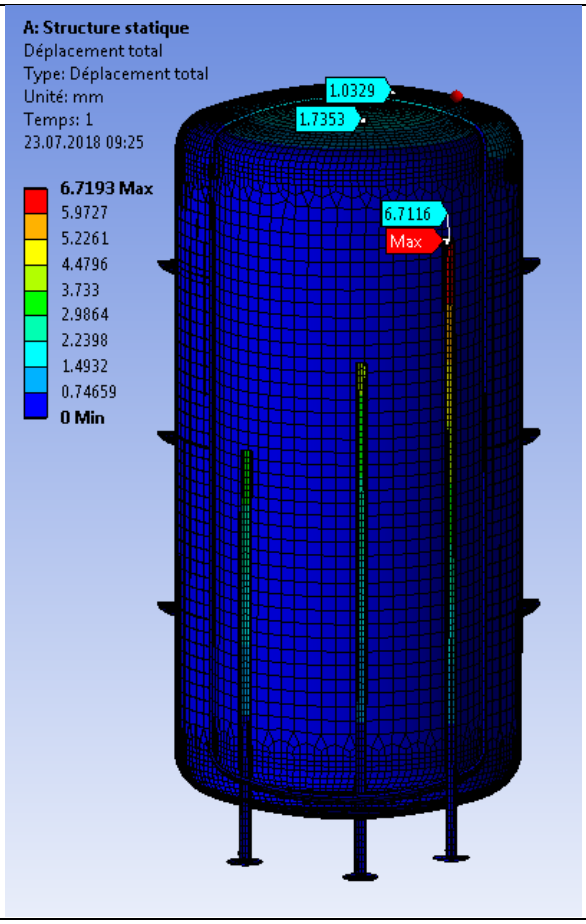

Table 37 : displacement, prototype 1

The major displacement is at the top of the higher tube. This large displacement isn't critical because the tube bend on the inside of the tank and the constraints aren't high in the tube (the displacement is due to de deformation of the inner curved bottom).
The displacement of the top of the tank is acceptable as well because the inner tank does not interfere with the outer tank.

- Conclusion

The prototype 1 is good regarding buckling but the constraint in the small radius of the inner tank and the welds of the tubes are too high (plastic deformation at these location). This prototype cannot be use as an industrial solution because of its lack of resistance.

Prototype two

- Overview

As the first prototype, the outer tank is reinforced with C parts to resist. The positioning of the inner tank in the outer tank is made with radial tubes welded at the inner side of the outer tank and the outer side of the inner tank. These little tubes are only located on the cylindrical parts to simplify the building. The feet are weld outside cylindrical part of the outer tank.
This second prototype uses different thickness for the cylinder and curved parts of the inner tank in order to minimize constraints in the smaller radius of the curved part.

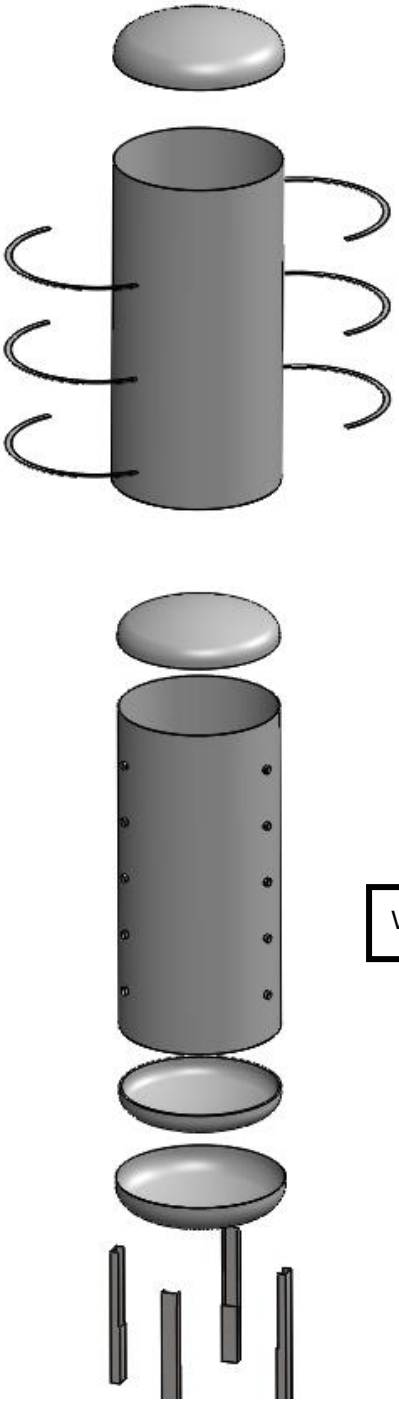

Figure 31 : overview prototype 2 of 15 spaces

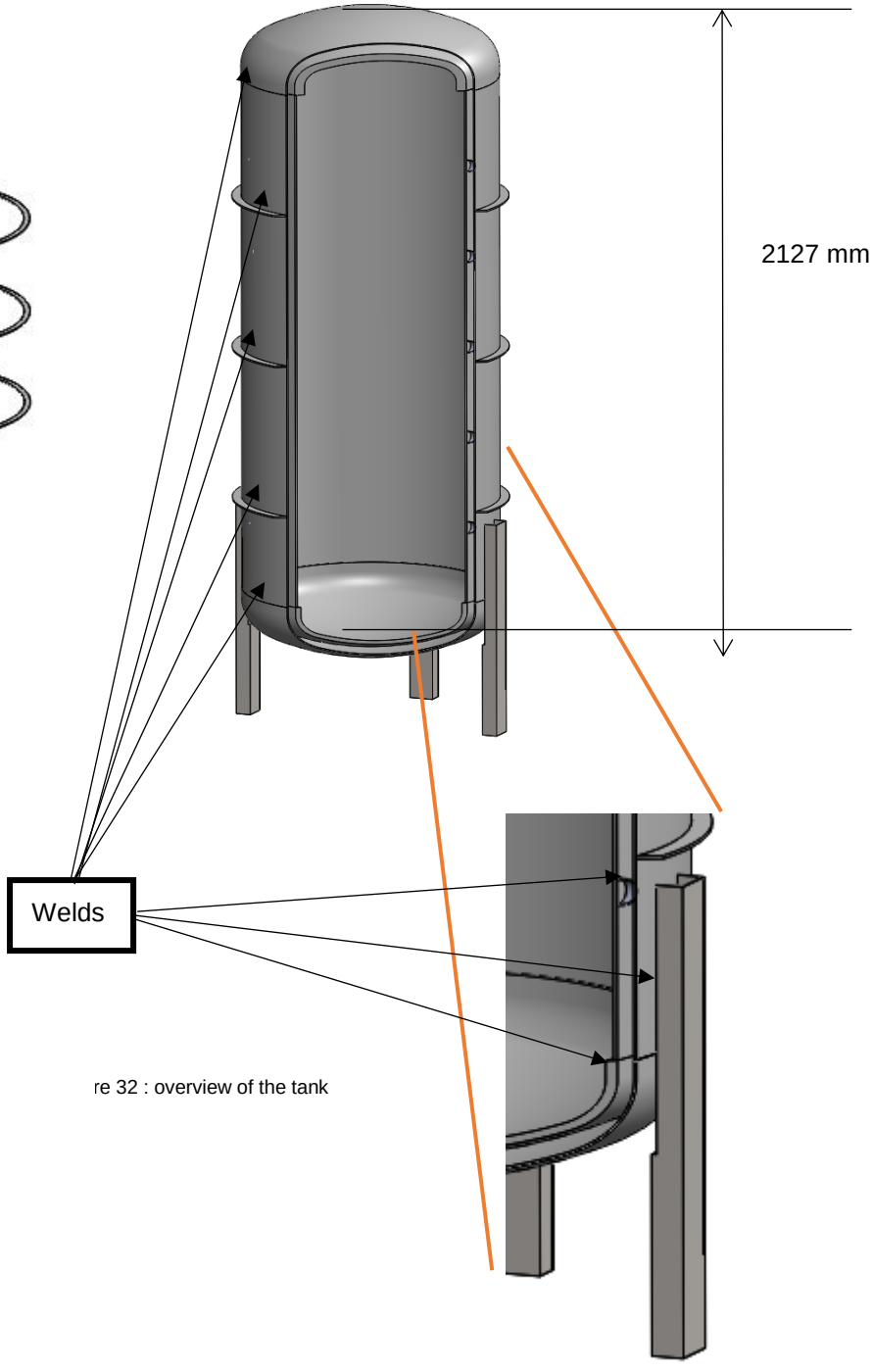

re 32 : overview of the tank

Analytical calculation

- Inner tank

Outer diameter	D_a	800	[mm]
Characteristic of material resistance	K	200	[MPa]
Security factor	S	2	[-]
Welding factor	v	0.8	[-]
Over thickness [2]	c	1.5	[mm]
Inner pressure	p_i	1.6	[MPa]
Minimal thickness	s_{min}	***9.3***	***[mm]***

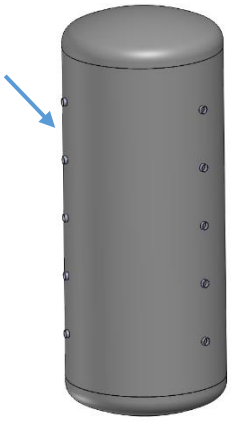

Table 38: inner tank, cylindrical part

Outer diameter	D_a	800	[mm]
Characteristic of material resistance	K	200	[MPa]
Security factor	S	2	[-]
Welding factor	v	0.8	[-]
Over thickness	c	1.6	[mm]
Inner pressure	p_i	1.6	[MPa]
Coefficient	β	4.6	[-]
Minimal thickness	s_{min}	***19.9***	***[mm]***

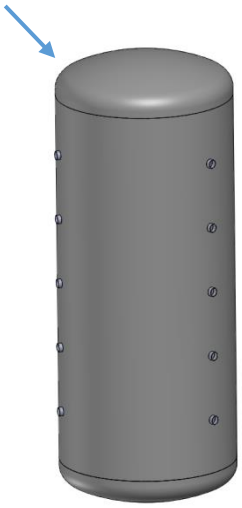

Table 39 : inner tank, curved bottom

The thickness of the two parts will be adapt depending the results of the simulation. The curved bottom and the cylinder part will have different thickness giving the big difference between the two analytical values.

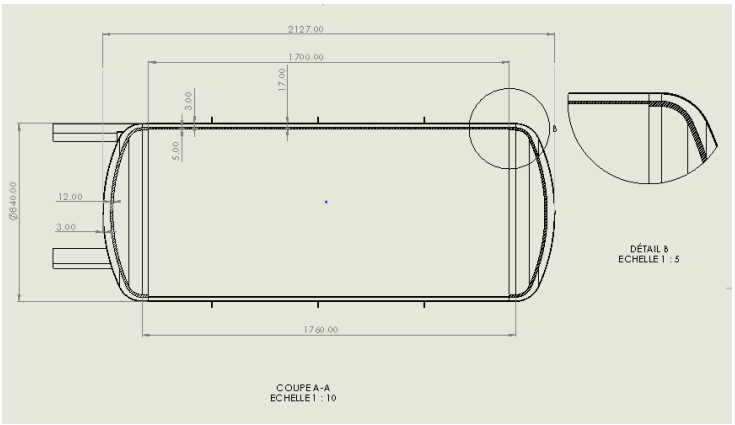

Outer tank

Outer diameter	D_a	1000	[mm]
Characteristic of material resistance	K	200	[MPa]
Security factor	S	2	[-]
Welding factor	v	0.8	[-]
Over thickness	c	1.4	[mm]
Outer pressure	p_e	0.1	[MPa]
Minimal thickness	s_{min}	***2.0***	***[mm]***

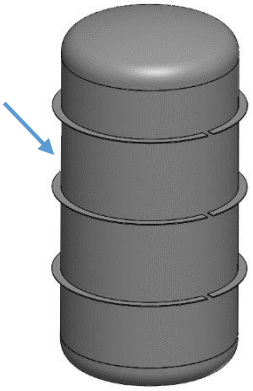

Table 40 : outer tank, cylindrical part

Outer diameter	D_a	1000	[mm]
Characteristic of material resistance	K	200	[MPa]
Security factor	S	2	[-]
Welding factor	v	1	[-]
Over thickness	c	1.4	[mm]
Outer pressure	p_e	0.1	[MPa]
Coefficient	β	4.6	[-]
Minimal thickness	s_{min}	***2.5***	***[mm]***

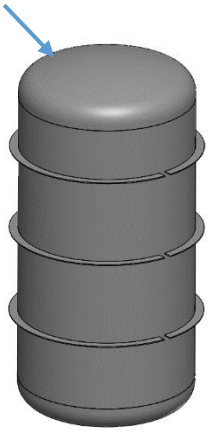

Table 41 : outer tank, curved bottom

Outer diameter	D_a	1000	[mm]
Wall thickness	a	3	[mm]
Young's modulus	E	210	[GPa]
Poisson's ratio	v	0.3	[-]
Distance between reinforcement	L	500	[mm]
Critical pressure (with reinforcement)	p_{cr}	***5.66***	***[bar]***

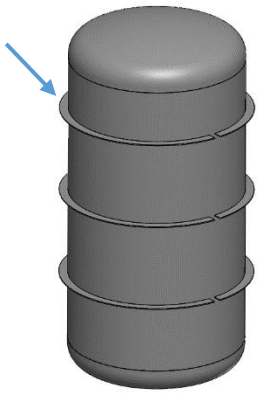

Table 42 : critical pressure (buckling)

For the outer tank, the thickness for the cylinder part and the curved bottom is nearly the same, so a common thickness will be use in the simulation.
The solution with three reinforcement is acceptable because the critical pressure is 5.6 times higher than the atmospheric pressure, pressure that is the same anywhere on earth.

- Feet

Geometry			
External side	x_{e1}	80	[mm]
	x_{e2}	50	[mm]
Internal side	x_{i1}	76	[mm]
	x_{i2}	46	[mm]
Area	S_{feet}	504.0	[mm^2]
Second moment of area	I_y	216872.0	[mm^4]
Quantity of feet	n	4	[-]
Material			
Young's Modulus	E	210	[GPa]
Poisson's ratio	v	0.3	[-]
Load			
Tank mass	m_{res}	664	[kg]
Water mass	m_{eau}	1000	[kg]
Overall weight	F_g	16323.8	[N]
Compression			
Compression constraint	σ_{feet}	**8.10**	**[MPa]**
Yield strength	F_e	207	[MPa]

Buckling			
Maximal length	l	450	[mm]
Buckling length (case l_k = 0.7 l)	l_k	315	[mm]
Maximal load before buckling	F_k	4465	[N]
Load per foot	**$F_{g,1}$**	**4081**	**[N]**

Table 43 : feet calculation (compression and buckling)

With four feet, the compression constraint is much lower than the yield strength. The maximal buckling load is 4465 [N], which is 10% higher than the actual load.

Simulation

- Geometry

Mesh	Inner pressure	Outer pressure
Shell, quadrilateral	$p_i = 16\ [bar]$	$p_e = 1\ [bar]$
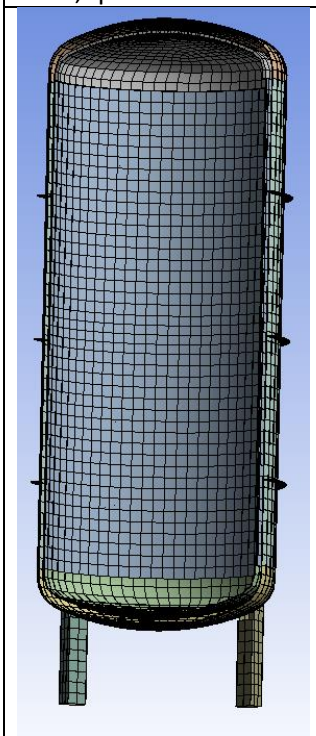	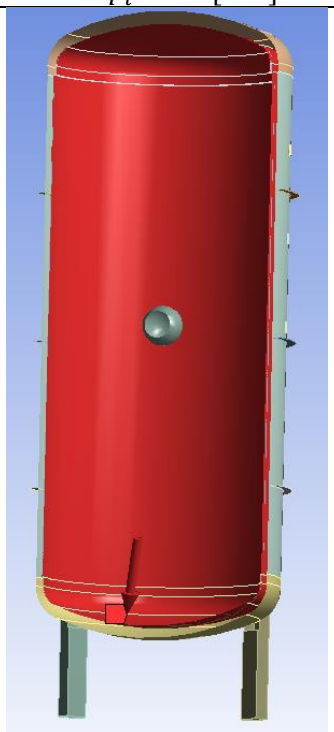	

Water	Gravity
$m = 1000\ [kg]$	$g = 9.81\ \left[{}^{m}/_{s^2}\right]$

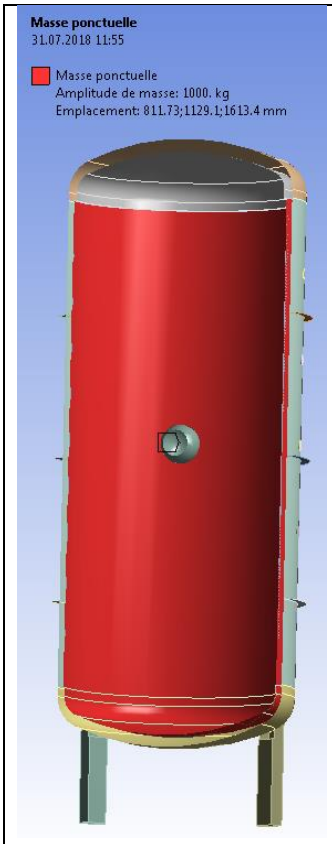

Table 44 : loads, prototype 2

Thickness	
Inner tank, cylindrical part	5 [mm]
Inner tank, top	12 [mm]
Inner tank, bottom	12 [mm]
Outer tank, cylindrical part	3 [mm]
Outer tank, top	3 [mm]
Outer tank, bottom	3 [mm]
C's reinforcements	3 [mm]
Feet	2 [mm]
Overall mass	
462 [kg]	

Table 45 : geometry, prototype 2

Shear constraint

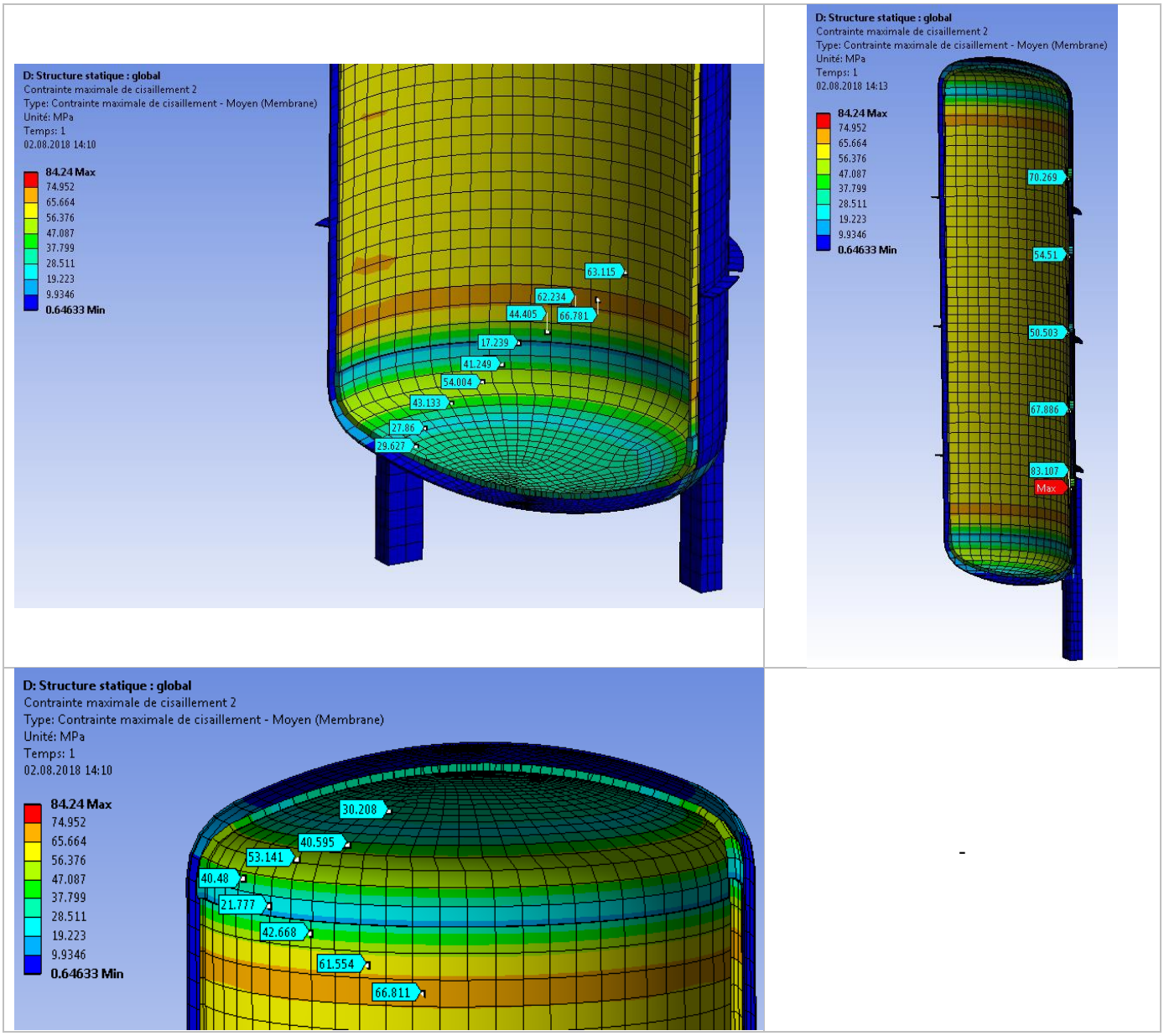

Table 46 : membrane constraint, prototype 2

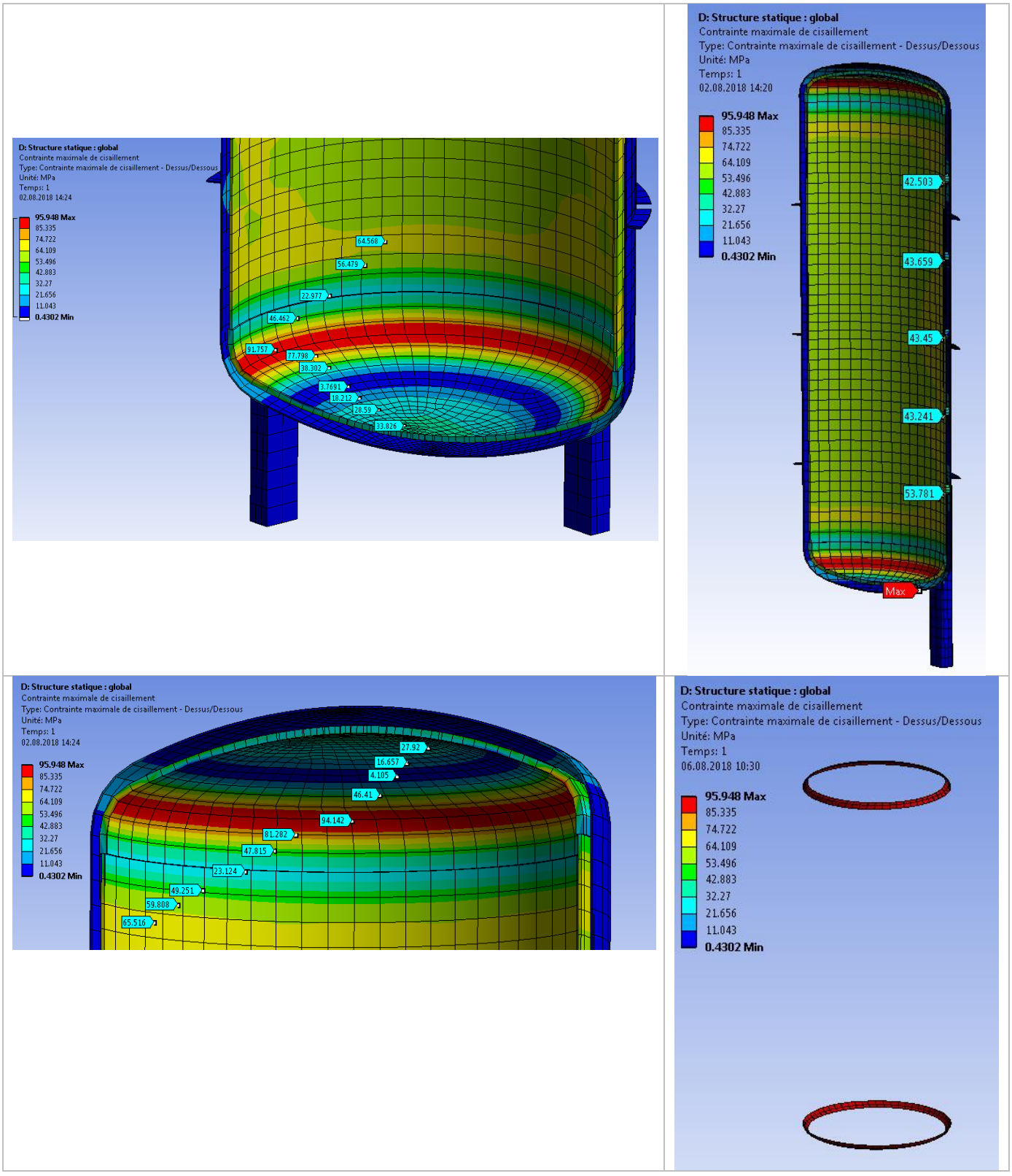

Table 47 : global constraint, prototype 2

Membrane			
Primary general constraint		$f = 172.4\ [MPa]$	$\sigma_{eq} = 2 \cdot \tau_{max} = 2 \cdot 66.8 = 133.6\ [MPa]$
Primary local constraint		$1.5 \cdot f = 258.6\ [MPa]$	$\sigma_{eq} = 2 \cdot \tau_{max} = 2 \cdot 84.24 = 168.48\ [MPa]$
		Theoretical	Effective
Local zone	Inner tank	$l_1 \leq \sqrt{R \cdot e} = 54.8\ [mm]$	-
	Outer tank	$l_2 \leq \sqrt{R \cdot e} = 80\ [mm]$	-
Global			
Primary global constraint		$1.5 \cdot f = 258.6\ [MPa]$	$\sigma_{eq} = 2 \cdot \tau_{max} = 2 \cdot 95.948 = 191.896\ [MPa]$
		Theoretical	Effective
Local zone	Inner tank	$l_1 \leq \sqrt{R \cdot e} = 54.8\ [mm]$	$l_1 \cong 40\ [mm]$
	Outer tank	$l_2 \leq \sqrt{R \cdot e} = 80\ [mm]$	-

Table 48 : constraints results, prototype 2

The membrane constraint are lower than the primary general constraint so there is no local zone regarding this sort of constraint and. The global constraint is good too, being lower than the primary global constraint. There is a local zone here but its length is smaller than the maximal length for local zone.
The cylindrical connectors (connecting the two tanks) have a maximal shear constraint of 54 [MPa]. This does not allow the use of borosilicate glass for these parts because of its lack of resistance, but stainless steel is possible. The heat transfer will be higher but the resistance will be sufficient.
An alternative should be to use cylindrical connectors at the top and bottom and use borosilicate glass instead of stainless steel.

- Buckling

Mode 1 Load multiplicator : 9.6	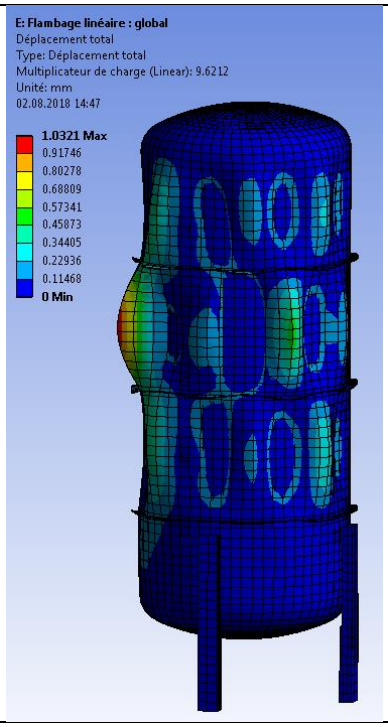

Table 49 : buckling, prototype 2

The minimal buckling load is 9.6 times higher than the nominal load and 1.5 times more than prototype 1. There is no risk of buckling of the structure with the actual load parameters.

- Displacement

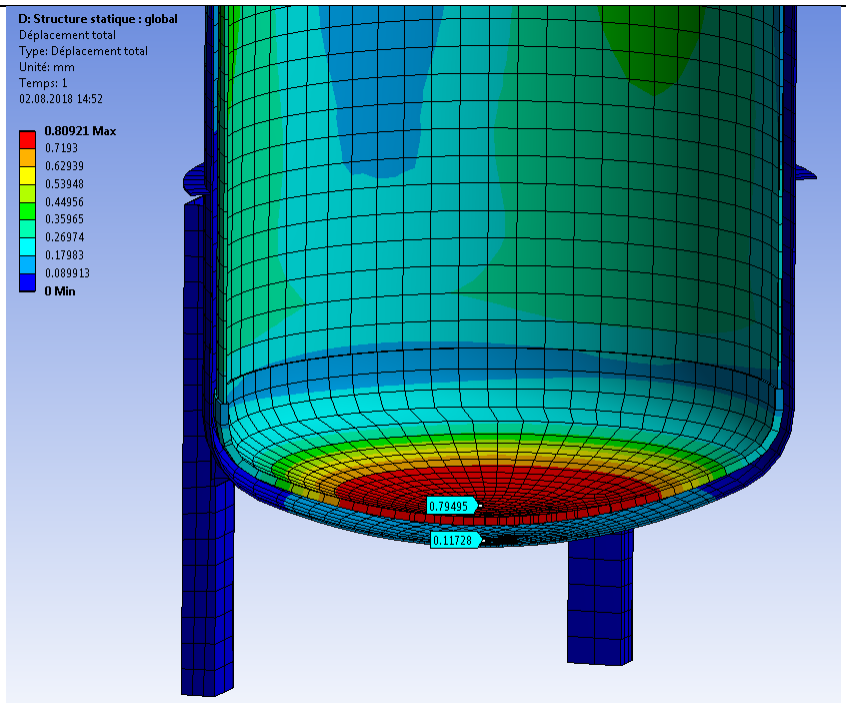

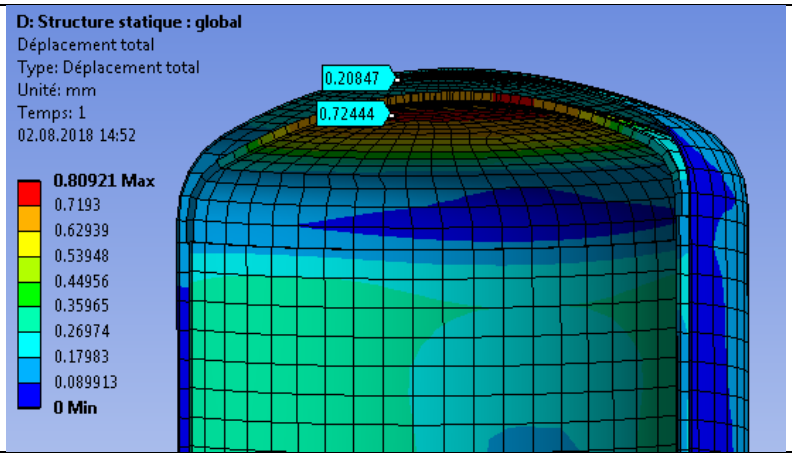

Table 50 : displacement, prototype 2

The biggest displacement is at the top and bottom of the inner tank. These values for displacement are acceptable here because there is no contact between the inner tank and the outer tank. There is also no plastic deformation here, not like in prototype 1.

- Conclusion

This prototype is better than the first one, having lower constraint and higher buckling factor. The mass has been reduce for about 200 kg compared to prototype 1.

- Comparison

Prototype 1		Prototype 2	
Mass			
655 [kg]		462 [kg]	
Stress (global)			
Inner tank	Pipe welds	Inner tank	Cylindrical reinforcements
314.4[MPa]	377.5 [MPa]	191.8 [MPa]	108 [MPa]
Stress (membrane)			
Inner tank	Pipe welds	Inner tank	Cylindrical reinforcements
189.7 [MPa]	237.7 [MPa]	133.6 [MPa]	168 [MPa]
Load multiplication (buckling)			
6.2		9.6	

-

Table

Figure

Annexes

[1] Von Karl-Heinz Decker. *Maschinenelemente Gestaltung und Berechnung, 1990.*

Tab. A 4.26 Sicherheitsbeiwerte S und Wanddickenzuschläge c für Druckbehälter und Dampfkessel (nach AD-Merkblatt A0)

Sicherheitsbeiwert S	bei Walz- und Schmiedestählen unter innerem Überdruck 1,5 unter äußerem Überdruck 1,8	bei Stahlguß 2 2,4
Wanddickenzuschlag $c = c_1 + c_2$		
c_1 Zuschlag zur Berücksichtigung von Wanddickenunterschreitungen: Minustoleranz nach der Maßnorm DIN 1543 bei Blechen von 3 bis unter 8 mm **0,4 mm** 8 15 mm **0,5 mm** 15 25 mm **0,6 mm** bei Rohren ≈ 15% der Wanddicke	von 25 bis unter 40 mm **0,8 mm** 40 80 mm **1,0 mm** 80 150 mm **1,0 mm**	
c_2 Abnutzungszuschlag: bei ferritischen Stählen = 1 mm. Er entfällt bei $s_e \geqq 30$ mm, bei Rohren und bei ausreichendem Schutz durch Verbleiung, Gummierung, Kunststoffüberzügen, bei austenitischen Stählen und bei Nichteisenmetallen. Galvanische Überzüge gelten nicht als Schutz. Bei stark korrodierendem Beschickungsmittel ist ein höherer Zuschlag als 1 mm zu vereinbaren.		

Tab. 4.23 Berechnungsbeiwerte β für gewölbte Böden, gültig für den gesamten Kalotten- und Krempenteil, bei $d_i / D_a = 0$ nur für den Krempenteil (zusammengestellt nach AD-Merkblatt B3)

$\frac{s_e - c}{D_a}$	Klöpperboden d_i/D_a								Korbbogenboden d_i/D_a								
	0	0,15	0,2	0,25	0,3	0,4	0,5	0,6	0	0,1	0,15	0,2	0,25	0,3	0,4	0,5	0,6
0,001	6	7	8						3,2	4,2	5,6	7,1	9				
0,002	4,6	5,4	6,1	7	8,2				2,7	3,4	4,5	5,5	6,4	7,5			
0,003	3,9	4,6	5,3	6,1	7	9			2,4	3	3,9	4,7	5,6	6,4	8		
0,004	3,6	4,3	4,8	5,6	6,3	7,9			2,3	2,8	3,6	4,3	5	5,7	7,2	8,8	
0,005	3,3	4	4,5	5,2	5,9	7,3	8,7		2,2	2,6	3,4	4	4,6	5,3	6,5	8	
0,01	2,7	3,3	3,7	4,3	4,7	5,7	6,6	7,5	1,9	2,3	2,8	3,2	3,8	4,2	5	6	6,9
0,02	2,6	2,9	3,3	3,5	3,8	4,5	5,2	5,9	1,8	2,3	2,5	2,7	3,1	3,4	4	4,7	5,3
0,03	2,5	2,9	2,9	3,2	3,4	4	4,6	5,3	1,8	2,2	2,5	2,6	2,7	3	3,6	4	4,7
0,04	2,5	2,8	2,8	3	3,3	3,7	4,3	4,7	1,7	2,2	2,4	2,5	2,6	2,8	3,3	3,7	4,3
0,05	2,4	2,8	2,8	2,9	3,2	3,5	3,9	4,4	1,7	2,2	2,4	2,4	2,4	2,6	3,2	3,5	4
0,1	2,4	2,8	2,8	2,9	2,9	3	3,4	3,7	1,7	2,2	2,4	2,4	2,4	2,6	2,7	2,9	3,2

Tab. A 4.25 Festigkeitskennwert K in N/mm² von Rohrwerkstoffen und Stahlguß (Auszug aus den DIN-Normen)

Stahlsorte		Dicke mm über	Dicke mm bis	Streckgrenze bei °C 50	100	150	0,2%-Dehngrenze bei °C 200	250	300	350	400	450	500
Warmfeste Stähle DIN 17175	**St 35.8**		16	235	218	202	185	165	140	120	110	105	
		16	40	225	210	195	180	160	135	120	110	105	
	St 45.8		16	255	238	222	205	185	160	140	130	125	
		16	40	245	228	212	195	175	155	135	130	125	
	17 Mn 4		40	270	258	247	235	215	175	155	145	135	
	19 Mn 5		40	310	292	273	255	235	206	180	160	150	
	15 Mo 3		10	285	270	255	240	220	195	185	175	170	165
		10	40	270	255	240	225	205	180	170	160	155	150
	13 CrMo 4 4		10	305	288	272	255	245	230	215	205	195	190
		10	40	290	273	257	240	230	215	200	190	180	175
	10 CrMo 9 10		40	280	268	257	245	240	230	215	205	195	185
	14 MoV 6 3		40	320	303	287	270	255	230	215	200	185	170
Unlegierte Stähle DIN 1626, 1628, 1629, 1630	**St 37.0 und St 37.4**		16	235	218	202	185	165	140				
		16	40	225	208	192	175	155	135				
	St 44.0 und St 44.4		16	275	248	232	215	195	165				
		16	40	265	245	225	205	185	160				
	St 52.0 und St 52.4		16	355	318	282	245	225	195				
		16	40	345	308	272	235	215	190				

Stahlgußsorte		0,2%-Dehngrenze bei °C 20	50	100	150	200	250	300	350	400	450	500	550
Warmfester Stahlguß DIN 17245	**GS-C25**	245	245	222	198	175	160	145	135	130	125		
	GS-22 Mo 4	245	245	227	208	190	177	165	155	150	145	135	
	GS-17 CrMo 5 5	315	315	295	275	255	242	230	215	205	190	180	160
	GS-18 CrMo 9 10	400	400	385	370	355	350	345	330	315	305	280	240
	GS-17 CrMoV 5 11	440	440	422	403	385	375	365	350	335	320	300	260
	G-X 8 CrNi 12	355	355	328	302	275	270	265	260	255			
	G-X 22 CrMoV 12 1	590	590	560	530	500	485	470	460	445	420	365	300

Tab. A 4.24 Festigkeitskennwert K in N/mm² von Blechwerkstoffen (Auszug aus den DIN-Normen)

	Stahlsorte	Dicke mm über	Dicke mm bis	Streckgrenze bei °C 50	100	150	0,2%-Dehngrenze bei °C 200	250	300	350	400	450	500
Warmfeste Stähle DIN 17155	**UH I**		16	195	175	155							
		16	40	185	168	152	135	115	95	80	70		
		40	60	175	162	148							
	H I		16	235	218	202	185	165	140	120	110	105	
		16	40	225	210	195	180	165	135	120	110	105	
		40	60	215	202	188	175	165	135	120	110	105	
	H II		16	265	245	225							
		16	40	255	238	222	205	185	155	140	130	125	
		40	60	245	232	218							
	17 Mn 4		16	290	275	260							
		16	40	285	272	258	245	225	205	175	155	135	
		40	60	280	268	257							
	19 Mn 6		16	355	325	295							
		16	40	345	318	292	265	245	225	205	175	155	
		40	60	335	312	288							
	15 Mo 3		10	285	270	255	240	220	195	185	175	170	165
		10	40	270	255	240	225	205	180	170	160	155	150
		40	60	260	243	223	210	195	170	160	150	145	140
	13 CrMo 4 4		10	300	285	270	255	245	230	215	205	195	190
		10	40	295	280	265	240	230	215	200	190	180	175
		40	60	295	273	252	230	220	205	190	180	170	165
	10 CrMo 9 10		16	310	288	267							
		16	40	300	282	263	245	240	230	215	205	195	185
		40	60	290	272	253	235	230	220	205	195	185	175
Feinkornbaustähle DIN 17102	**WSt 255**		35	255	226	206							
		35	70	235	216	201	186	167	137	118	108		
	WSt 285		35	285	255	235							
		35	70	265	245	226	206	186	157	137	118		
	WSt 315		35	315	275	255							
		35	70	295	265	245	226	206	177	157	137		
	WSt 355		35	355	304	284							
		35	70	335	294	275	255	235	216	196	167		
	WSt 380		35	375[1]	333	314							
		35	70	345	324	304	284	265	245	216	186		
	WSt 420		35	410[1]	363	343							
		35	70	385	353	333	314	284	265	235	206		
	WSt 460		35	450[1]	402	373							
		35	70	420	392	363	343	314	294	265	235		
	WSt 500		35	480[1]	422	392							
		35	70	450	412	382	363	333	314	284	255		
Baustähle DIN 17100	**St 37-2, St 37-3** USt 37-2 RSt 37-2		16	235	218	202	185	165	140				
		16	40	225	208	192	175	155	135				
		40	65	215	200	185	170	150	130				
	St 44-2		16	275	248	232	215	195	165				
		16	40	265	245	225	205	185	160				
		40	65	255	237	218	200	180	155				
	St 52-3		16	355	318	282	245	225	195				
		16	40	345	308	272	235	215	190				
		40	65	335	300	265	230	210	185				

[1] bis 16 mm Dicke um ca. 10 N/mm² höher.

Mindestwanddicke von zylindrischen Mänteln mit $D_a/D_i \leqq 1{,}2$ *bei Druckbehältern bzw.* 1,7 *bei Dampfkesseln sowie von Rohren mit* $d_a \leqq 200$ mm *und* $d_a/d_i \leqq 1{,}7$

$$s = \frac{D_a \cdot p}{2\frac{K}{S}v + p} + c = \frac{D_i \cdot p}{2\frac{K}{S}v - p} + c \leqq s_e \qquad (4.18)$$

s	in mm	erforderliche Mindestwanddicke,
s_e	in mm	ausgeführte Wanddicke,
D_a, D_i	in mm	Außen- bzw. Innendurchmesser des zylindrischen bzw. kugeligen Mantels oder gewölbten Bodens, bei Rohren = d_a bzw. d_i,
p	in N/mm²	Berechnungsdruck = höchstzulässiger Betriebsüberdruck (1 N/mm² = 1 MPa = 10 bar oder 1 bar = 0,1 N/mm²),
β		Berechnungsbeiwert für gewölbte Böden nach Tab. 4.23, für kugelige Mäntel und Halbkugelböden ist $\beta = 1$,
K	in N/mm²	Festigkeitskennwert des Werkstoffs nach den Tabn. A 4.24 und A 4.25,
S		Sicherheitsbeiwert nach Tab. A 4.26,
v		Schweißnahtfaktor, der die Wertigkeit der Schweißnaht gegenüber dem Blech berücksichtigt, in der Regel = 0,8. Höherbewertung bis $v = 1$ nach vorausgegangenen Prüfungen. Bei ungeschweißten Teilen und bei äußerem Überdruck ist $v = 1$,
c	in mm	Wanddickenzuschlag nach Tab. A 4.26.

[2] Extract from the Standard EN 13445

5.2.3 Relation entre les définitions relatives à l'épaisseur

Les relations entre les différentes définitions relatives à l'épaisseur sont illustrées Figure 5-1.

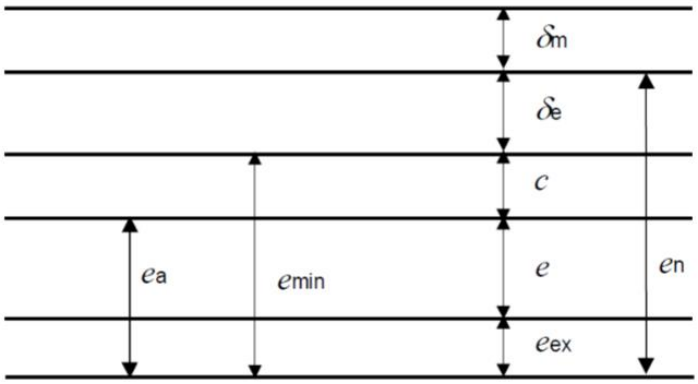

Légende

e est l'épaisseur requise

e_n est l'épaisseur nominale

e_{min} est l'épaisseur minimale possible après fabrication ($e_{min} = e_n - \delta_e$)

e_a est l'épaisseur utile ($e_a = e_{min} - c$)

c est la surépaisseur de corrosion ou d'érosion

δ_e est la valeur absolue de la tolérance négative éventuelle relative à l'épaisseur nominale (prise dans les normes de matériaux par exemple)

δ_m est la surépaisseur relative à l'amincissement possible pendant la fabrication

e_{ex} est l'épaisseur complémentaire pour atteindre l'épaisseur nominale

[3]-https://www.techniques-ingenieur.fr/base-documentaire/mecanique-th7/stockage-et-transfert-des-fluides-des-machines-hydrauliques-et-thermiques-42174210/tuyauteries-resistance-des-elements-bm6720/dimensionnement-calcul-de-resistance-a-la-pression-bm6720niv10003.html#niv-sl3974465

Les contraintes directes sont régies par les mêmes formules que la pression intérieure (figure **2**). La tension de compression maximale se produit à la face interne et vaut :

$$\sigma_{ti} = \frac{2p_e R_e^2}{R_e^2 - R_i^2} \qquad (8)$$

Pour les tubes minces, il suffit d'inverser le signe de la pression et l'on calcule :

$$\sigma_t = \frac{-p_e R_m}{a}$$

et

$$\sigma_\ell = \frac{-p_e R_m}{2a}$$

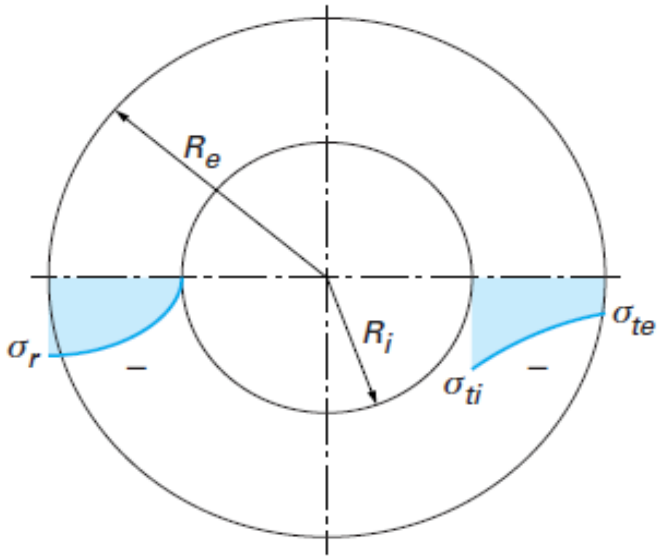

[4] CODAP 2005 Division 2, Partie C-Conception et Calculs

Caractéristique matériau		
Type	316L	1.4404
Rp 0.2	220	[MPa]
Rp 1.0		[MPa]
Re		[MPa]
Rm	520	[MPa]
Technical Pocket Guide (Schaffler)		

Contrainte nominale de calcul			
Rp 1.0 / 1.2	183.3	[MPa]	Calcul
Rm / 3	173.3	[MPa]	
f	173.3	[MPa]	
f	25	[ksi]	ASME
	172.37	[MPa]	
Zone locale (interne)	63.25	[mm]	
Zone locale (externe)	54.8	[mm]	

Zones		
Contrainte maximale générale de membrane	172.4	[MPa]
Contrainte minimale pour un zone locale	189.6	[MPa]
Contrainte maximale locale de membrane	258.6	[MPa]

[5] https://engstandards.lanl.gov/esm/pressure_safety/process_piping_guide_R2.pdf

- Prototype one: excel data and result

Données			
Données tube			
Rayon extérieur	R_e	16.7	[mm]
Rayon intérieur	Ri	12.7	[mm]
Rayon moyen	R_m	14.7	[mm]
Épaisseur de paroi	s_e	4	[mm]
Section	S_{feet}	369.5	[mm^2]
Moment quadratique	I_y	40656.3	[mm^4]
Nombre de pieds	n	4	[-]
Données matériau			
Module élastique	E	210	[GPa]
Module de Poisson	v	0.3	[-]
Limite élastique	F_e	207	[MPa]
Charge			
Masse réservoir	m_{res}	664	[kg]
Masse eau	m_{eau}	1000	[kg]
Accélération gravitationnelle	g	9.81	[m/s^2]
Poids	F_g	16323.8	[N]

Calculs			
Compression			
Contrainte	σ_{feet}	11.05	[MPa]
Flambage			
Longueur maximale d'un pied	l	170	[mm]
Longueur de flambage	l_k	119	[mm]
Force limite de flambage	F_k	5865.5	[N]
Poids par pied	$F_{g,1}$	4080.96	[N]

- Prototype two: excel data and result

Données			
Données pieds			
Côtés externes	x_{e1}	80	[mm]
	x_{e2}	50	[mm]
Côtés internes	x_{i1}	76	[mm]
	x_{i2}	46	[mm]
Section	S_{feet}	504.0	[mm^2]
Moment quadratique	I_y	450592.0	[mm^4]
	I_y	216872.0	[mm^4]
	I_y	216872.0	[mm^4]
Nombre de pieds	n	4	[-]
Données matériau			
Module élastique	E	210	[GPa]
Module de Poisson	v	0.3	[-]
Limite élastique	F_e	207	[MPa]
Charge			
Masse réservoir	m_{res}	664	[kg]
Masse eau	m_{eau}	1000	[kg]
Accélération gravitationnelle	g	9.81	[m/s^2]
Poids	F_g	16323.8	[N]

Calculs			
Compression			
Contrainte	σ_{feet}	8.10	[MPa]
Flambage			
Longueur maximale d'un pied	l	450	[mm]
Longueur de flambage	l_k	315	[mm]
Force limite de flambage	F_k	4465.3	[N]
Poids par pied	$F_{g,1}$	4080.96	[N]

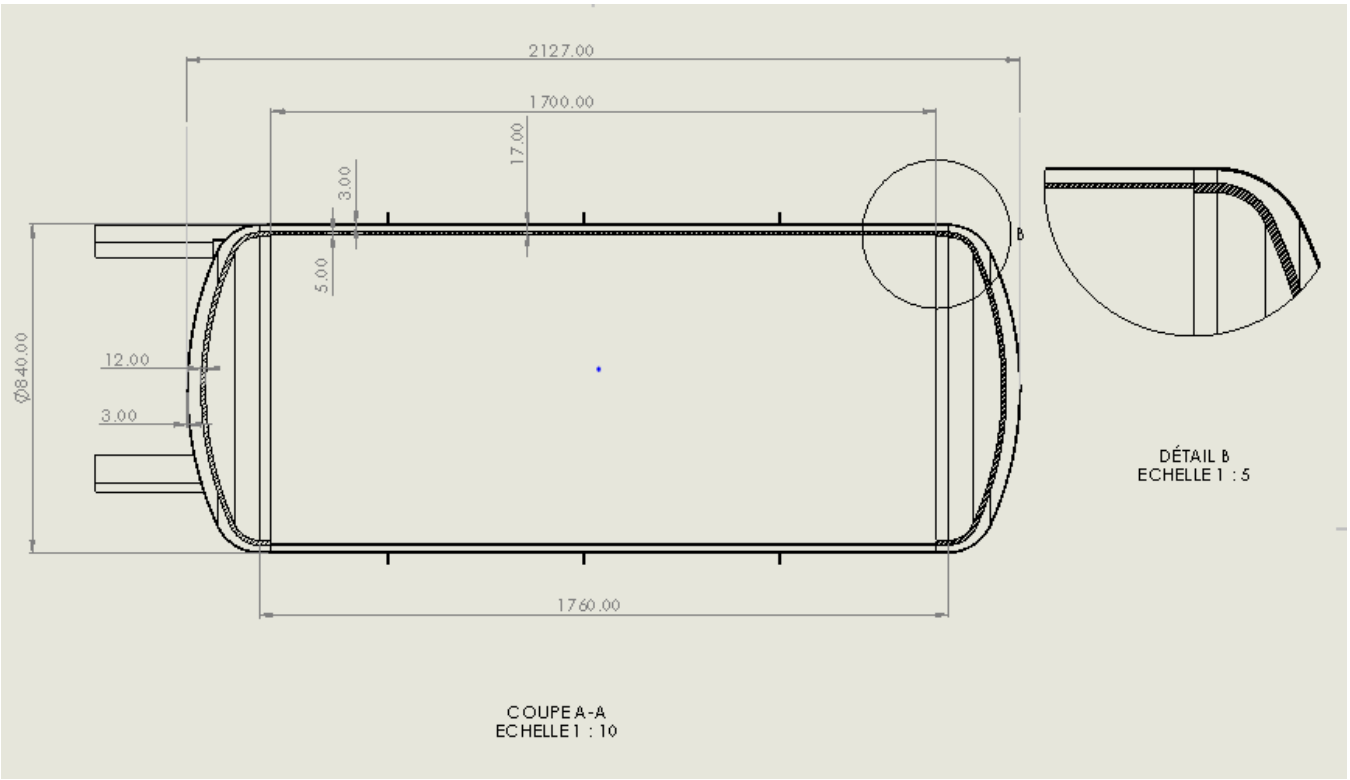
2127.00
1700.00
17.00
3.00
5.00
Ø840.00
12.00
3.00
1760.00
B
DÉTAIL B
ECHELLE 1 : 5
COUPE A-A
ECHELLE 1 : 10

11.2 Appendix 2: FEA structural analysis report of design 3

HAUTE ÉCOLE
D'INGÉNIERIE ET DE GESTION
DU CANTON DE VAUD
www.heig-vd.ch

Project :			VITES		
Subject :			Analyse structurelle de la version 09/18		
From :	COMATEC	To :	TVP Solar	Date :	08.03.2019
Author(s) :	Bonhôte Philippe				

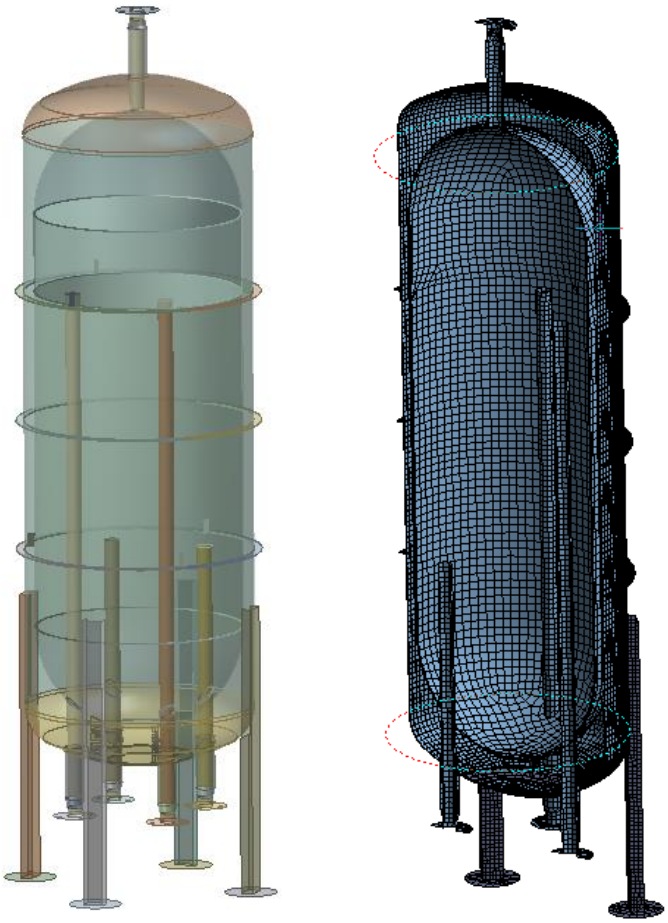

Table des matières

Introduction

Ce document décrit les calculs de vérification réalisés sur la structure finale proposée par TVP (nommé pour nous par son nom de fichier : vacuum_tank_asm.stp).

Les modifications apportées pour cette version sont :

L'utilisation de bouts sphériques pour la cuve interne (à la place de fonds bombés)

L'introduction de 4 tubes renforcés pour le remplissage (au lieu des trois tubes initialement proposés)

L'ajout du tube supérieur

La modification des systèmes de soutien limiteurs de chocs entre cuves

La modification des pieds de support

La figure présente la version considérée dans ce rapport en comparaison des versions précédemment calculées. La version considérée est celle dont le nom est « vacuum_tank_asr 3). Elle se trouve à droite sur la figure.

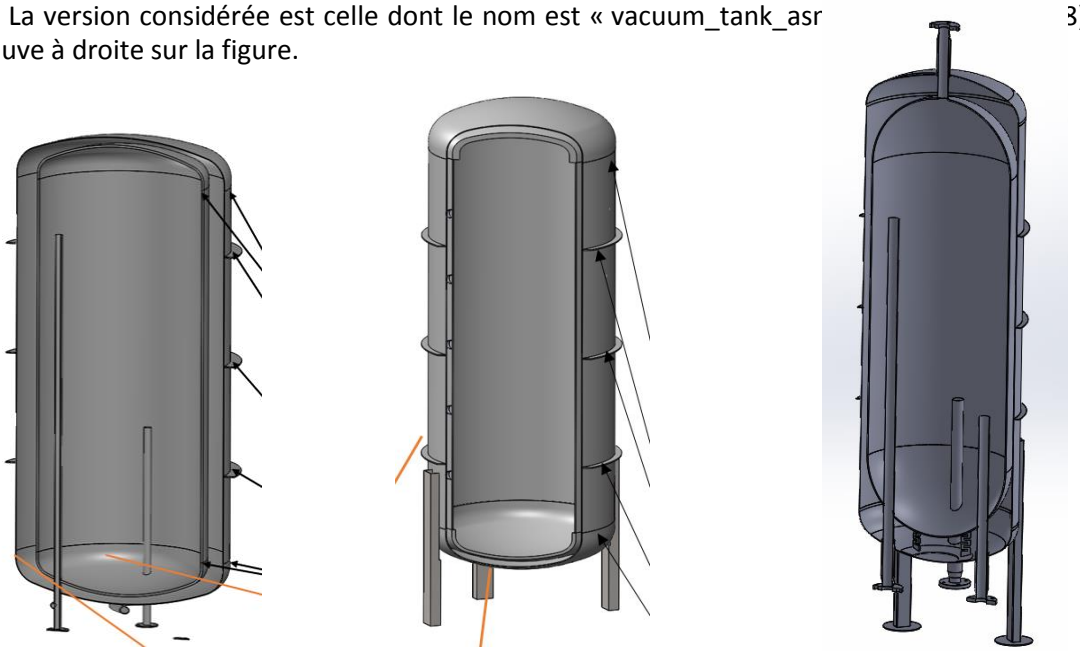

Figure 33 : Evolution des versions avec à gauche les 2 versions initiales évaluées dans le précéd rapport et à droite la version donnée par le fichier « vacuum_tank_asm.stp».

Les modifications structurelles apportées sont conformes aux recommandations et aux pré-dimensionnements présentés dans le rapport de calcul relatif à la précédente version. Il ne devrait donc pas y avoir de surprise en termes de dimensionnement mécanique :

La partie cylindrique de la cuve interne présente une épaisseur de 6mm au lieu de 5mm. Les fonds bombés de 12mm ont été remplacés par des bouts sphériques de 6mm d'épaisseur. Les contraintes dans les bouts sphériques sont en principe inférieures à celle présentes dans la partie cylindrique en raison de la double courbure. Ces modifications devraient donc être validées sans soucis en termes de résistance mécanique.

La cuve extérieure conserve la même épaisseur et la même structure de renforts extérieurs. Ainsi la marge de stabilité de cette enveloppe devrait être plus ou moins équivalente à la précédente version.

La liaison au sol est réalisée par des pieds à profils fermés de section semblable à la version précédente qui a été validée. La légère augmentation de longueur ne devrait pas remettre en cause la stabilité qui présentait une bonne marge.

Evaluation analytique succincte

Contrainte de membranes engendrées par la pression

Pour évaluer au premier ordre la sévérité des contraintes engendrées par la pression interne, il est possible d'établir un récapitulatif des contraintes équivalentes maximales de membranes primaires pour les différents éléments considérés. En observant que l'essentiel des efforts de supportage sont repris par les pieds et non par la tubulure, nous pouvons nous préoccuper essentiellement des efforts engendrés par la pression :

Pour les tubes et parois cylindriques : $\sigma_{eq} = p_i \frac{\sqrt{2}}{4} \frac{D_i}{a}$ *(circonférentiels et longitudinaux déjà combinés)*

Pour les fonds bombés : $\sigma_{eq} = p_i \frac{1}{4} \frac{D_i}{a}$

Avec les paramètres suivants :

Diamètre intérieur	**D_i**
Epaisseur de paroi	a
Différence de Pression nominale entre intérieur / extérieur	p_i
Contrainte de Von Mises équivalente	σ_{eq}

Table 51 : paramètres pour le calcul de la contrainte nominale engendrée par la pression dans des enveloppes minces

Résultats pour les différentes parties de la structure :

	D_i (mm)	a (mm)	P (MPa)	σ_{eq} (MPa)	f (MPa)
Enveloppe intérieure bouts sphériques	788	6	1.7	56	172
Enveloppe intérieure paroi cylindrique	788	6	1.7	79	172
Enveloppe extérieure paroi cylindrique	874	3	0.1	11	172
Tubes de remplissage, évacuation	56.3	2	1.6	16	172

Table 52 : Comparaison des contraintes de membranes équivalentes primaires pour les différentes parties de la structure

Il apparaît que les contraintes nominales relevées dans les différents éléments de la structure ne sont pas surchargés puisque les contraintes équivalentes sont toutes inférieures à la limite f=172MPa.

Stabilité et contraintes engendrées par le poids propre et la pression extérieure

Pour le reste des cas de charges, il est possible de se référer aux calculs analytiques réalisés dans le précédent rapport puisque l'enveloppe extérieure et les renforts n'ont pas fondamentalement changés. De même, les grandeurs qui régissent la stabilité et les contraintes dans les pieds n'ont pas été modifiées significativement depuis la dernière version.

Pour l'évaluation des changements effectifs, l'approche numérique sera plus significative.

Modèle numérique

L'évaluation de la résistance mécanique de la structure a aussi été réalisée avec un modèle numérique. Ce modèle, évalue la résistance statique des enveloppes et des pieds aux effets du poids propre et des pressions internes et externes. Il évalue également la stabilité de l'enveloppe extérieure à la pression atmosphérique ainsi que celle des pieds sous l'effet du poids propre.

Géométrie

La géométrie a été fournie par TVP. Le nom du fichier est « vacuum_tank_asm.stp». La géométrie est présentée par la figure ci-dessous.

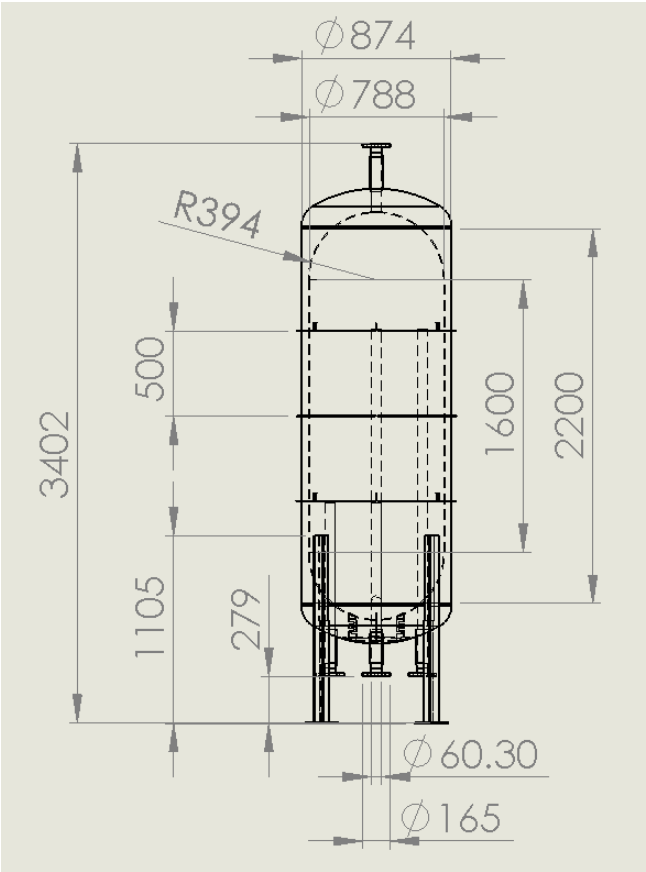

Figure 34 : Dimensions générale de la structure donnée par le fichier « vacuum_tank_asm.stp».

La masse de la structure a été calculée pour de l'acier à 545 kg (modèle géométrique, pas EF !)

Modèle numérique

La structure a été modélisée à l'aide de la version 18 du logiciel de calcul ANSYS.

Le modèle a été construit en utilisant des éléments de coques type SHELL 181, des éléments solides-coques de type SOLSH 190 et des éléments de contact et de cible type 170, 174 et 175.

Le modèle comporte au total 66576 nœuds et 37041 éléments.

La masse calculée du modèle est égale à 544 kg (modèle EF).

Le maillage considéré ainsi que la présentation de la répartition des matières et des épaisseurs de coques sont présentés à la figure ci-dessous.

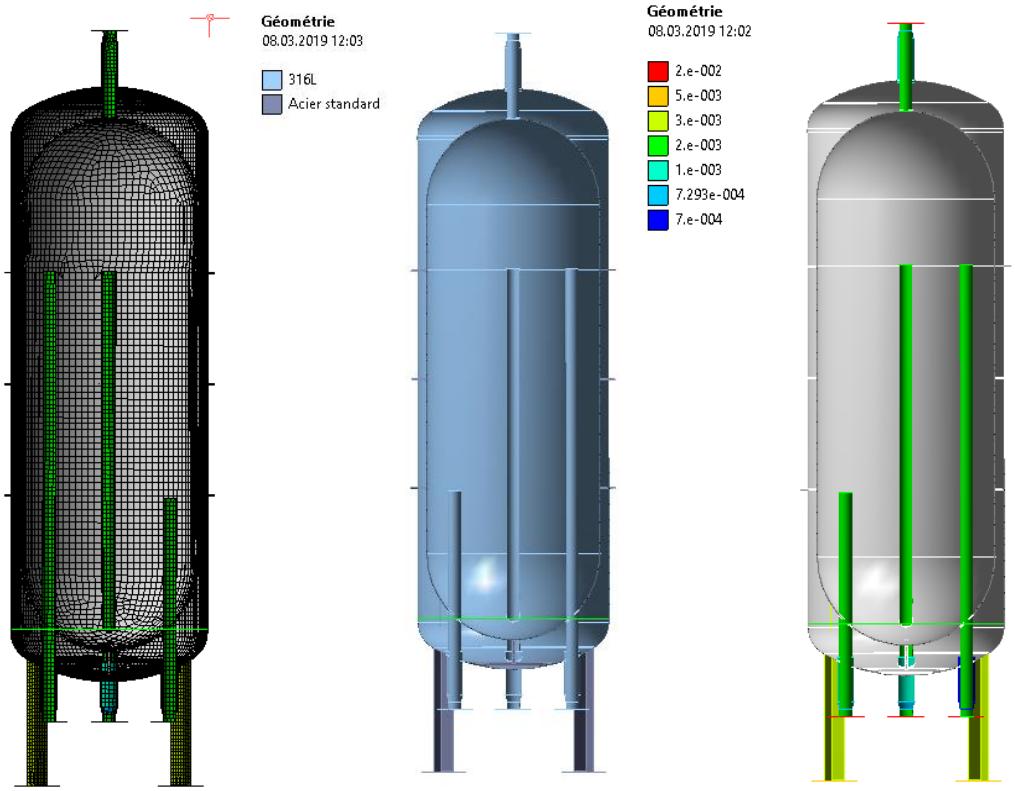

Figure 35 : Présentation du maillage, des matières et des épaisseurs de coques considérés pour le modèle (masse totale calcuée 544kg).

Conditions aux limites, cas de charges

Trois cas de charges ont été considérés avec les pieds fixés au sol :

1. Effet de la pression interne (16 bar) :
   - Pression appliquée sur la paroi intérieure de 17 bars (1,7 MPa)
   - Forces de traction sur les bouts des tubes pour remplacer l'effet des tubes manquants 4486N.
2. Effet de la pression externe (1 bar) :
   - Pression appliquée sur la paroi extérieure de 1 bar (0,1 MPa)
   - Forces de traction sur les bouts des tubes pour remplacer effet des tubes manquants 453N.
3. Effet de la gravité et de la masse de liquide (réaction d'appui calculée au sol : 15166N) :
   - Pression hydrostatique avec une référence en haut du réservoir (masse totale équivalente à 1t de liquide)
   - Gravité imposée à l'ensemble de la structure.

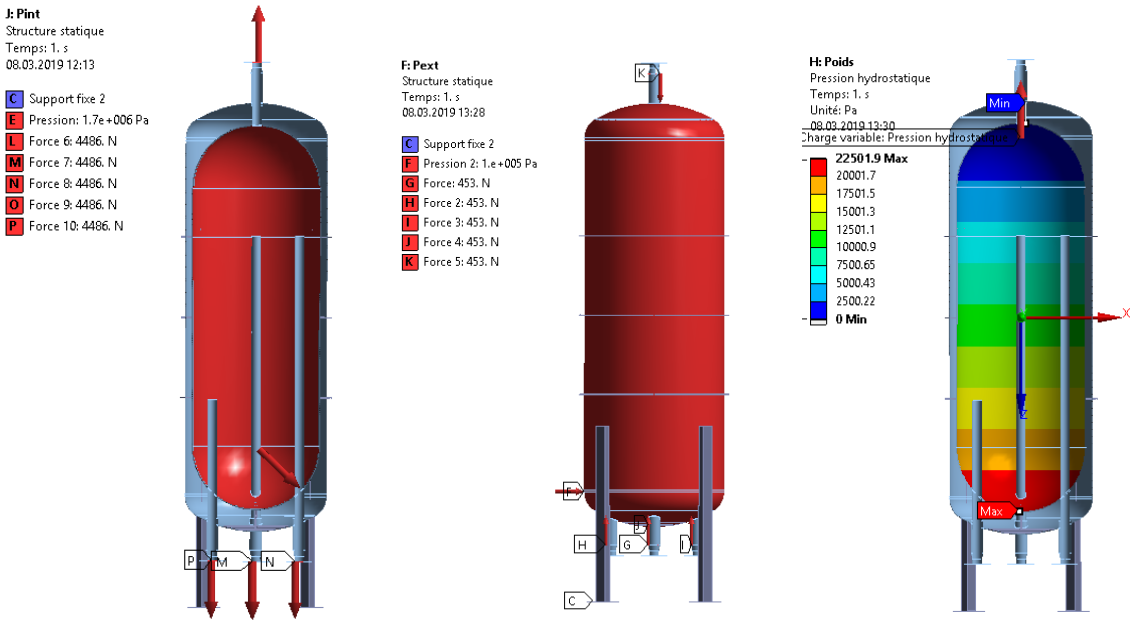

Figure 36 : Présentation des cas de charge considérés ; à gauche pression intérieure de 17 bars (absolu), au milieu pression extérieure de 1 bar, à droite gravité (1,55t)

Condition de calculs et liaisons

La liaison entre les pièces a été réalisée soit par « fusionnement » des nœuds aux interfaces (liaison conformes) lorsque cela était possible, soit par une approche de type contacts collés (MPC et pénalité). La qualité des liaisons a été évaluée par extraction des modes propres d'ordre élevé et observation du comportement de ces dernières.

Le conditionnement du problème numérique a été jugé comme relativement bon avec un rapport d'environ 10'000 entre les termes extrêmes de la matrice de raideur.

Résultats

Contraintes totales dans la structure engendrées par la somme des cas de charges 1) 2) et 3)

La figure ci-dessous présente la répartition des contraintes dans la structure engendrées par la superposition des 3 cas de charges décrits.

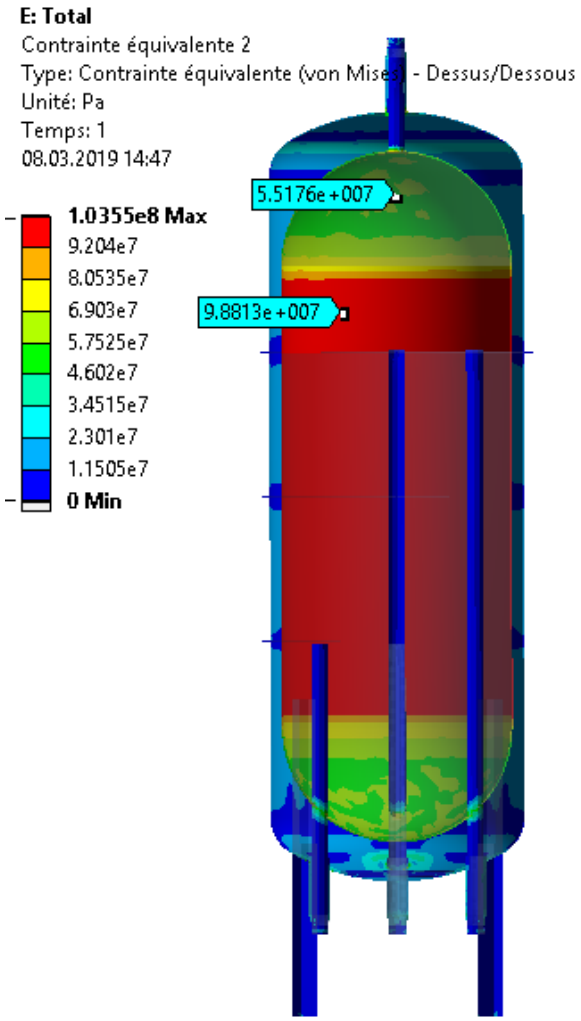

Figure 37 : Répartition des contraintes (selon Von Mises) dans la structure engendrées par la superposition de l'ensemble des cas de charge.

La contrainte maximale selon Von-Mises dans la paroi de l'enveloppe intérieure ne dépasse pas 100MPa ce qui est acceptable par rapport à la limite f qui vaut 172MPa pour le 316L. Par ailleurs, la contrainte locale ne dépasse pas non plus 104MPa ce qui est acceptable vis-à-vis de la limite tolérée à 1,5*f, soit 258 MPa.

Contraintes dans la structure engendrées uniquement par la pression intérieure de 17 bars absolus

La figure ci-après présente la répartition des contraintes dans la structure engendrées uniquement par la pression interne de 17 bars absolus.

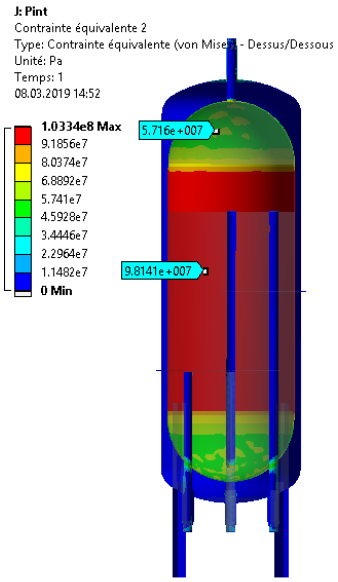

Figure 38 : Répartition des contraintes (selon Von Mises) dans la structure engendrées uniquement par la pression intérieure absolue égale à 17 bars.

La contrainte maximale selon Von-Mises dans la paroi de l'enveloppe intérieure ne dépasse pas 100MPa ce qui est acceptable par rapport à la limite f qui vaut 172MPa pour le 316L. Par ailleurs, la contrainte locale ne dépasse pas non plus 104MPa ce qui est acceptable vis-à-vis de la limite tolérée à 1,5*f, soit 258 MPa.

Contraintes dans la structure engendrées par les autres cas de charge

Les figures ci-après présentent séparément la répartition des contraintes dans la structure engendrées par la pression extérieure de 1bar et par le poids propre.

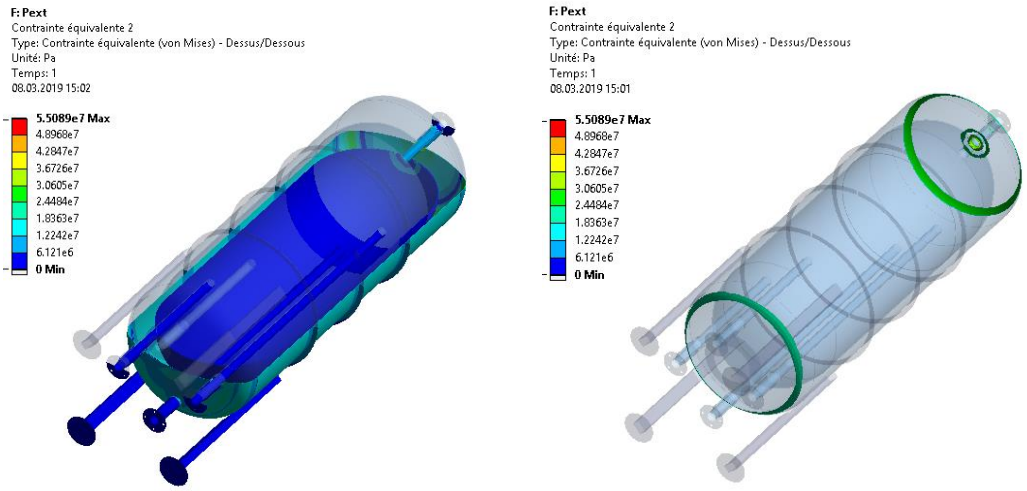

Figure 39 : Répartition des contraintes (selon Von Mises) dans la structure engendrées uniquement par la pression extérieure de 1 bar. A droite volume dans lequel la contrainte dépasse 24MPa.

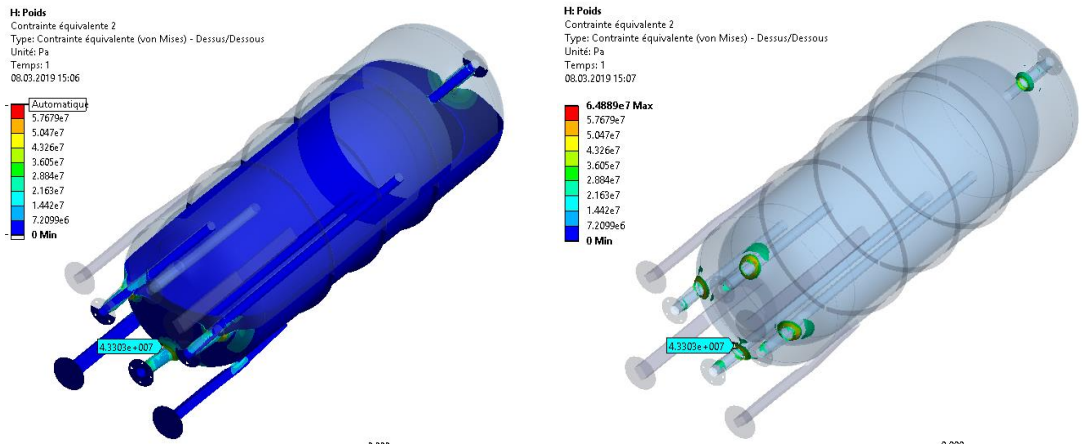

Figure 40 : Répartition des contraintes (selon Von Mises) dans la structure engendrées uniquement par l'effet du poids propre avec une tonne de liquide.
A droite volume dans lequel la contrainte dépasse 24MPa.

La contrainte maximale selon Von-Mises dans la structure ne dépasse pas dans les deux cas considérés 60 MPa de manière très locale. La taille de la zone sur laquelle la contrainte dépasse 25MPa n'excède pas 35mm ce qui est faible par rapport à la taille de la structure (zone considérée comme locale par le CODAP : $l = \sqrt{R \cdot e} \approx \sqrt{400 \cdot 3} = 35 \text{ mm}$). Le dimensionnement selon ces cas de charge n'est donc pas limité par les contraintes. Il faut évaluer la stabilité et donc la marge de flambage.

Evaluation de la marge de sécurité vis-à-vis du flambage pour les cas 2) et 3)

Les figures ci-après présentent les modes de flambages influents pour les deux cas de charges critiques, à savoir :

2. la pression extérieure de 1 bar sur la paroi du vaccum
3. le poids propre de la structure pleine de liquide sur les pieds
   -

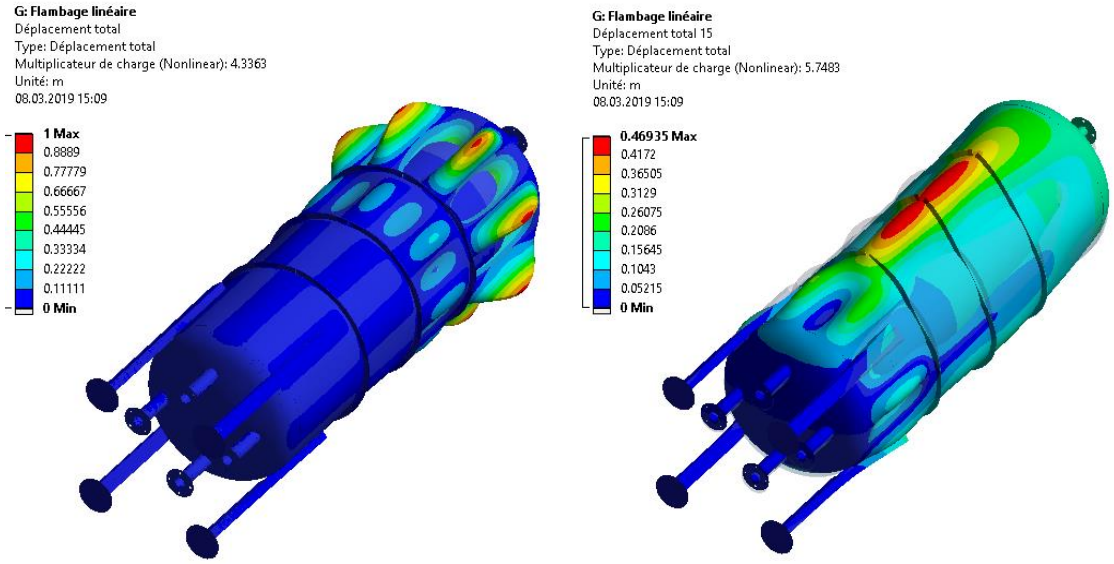

Figure 41 : Modes de flambages relevant pour la structure soumise à la pression extérieure de 1 bar. Les facteurs de marges valent respectivement 4,3 et 5,7.

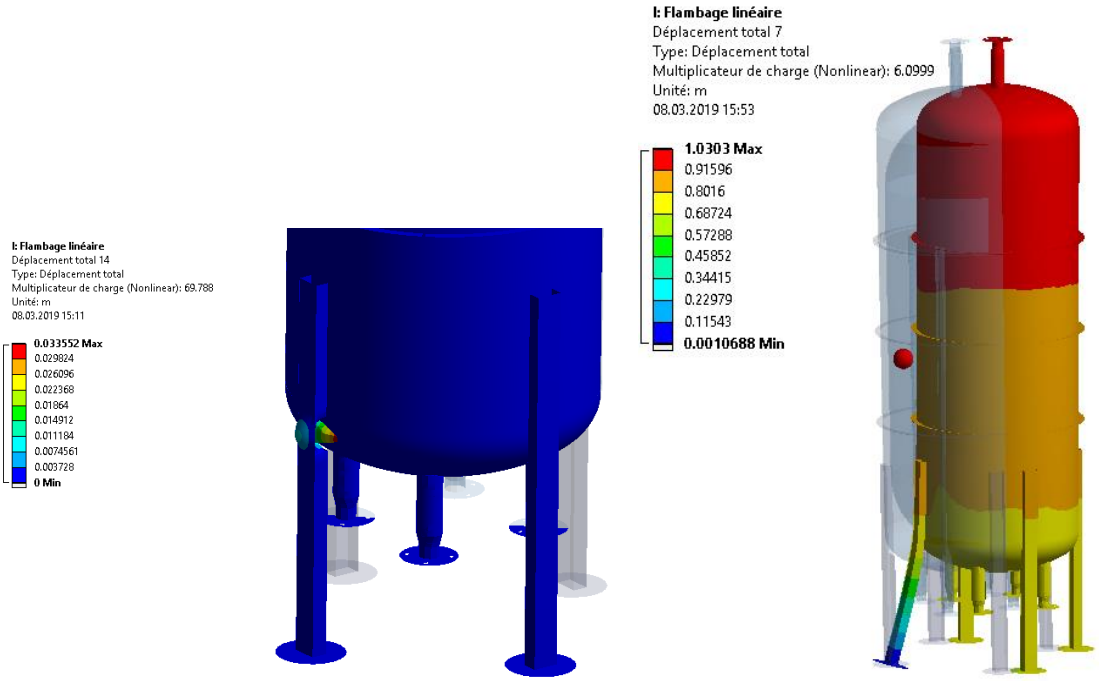

Figure 42 : Premier mode de flambage relevants pour la structure soumise à son poids propre au à celui du liquide. Le facteur de marge vaut environ 70 si les pieds sont vissés au sol (image de gauche). Le facteur de marge vaut environ 6 si les pieds sont juste posés au sol (image de droite).

Pour les deux cas de charge, la marge de stabilité au flambage est supérieure à 4.

Selon le document BM 6720 p17 des techniques de l'ingénieur, on demande que le facteur de marge soit supérieur à 3 ce qui est le cas pour la présente étude.

Conclusions

La structure proposée est correctement dimensionnée du point de vue statique mécanique (dimensionnement à pression nominale). Il devrait donc être possible de lui faire passer les spécifications selon le CODAP ou selon les normes de l'ASME.

Le fluage n'a pas été considéré car la température de fonctionnement est relativement faible (160°C) par rapport à la température de fusion de l'acier.

En comparaison des précédentes versions, voici les éléments relevant de ce rapport :

Prototype 1		Prototype 2		Prototype 3
Mass				
655 [kg]		462 [kg]		545 [kg]
Stress (global)				
Inner tank	Pipe welds	Inner tank	Cylindrical reinforcements	Inner tank
300 [MPa]	378 [MPa]	192 [MPa]	108 [MPa]	98 [MPa]
Stress (membrane)				
Inner tank	Pipe welds	Inner tank	Cylindrical reinforcements	Inner tank
190 [MPa]	240 [MPa]	134 [MPa]	168 [MPa]	103 [MPa]
Load multiplication (buckling)				
6.2		9.6		4.3

Tableaux

Figures